

# BER Performance Analysis of FSO Communication System over Málaga ( $\mathcal{M}$ ) Turbulence Channel with Zero and Non-zero Boresight Pointing Errors for Different Modulation Techniques.

---

**Course Code: ETE 498**  
**Fall 2020**

**Submitted By-**

Burhan Uddin Shakil  
Student ID: 2017-1-55-003

Md. Imtiaz Ahmed  
Student ID: 2017-1-55-004

Amrin Akter  
Student ID: 2017-1-55-042

**Submitted To-**

Department of Electronics and Communication Engineering

**Supervised by-**

S.M.Raiyan Chowdhury  
Lecturer

Department of Electronics and Communication Engineering



East West University (EWU)  
Jahirul Islam City, Aftabnagar, Dhaka, Bangladesh

# Certification

This is to certify that the work presented in the thesis is an outcome of the investigation carried out by the authors under the supervision of Lecturer S.M.Raiyan Chowdhury,Department of Electronics and Communication Engineering.This thesis is done due to the partial fulfillment of the requirement for the degree of Bachelors of Science in B.Sc in Electronics and telecommunication Engineering.

## Authors



---

Imtiaz Ahmed Emon



---

Burhan Uddin Shakil



---

Amrin Akter

## Signature of the Supervisor



---

S.M.Raiyan Chowdhury

Lecturer

Department of Electronics and Communication Engineering  
East West University (EWU)

# **Acknowledgments**

First and foremost, we would like to thank Almighty Allah for His blessings to overcome this current circumstance and continue our work. We cannot express enough thanks to our thesis supervisor S.M.Raiyan Chowdhury for his guidance and for always being there as a mentor. He showed us the path to go through. we were very tensed before starting our thesis as we have to deal with everything in the middle of the corona outbreak on the online platform, but after talking with our supervisor we got the mental strength to start our research. He shared his experienced and wisdom with us while conducting our work. His suggestions helped us to think in a better way. We deeply want to thank our family members and friends for always being understanding, supportive and believing in us even at the moment we were out of confidence.

# Abstract

Free Space Optical (FSO) Communication system defines a line of sight communication of light in the visible or infrared region for transferring data between two distant points. FSO communication is providing high bandwidth over RF communication. It is a license-free, low cost, the transmission of the system is secure and free from Electromagnetic Interference (EMI). In the FSO communication data rate faster than any other wireless communication technology. However, as the emitted light signal travels through the atmosphere, the atmospheric turbulence induces attenuation and fluctuations. In this thesis, we evaluated the average bit error performance of FSO communication systems by using coherent and noncoherent modulation schemes such as BPSK, DPSK, QPSK, NRZ-OOK, RZ-OOK, M-QAM, M-PPM, M-PAM. By consider Málaga ( $\mathcal{M}$ ) distribution atmospheric turbulence, atmospheric attenuation and pointing error a channel fadding model is design. We have worked for the ABER performance for zero and non-zero boresight pointing error, different propagation link distances, different weather conditions, and different beamwidth. Our main objective from this work is to find out the best suitable modulation schemes for the FSO communication system over Málaga ( $\mathcal{M}$ ) distribution. To analyze the average bit error performance we have used both theoretical analysis and Matlab simulation. Now we can say that our simulation results of average bit error performance can help the design of future FSO communication systems.

**Keywords:** Free-space optics (FSO), Málaga ( $\mathcal{M}$ ) atmospheric turbulence channel, average bit-error-rate (ABER), zero boresight pointing error, non-zero boresight pointing error, BPSK, QPSK, DPSK, RZ-OOK, NRZ-OOK, M-PPM, M-PAM and M-QAM.

# **Nomenclature**

FSO : Free Space Optics

ABER: Average bit error rate

BPSK: Binary phase shift keying

QPSK: Quadrature phase shift keying

DPSK: Differential phase shift keying

OOK: On-Off keying

NRZ: Non return zero

RZ: Return zero

PAM: Pulse amplitude modulation

PPM: Pulse position modulation

MIMO: Multiple input multiple output

SNR: Signal to noise ratio

LOS: Line of sight

RF: Radio Frequency

OWC: Optical wireless communication

VLC: Visible light communication

AWGN: Additive Gaussian noise

# TABLE OF CONTENTS

	Page
<b>List of Tables</b>	<b>vii</b>
<b>List of Figures</b>	<b>viii</b>
<b>1 Introduction</b>	<b>1</b>
1.1 Overview . . . . .	1
1.2 Advantages of FSO . . . . .	3
1.3 Applications of FSO . . . . .	4
1.4 Drawbacks of FSO . . . . .	6
<b>2 Background and Literature Review</b>	<b>9</b>
2.1 Contribution of This Thesis . . . . .	11
2.2 Research Methodology . . . . .	11
2.3 Thesis Structure . . . . .	12
<b>3 Free-Space Optical Communication</b>	<b>13</b>
3.1 Introduction . . . . .	13
3.2 Fundamental of Free Space Optical Communication . . . . .	13
3.2.1 Basic Block Diagram of FSO . . . . .	14
3.3 Classification of FSO Systems Based on Detection Techniques . . . . .	18
3.4 Atmospheric Turbulence Statistical Fading Models . . . . .	19
3.4.1 Lognormal(LN) Turbulence Scenario . . . . .	21
3.4.2 Gamma-Gamma(CC) Turbulence Scenario . . . . .	22
3.4.3 Rician-Lognormal (RLN) Turbulence Scenario . . . . .	23
<b>4 System and Channel Models</b>	<b>24</b>
4.1 Introduction . . . . .	24
4.2 System Model . . . . .	24
4.3 Málaga ( $\mathcal{M}$ ) Atmospheric Turbulence Model . . . . .	25
4.3.1 Málaga ( $\mathcal{M}$ ) Probability Density Function . . . . .	28

---

**TABLE OF CONTENTS**

4.4	Pointing Error . . . . .	30
4.4.1	Zero Boresight Pointing Error Model . . . . .	33
4.4.2	Non-Zero Boresight Pointing Error Model . . . . .	34
4.5	Atmospheric Effects . . . . .	36
4.5.1	Atmospheric loss . . . . .	37
4.6	Channel Statistical Model . . . . .	38
<b>5</b>	<b>Modulation Techniques and BER Analysis</b>	<b>40</b>
5.1	Introduction . . . . .	40
5.2	Binary Phase Shift Keying (BPSK) . . . . .	42
5.3	Quadrature Phase Shift Keying (QPSK) . . . . .	42
5.4	Differential Phase Shift Keying (DPSK) . . . . .	43
5.5	On-Off Keying (OOK) . . . . .	44
5.6	Quadrature Amplitude Modulation (QAM) . . . . .	45
5.7	Pulse Amplitude Modulation (PAM) . . . . .	46
5.8	Pulse Position Modulation (PPM) . . . . .	46
5.9	BER Analysis In-Terms of Atmospheric Turbulence for Different modulation .	47
<b>6</b>	<b>Simulation output</b>	<b>50</b>
6.1	Simulation Parameters . . . . .	50
6.2	Model Validation . . . . .	51
6.3	Result and Discussion . . . . .	51
6.3.1	ABER Performance of Zero and Non-zero Boresight Pointing Errors for Different Turbulence Condition . . . . .	51
6.3.2	ABER Performance for Different Propagation link Distance . . . . .	61
6.3.3	ABER Performance for Different Weather Conditions . . . . .	70
6.3.4	ABER Performance for Different Beam-Width . . . . .	87
<b>7</b>	<b>Conclusion</b>	<b>97</b>
7.1	Overall Conclusion and Future work . . . . .	97
7.2	Challenges of FSO . . . . .	99
<b>References</b>		<b>100</b>

## LIST OF TABLES

TABLE	Page
4.1 List of most popular existing distribution models for FOS communications that can generation by using the proposed Málaga ( $\mathcal{M}$ )distribution model. . . . .	30
4.2 Attenuation coefficients for different weather conditions[94] . . . . .	37
6.1 Simulation parameters [59] . . . . .	50

## LIST OF FIGURES

<b>FIGURE</b>	<b>Page</b>
1.1 Physical diagram of FSO system . . . . .	2
1.2 Atmospheric effects on a FSO system [14] . . . . .	7
3.1 Block Diagram of a terrestrial FSO . . . . .	17
3.2 Block diagram of a non-coherent or direct detection optical receiver. . . . .	18
3.3 Block diagram of a coherent detection optical receiver. . . . .	19
3.4 Atmospheric Channels with turbulent eddies . . . . .	20
4.1 Practical propagation of laser beams in Málaga ( $\mathcal{M}$ ) atmospheric turbulence . . . . .	24
4.2 Laser beam propagation scheme under a Málaga ( $\mathcal{M}$ ) distributed FSO link.[51] . . .	27
4.3 Beam footprint with misalignment on the detector plane [7] . . . . .	32
6.1 ABER performance of BPSK for zero and non-zero boresight pointing errors. . . . .	52
6.2 ABER performance of QPSK for zero and non-zero boresight pointing errors. . . . .	53
6.3 ABER performance of DPSK for zero and non-zero boresight pointing errors. . . . .	54
6.4 ABER performance of NRZ-OOK for zero and non-zero boresight pointing errors. . . . .	55
6.5 ABER performance of RZ-OOK for zero and non-zero boresight pointing errors. . . . .	55
6.6 ABER performance of 4-QAM for zero and non-zero boresight pointing errors. . . . .	56
6.7 ABER performance of 8-QAM for zero and non-zero boresight pointing errors. . . . .	56
6.8 ABER performance of 16-QAM for zero and non-zero boresight pointing errors. . . . .	57
6.9 ABER performance of 4-PAM for zero and non-zero boresight pointing errors. . . . .	58
6.10 ABER performance of 8-PAM for zero and non-zero boresight pointing errors. . . . .	58
6.11 ABER performance of 16-PAM for zero and non-zero boresight pointing errors. . . . .	59
6.12 ABER performance of 4-PPM for zero and non-zero boresight pointing errors. . . . .	59
6.13 ABER performance of 8-PPM for zero and non-zero boresight pointing errors. . . . .	60
6.14 ABER performance of 16-PPM for zero and non-zero boresight pointing errors. . . . .	60
6.15 ABER performance of BPSK for different propagation link distance . . . . .	61
6.16 ABER performance of QPSK for different propagation link distance . . . . .	62
6.17 ABER performance of DPSK for different propagation link distance . . . . .	63

6.18 ABER performance of NRZ-OOK for different propagation link distance . . . . .	63
6.19 ABER performance of RZ-OOK for different propagation link distance . . . . .	64
6.20 ABER performance of 4-QAM for different propagation link distance . . . . .	65
6.21 ABER performance of 8-QAM for different propagation link distance . . . . .	65
6.22 ABER performance of 16-QAM for different propagation link distance . . . . .	66
6.23 ABER performance of 4-PAM for different propagation link distance . . . . .	66
6.24 ABER performance of 4-PPM for different propagation link distance . . . . .	67
6.25 ABER performance of 8-PPM for different propagation link distance . . . . .	67
6.26 ABER performance of 16-PPM for different propagation link distance . . . . .	68
6.27 Comparison between four different modulationn for different propagation link distance	68
6.28 ABER performance of BPSK for different weather condition under strong turbulence.	70
6.29 ABER performance of BPSK for different weather condition under weak turbulence.	71
6.30 ABER performance of QPSK for different weather condition under strong turbulence.	72
6.31 ABER performance of QPSK for different weather condition under weak turbulence.	72
6.32 ABER performance of DPSK for different weather condition under strong turbulence.	73
6.33 ABER performance of DPSK for different weather condition under weak turbulence.	73
6.34 ABER performance of NRZ-OOK for different weather condition under stong turbulence. . . . .	74
6.35 ABER performance of NRZ-OOK for different weather condition under weak turbulence. . . . .	75
6.36 ABER performance of RZ-OOK for different weather condition under strong turbulence. . . . .	75
6.37 ABER performance of RZ-OOK for different weather condition under weak turbu-lence. . . . .	76
6.38 ABER performance of 4-QAM for different weather condition under strong turbulence.	76
6.39 ABER performance of 4-QAM for different weather condition under weak turbulence.	77
6.40 ABER performance of 8-QAM for different weather condition under weak turbulence.	77
6.41 ABER performance of 8-QAM for different weather condition under strong turbulence.	78
6.42 ABER performance of 16-QAM for different weather condition under strong turbu-lence. . . . .	78
6.43 ABER performance of 16-QAM for different weather condition under weak turbu-lence. . . . .	79
6.44 ABER performance of 4-PAM for different weather condition under strong turbulence.	80
6.45 ABER performance of 4-PAM for different weather condition under weak turbulence.	80
6.46 ABER performance of 8-PAM for different weather condition under strong turbulence.	81
6.47 ABER performance of 8-PAM for different weather condition under weak turbulence.	81

6.48 ABER performance of 16-PAM for different weather condition under strong turbulence. . . . .	82
6.49 ABER performance of 16-PAM for different weather condition under weak turbulence. . . . .	82
6.50 ABER performance of 4-PPM for different weather condition under strong turbulence. . . . .	83
6.51 ABER performance of 4-PPM for different weather condition under weak turbulence. . . . .	84
6.52 ABER performance of 8-PPM for different weather condition under strong turbulence. . . . .	84
6.53 ABER performance of 8-PPM for different weather condition under weak turbulence. . . . .	85
6.54 ABER performance of 16-PPM for different weather condition under strong turbulence. . . . .	85
6.55 ABER performance of 16-PPM for different weather condition under weak turbulence. . . . .	86
6.56 ABER performance of BPSK for different beam width. . . . .	87
6.57 ABER performance of QPSK for different beam width. . . . .	88
6.58 ABER performance of DPSK for different beam width. . . . .	89
6.59 ABER performance of RZ-OOK for different beam width. . . . .	89
6.60 ABER performance of NRZ-OOK for different beam width. . . . .	90
6.61 ABER performance of 4-QAM for different beam width. . . . .	91
6.62 ABER performance of 8-QAM for different beam width. . . . .	91
6.63 ABER performance of 16-QAM for different beam width. . . . .	92
6.64 ABER performance of 4-PAM for different beam width. . . . .	93
6.65 ABER performance of 8-PAM for different beam width. . . . .	93
6.66 ABER performance of 16-PAM for different beam width. . . . .	94
6.67 ABER performance of 4-PPM for different beam width. . . . .	94
6.68 ABER performance of 8-PPM for different beam width. . . . .	95
6.69 ABER performance of 16-PPM for different beam width. . . . .	95

# **Chapter 1**

## **Introduction**

### **1.1 Overview**

Communication is the most important part for human beings to build a form of community to survive. Communication means sharing information through acting, speaking, writing or using another medium through the same system of signs between people. Communication has undergone various changes, beginning with cave drawings and continue with various forms of wireless communication, after man arrived on earth.

Wireless communication is pushed through a complex phenomenon termed as radio or optical wave propagation. It's far characterized via a couple of outcomes inclusive of multipath fading and shadowing. The statistical behavior of these effects is characterized with the aid of unique turbulence fashions depending on the character of the communication environment. To encompass the practicality concern of the currently available turbulence channel models and beyond, it is important to research these effects. Therefore, researching large-scale fading alongside small-scale fading is very simple and tempting as the multi-hop relay networks are evolving in the current days. Various multipath fading and shadowing statistics are encountered by geographically distributed nodes [11]. Therefore it is important to model hybrid fading turbulence networks, where multipath fading and shadowing are modelled together,for the performance analysis of different systems of communication. Three impairments are primarily experienced by the signal transmitted by the wireless channel : (i) pathloss, (ii) shadowing and (iii) fading. Pathloss is specifically a large-scale propagation effect that characterizes the difference over large distances in the power of the transmitted signal [39]. Pathloss may be a deterministic amount and is usually modeled as a function of distance  $d$ . The general model for pathloss is  $PL \propto d^{-\alpha}$ , where the exponent of path loss is  $\alpha$ . Due to pathloss, the signal power reduces rapidly [39].

Optical wireless communication is a core part of wireless communication. OWC is a technology which involves the transmission over the free space channel of information-laden optical radiation. The interest in optical wireless communication (OWC) as a promising short-range communication technology has recently increased largely due to the need for higher data speeds in support of communication applications [38]. It offers flexible networking solutions that are also cost-effective for indoor and outdoor applications, providing high-speed broadband connectivity [34].

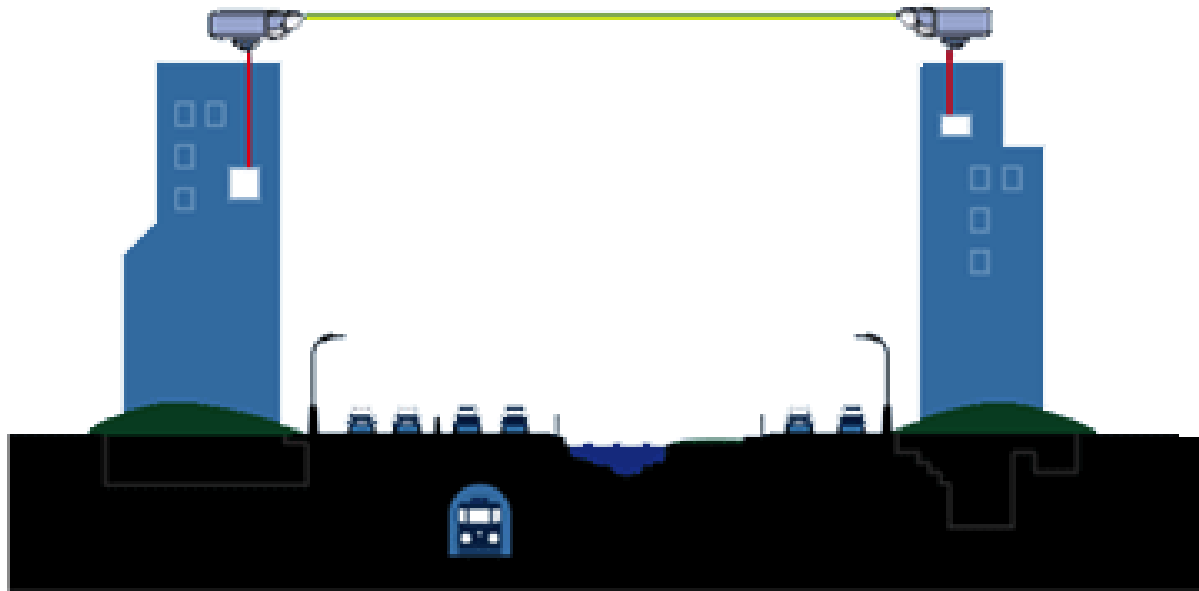


**Figure 1.1:** Physical diagram of FSO system

OWC is classified into three fundamental types and they are Free-Space Optical (FSO) communications, Visible Light Communications (VLC), and Ultra-Violet (UV) Communications [40]. Communication with Free Space Optical (FSO) has attracted significant interest because of its privileges, such as large available and unlicensed bandwidth, long Operational range, spatial reusability, protection and electromagnetic interference immunity [38]. Recently, FSO connectivity has gained rising interest for commercial and military applications [70]. FSO transmits data in the form of a narrow conical beam by means of a low-power laser or light-emitting diode (LED) in the Terahertz spectrum, close to fiber [68]. Rather than enclosing the stream of data in a glass, it is transferred by fiber through the air and operates in the near infrared (IR) band. In comparison to the well known RF wireless systems, FSO is all-optical. So without the considerable expense of digging up sidewalks to install a fiber connection, one gets the speed of a fiber. This technology does not require an installation license from the government [68]. As soon as the line-of-sight (LOS) link between the laser and the receiver becomes available, it

can be readily deployed. This means that the fiber backbone has no hassles, no backlog and no intermediary devices.

FSO gets to be appealing innovation where fiber establishment and the correct of way are exceptionally costly. FSO mentions application areas like metropolitan networks, backhaul wireless systems, in-door links, inter-building communication, service acceleration, fiber backup, military purposes, security, and satellite communications, etc. Because of the low loss links and small-sized antennas, FSO is an excellent candidate for deep space probes and inter-satellite communication [68]. Each FSO transponder is expected to grow to hundreds of wavelengths (transmitter and receiver). The tens of Terabit/s range will potentially reach future developments of this technology.

As the FSO link can be easily installed within 24 hours or less, there is a growing interest in applications for military and homeland security. Connecting remote, non-permanent sites, border control and surveillance sites, difficult terrains, and battlefields with very high bandwidth links is very practical. In addition, the FSO is increasingly becoming an essential part of disaster response efforts for governments and major businesses [48]. In addition, FSO also has a growing share of the market in active systems of imaging and remote sensing. For defense and homeland security, these applications are particularly appealing. Moreover, considering the LOS's extreme difficulty, there is a recent rising interest in exploiting FSO in military and challenging terrain mobile networks [68]. Indeed the deployment of widespread wireless commercial communication systems results in governmental pressure and reductions in the bandwidth available for military use. Military applications need a higher capacity communication system because they need to share vast volumes of audio, video and data. In essence, wars and conflicts of the modern era involve a real-time transmission of immense knowledge directly from the field to the command center. Another future market for FSO information technology is naval communications [70].

## 1.2 Advantages of FSO

In the FSO system, there are a versatile networking solution that fulfills the broadband promise. Free Space Optics (FSO) also provide required combination of properties required to transport information to the backbone of optical fiber: almost limitless bandwidth, ease of deployment and power, Low-cost set-up and service, fiber optic cable bandwidth at par, light-speed reception, signal interception tolerance, and license- and regulation-free use. The licensing and the control freedom system translate into convenience, the speed and the implementation of the low cost. Since Free Space Optics (FSO) wireless optical transceivers are responsible for transmitting and receiving through windows, it is possible to install Free Space Optics (FSO) systems within

buildings, reducing the need to fight for roof space, simplifying wiring and cabling, and enabling equipment to operate in a very favorable setting. For the FSO System, the line of sight (LOS) between the two ends of the connection is the important thing. Other similar types of advantages are given below:

- **Cost:** For the FSO system in comparison to RF, FSO system have lower SWaP, making them inexpensive to deploy to storage and sustain long period. RF antenna is greater than the regular aperture diameter of the FSO receiver but it is not so small that is not possible to produce [105].
- **Bandwidth:** FSO operations are often performed within the Terahertz range, a region that is permitted and very wide. One terahertz has a frequency of one million megahertz and is equal to a standard transmission spectrum for the optics between 186 THz and 199 THz, which results in nearly 13 million frequencies usable only on the Megahertz stage [103].
- **Transmission speed:** In comparison to other communication systems, it is important to take into account the transmission speed of FSO systems. As with other optical communication systems, FSO interacts with speeds above the potential light speed limit, making them faster than traditional electronic systems. It is easier to equate FSO systems with other fiber optical transmission systems. FSO signals scatter where the " $n = 1.000273$ " refractive index is often generalized to " $n = 1$ " (a major disparity in vacuum motions and a " $n = 1.000000$ " refractive index). (FSO signals spread freely. The refractive index of the fiber is greater than that of the air. This causes the light that travels through the fiber to completely internally mirror, causing light to scatter through the core. For an upwards refractive ratio, FSO will also have an average base propagation speed than fiber-optic cables [3].
- **Easy Deployment and Redeployment:** In the FSO system, the installation process time is very low. Approximately, there are less than 4 hours to take the installation in the FSO system. From one place to another it can redeployed easily [105].

### 1.3 Applications of FSO

FSO communication link is currently in use for many services at many places. These are described below in details:

- **Storage Area Network (SAN):** A storage area network (SAN) offers access to the data storage in the block level through a high-speed network. It integrates servers like disk

arrays, RAID hardware, and tape libraries with storage devices. The server's operating system considers the SAN devices in these configurations as if they were directly connected. To form a SAN, FSO link can be used. It is a network known to provide access to centralized data storage at the block level [52].

- **Outdoor wireless access:** It can be used for communication by wireless service providers and as is required for microwave bands, no license is required to use the FSO.
- **Last-mile access:** For much of the telecommunication, cable television, and Internet sectors, the last mile has always been a bottleneck. By deploying it along with other networks in the final mile, FSO can provide a solution to this problem. It is very expensive for service providers to lay user cables in the last mile as the price of digging to lay fiber is too high that it will make sense to lay as much fiber as possible. FSO can be used by integrating it in the last mile along with other networks to solve such a problem. It is a high-speed connection. It is often used to circumvent other kinds of networks local-loop schemes. [97].
- **Enterprise connectivity:** FSO systems can be mounted quickly. This role makes it applicable to connect two buildings or other assets to interconnect LAN segments. So, without the cost of dedicated fiber optic links, FSO systems will cross several buildings in the corporative and campus networks that allow ultra-high speeds.
- **Fiber backup:** In the event of a transmission failure via a fiber connection, FSO can also be used to provide a backup link [97].
- **Metro-network extensions:** In expanding the fiber rings of an existing metropolitan area, metro-network extensions may be used. Within less time and connection, the FSO device can be deployed.
- **Backhaul:** Backhaul can be helpful in transmitting high speed and high data rate mobile phone traffic from antenna towers back to the PSTN. The transmission velocity will increase. On the other hand, FSO will prove to be of high use in cellular networks in transporting high-speed cellular telecommunications traffic as well as fast data rates from antenna towers to the PSTN, thereby increasing the transmission speed [97].
- **Service acceleration:** In the meantime, service acceleration can also be used to provide consumers with instant service while their fiber infrastructure is being implemented.
- **Bridging WAN Access:** In WAN, FSO is useful in promoting high-speed data networks for smartphone users and small satellite terminals and serving as a high-speed trucking network backbone [86].

- **Point-to-point connections:** It can be used to communicate between point-to-point connections, e.g. between two houses, two vehicles, and point-to-multipoint connections for short and long-range communication e.g. from aircraft to land or satellite to ground [82].
- **Military access:** As it utilizes narrow beam width for data transmission, FSO has the benefit of being protected and undetectable. Therefore, with limited preparation and less deployment time, it can provide safe connectivity in wide areas, which makes it most appropriate for military access. It is a safe that can securely link wide areas with minimal planning and deployment time and is therefore ideal for military applications [87].

## 1.4 Drawbacks of FSO

The benefits of free space optics are easy to receive. But since air for FSO is the medium of communication and the light travels through it, certain environmental problems are inevitable. Maximum atmospheric phenomenon normally occurred in the troposphere regions [32]. In spite of the incredible potential of the FSO link, due to atmospheric turbulence, FSO links face fading issues. It also suffers from various impairments, such as severe impact of path-loss, pointing degradation of error, and needs for line-of-sight (LOS). Atmospheric weaknesses, such as atmospheric turbulence and limiting conditions of visibility (snow, fog, and dust)(see Figure 1.2), often weaken the reliability of FSO links and can contribute to performance deterioration (outage likelihood and probability of error) [25]. Several methods have been proposed to reduce these impacts. These have approaches for physical and higher layers. On the physical layer, adoptable strategies have been shown to be forward error correction (FEC), dynamic thresholding, and time-delayed diversity (TDD) [102].

The figure (1.2) placed above, illustrates the parameters of FSO demerits such as Rain and Dust. Instead, there are many more factors that affect FSO during its transmission, such as scintillation, low clouds, fog, atmospheric and window attenuation, and obstructions [10]. This is very visible in the figure that how those obstacles could stand in the way of FSO transmission, for example, if we look at the Rain, they stand as a straight obstruction to FSO transmission.

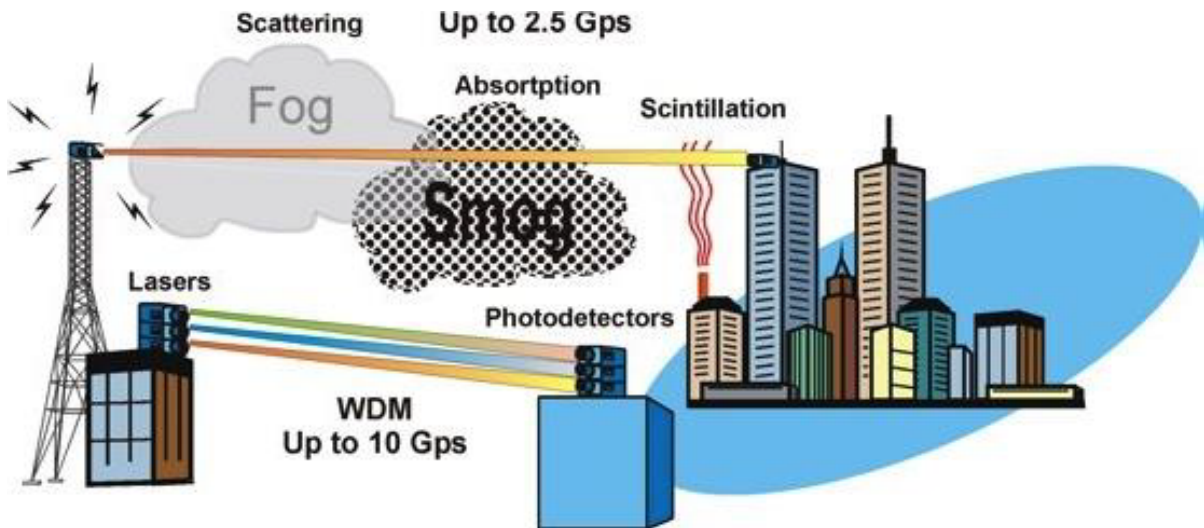


**Figure 1.2:** Atmospheric effects on a FSO system [14]

A few limitations of FSO are explained as follows:

- **Physical obstacle:** A single beam can be temporarily interrupted by trees, tall buildings and flying birds, but this appears to cause only fleeting interruptions, and transmissions are restored quickly and automatically. To solve this challenge, as well as other atmospheric conditions, Light Pointe uses multi-beam systems (spatial diversity) to allow for greater availability [1].
- **Scintillation:** Heated air arising from the earth or man-made structures such as heating ducts produce differences in temperature between multiple air pockets. This can induce signal amplitude variations, contributing to "image dancing" at the end of the FSO receiver [1].
- **Geometric losses:** Because of the scattering of the beam, geometric losses that can also be considered as optical beam attenuation are induced and the signal power level reduces as it travels from the transmitted end to the receiver end [91].
- **Absorption:** The water molecules which are banned in the terrestrial atmosphere are responsible for absorption. The strength of photons is consumed by these ions. The optical beam power density is reduced and the propagation availability in an FSO device is significantly affected by absorption. Carbon dioxide may also induce signal absorption [89].
- **Scattering:** At the time of collision between the optical beam and the scatterer, scattering phenomena occur. This phenomenon is wavelength dependent phenomenon where there

is no change in optical beam energy. But there is just a directional transfer of optical energy, which corresponds to a drop in beam strength over longer wavelengths. Three kinds of atmospheric attenuation are split into [103].

- **Atmospheric attenuation:** Atmospheric attenuation is usually the natural consequence of fog and haze. Dust and rain are also based on it. Atmospheric attenuation is expected to be wavelength dependent, but this is not accurate. Haze is dependent upon wavelength. Attenuation in haze weather conditions at 1550 nm is smaller than other wavelengths [32].

# **Chapter 2**

## **Background and Literature Review**

With the update stages of communication, the necessary of high bandwidth is growing day by day. FSO communication can support the need of high data rate communication which can replace the radio frequency (RF) communication in several scenarios. RF can have data speeds of up to several Mbps, but spectrum congestion, intrusion and license-related problems are limited. RF can provide data rates of up to the several Mbps, but spectrum congestion, intrusion and license-related problems are limited. FSO is indeed a cost-effective and high-bandwidth connectivity strategy that has been gradually taken into account in recent advertisements of the program [60].

Due to the presence of turbulence in the propagating medium, there can exist many different models recommended to quantify the losses. As for example Gamma-Gamma [72], Log-normal[30], Weibull [23], K-distribution [83], and Negative Exponential [73], Nakagami, and so on. Not only do these models have different probability distribution function, but because of this, they are often used in various forms of turbulence conditions (such as weak, strong, or moderate) and their efficiency differs under different conditions as well. Lately a model, the distribution of Málaga ( $\mathcal{M}$ ), was recently proposed in [51] to model the fluctuation of irradiance of an unbounded optical wavefront propagating through a turbulent medium under all irradiance conditions in homogeneous isotropic turbulence [50]. The Málaga ( $\mathcal{M}$ ) atmospheric turbulence channel is acceptable in any turbulence scheme. By combining in a closed-form expression, the link performance of most of the irradiance statistical models are proposed in the literature. The transmitted signal can be affected by other effects as for example, scintillation effect, irradiance, misalignment between the transmitter and the receiver (pointing error) besides the atmospheric turbulence channel. These influences affect the output of the transmitted signal.

So, till now literature researchers have investigated a lots work to analize the performance of a FSO link by using Málaga ( $\mathcal{M}$ ) turbulence channels with and without pointing errors under heterodyne detection as well as IM/DD techniques. Here some of the work is shown in [15], as

performance analysis of Free-Space Optical Links over Málaga ( $\mathcal{M}$ ) turbulence channels with pointing errors. Where in [50] analyzing the impact of pointing errors on the performance of generalized atmospheric optical channels has done. Where Performance analysis of FSO Links in turbulent atmosphere showing in [18]. By using imprecise Málaga ( $\mathcal{M}$ ) [44] they investigate the performance analysis of FSO communication system first time in the literature. In [71] showing ABER analysis FSO system employing subcarrier intensity modulation (SIM) with binary phase-shift keying (BPSK). Performance analysis of (FSO) links for Outage Capacity Optimization with Pointing Errors doing in [33]. And in [99] they are considering atmospheric fading and investigate statistical model with nonzero boresight pointing error to see the performance of (FSO) communication systems. The issue of estimating jitter and mechanical boresight output in the presence of atmospheric turbulence analyze in [21]. Under Strong atmospheric turbulence condition effects of Pointing error of FSO link showing in [22]. Where in [13] analyzing ergodic capacity of FSP link with nonzero boresight Pointing error. In [84] investigating BER performance of FSO system over strong atmospheric turbulence channels with Pointing errors. Relay-aided FSO system performances over  $M$  distribution with pointing errors in presence of various weather conditions showing in [94], Where in [20] nonzero boresight pointing error impact on ergodic capacity of MIMO communication systems investigated.

We can use many existing coherent and non-coherent optical modulation schemes in the FSO communication system. Till now in literature, many researchers already analyzing the performance of the FSO system by using a different modulation scheme. Here in [62] showing Over weak to strong atmospheric turbulence channels Performance analysis of FSO communication system using different modulation schemes. Where in [78] they reviewing FSO msystem Using different modulation techniques. Under atmospheric turbulence conditions Performance analysis of FSO links based on various modulation techniques investigate in [63, 74]. BER Performance comparison of FSO communication system under various modulation techniques in the Presence of atmospheric turbulence are showing in [26, 41, 85, 104] this papers. In [58] doing BER analysis under Lognormal and Gamma-Gamma turbulence channel for different modulation techniques for FSO System. For free space optical communication performance investigation of MPM-QPSK modulation signal establish in [93]. By using subcarrier intensity modulation rectangular QAM in [9] they are doing Performance analysis over Málaga ( $\mathcal{M}$ ) turbulence channels with integer and non-integer  $\beta$ .

From the above literature review we can conclude that till now many researcher have worked with the performance analysis of FSO system. There exist works with Different modulation scheme, different atmospheric channels for the performance of BER. Some works have been done considering only the zero-boresight pointing error or non-zero boresight pointing error. Also some of them have worked with different propagation link distance or different beam width.

Further, we have seen that for different weather condition some have considered weak turbulence and some have considered strong turbulence. So, after completing the review to the best of our knowledge, we have found that there was no research work in literature which consider the BER performance analysis of the FSO system using the Málaga ( $\mathcal{M}$ ) atmospheric turbulence channel with the presence of both zero and non-zero boresight pointing errors in terms of different modulation schemes where different pointing error, different beam width,different propagation link distance and different weather condition (for both strong and weak turbulence) were varied in a single paper.

## 2.1 Contribution of This Thesis

We have provided the closed-form mathematical expressions for average bit error rate (ABER) performance of an IM/DD system over the Málaga ( $\mathcal{M}$ ) atmospheric turbulence channel. The included expressions of PDF are involved with the Meijer's G-function which can be calculated easily and precisely by using MATLAB. Using Monte Carlo simulations we have validated the mathematical analyzes.

We have worked with the performance of FSO system by evaluating the average bit error rate (ABER). In this thesis, different modulation schemes including BPSK,QPSK,DPSK, NRZ-OOK,NRZ-OOK,M-QAM,M-PPM,M-PAM are shown in the presence of zero and non-zero boresight pointing error over Malaga turbulence channel to analyses the performance of average bit error rate (ABER).

Also, we have presented the closed form expression for all of the modulation format that we have used in this thesis and added the results that we got from the simulation through MATLAB. The main objective of our thesis paper is to figure out the best modulation scheme among the provided modulation schemes for the FSO systems in terms of malaga atmospheric turbulence for different pointing error, different propagation link distance, different weather condition and different beam width.

## 2.2 Research Methodology

This section will provide the methodology that we have followed while doing this research work for our thesis.The software named *MATLAB R2019a* has been used as our simulation software throughout the session of thesis.moreover, *MATLAB* is a software which is especially used in the sector of signal processing , simulation , modelling, design, numerical data analysis and visualization of computer graphics. It has been highly recognized as an efficient platform over the last few years and thus the use of *MATLAB* has increased massively in research practices and also in educational institutions.The methodology's primary feature involves with the process

of our Simulation. The main aim behind the simulation was to analysis the impact of zero and non-zero boresight pointing error on ABER over the Málaga ( $\mathcal{M}$ ) atmospheric turbulence channel for four different condition using different modulation scheme such as for different values of boresight displacement, for different distances, for various weather conditions and for different beam widths. First of all the pdf of Málaga ( $\mathcal{M}$ ) atmospheric turbulence channel was build as a function in *MATLAB* for finding the further simulation output. Then for the four different conditions four code has been written to simulate the result in terms of different modulation scheme.

## 2.3 Thesis Structure

The thesis paper is structured according to the following pattern. First of all,in chapter 1 it begins with the introduction. The Background and literatur review is considered in Chapter 2. Then Next in Chapter 3, Free-Space optical communication is discussed broadly. Chapter 4 focuses on the Málaga ( $\mathcal{M}$ ) atmospheric turbulence channel in details for this thesis . Following this Chapter 5 represents the modulation technique and bit error rate analysis. In Chapter 6, the simulation output for different conditions has been provided . Finally, with a description of future work, challenges and overall conclusion in Chapter 7, this thesis is eventually concluded.

# **Chapter 3**

## **Free-Space Optical Communication**

### **3.1 Introduction**

In this chapter, we have mainly discussed about Free-Space Optical Communication. At first, we present a simple description of FSO. Then given the theory related to atmospheric turbulence statistical fading models. Also described some of the atmospheric turbulence model. In this thesis we have mainly used the Málaga ( $\mathcal{M}$ ) atmospheric turbulence. So, there is another chapter regarding Málaga ( $\mathcal{M}$ ) where we have described about this model in details.

### **3.2 Fundamental of Free Space Optical Communication**

Free - space optical communication is the transmission, utilizing optical radiation as the carrier channel through the atmosphere, of signals/data or information between the transmitter and the receiver. The data packet could be modulated by the optical carrier's intensity/phase or frequency. For FSO communication to actually occur, a line of sight (LOS) without any interference is important between the transmitter and the receiver [95]. Compared with traditional RF communication, FSO has enormous benefits. Particularly in comparison to radio frequency (RF), FSO link makes high data rate, very high optical bandwidth. FSO does not need drilling for the fiber to be laid as well as there is no need of permission from the landowners. Implementation can be done more quickly. Compared with fibre optic networking, the cost is smaller. The modules of the FSO are portable, small and can be replaced simply. It is difficult to intercept and detect the laser pulse, which allows FSO better compared to current RF and microwave communication for security purposes.

There are many FSO implementations such as temporary network access, campus LAN to LAN

communications, military secure communications, connectivity solution in the region where the fiber optic cables are less likely to be laid, etc [60] [43]. FSO can be utilized for satellite communication, i.e. also for inter-satellite communication and communication between earth station to the Low Earth Orbit (LEO) . Be that as it may with so numerous advantages of FSO there is a significant drawback of the environment such as absorption, scintillation and scattering which have been already described in chapter 1 section 1.4.

### **3.2.1 Basic Block Diagram of FSO**

FSO communication uses laser beam for transmitting the very high bandwidth digital information from one location to another across the atmosphere. This can be accomplished by using a small laser beam modulated from a transmitting station to a transmission station. It is distributed through the atmosphere and received at the receiver station afterwards. The basic block diagram of FSO system is shown in 3.1. In FSO, the transmitter, FSO communication channel or atmospheric channel and receiver are the three main functional elements. The elements of the FSO communication system's block diagram are discussed as follows:

#### **1. Transmitter :**

The transmitter converts the electrical signal into an optical signal and modifies the laser beam to transmit data across the atmospheric channel to the receiver. The original data can be modulated by different modulation techniques in the transmitter section. We have considered BPSK, OOK, QPSK, DPSK, PPM, PAM and QAM as strategies for modulation in this thesis. The transmitter is made up of four elements, as seen in figure 3.1: laser modulator, Laser driver, optical source (LED or Laser) and transmit telescope.

#### **I Modulator**

In Laser modulation the data were carried by the laser beam. Two common methods can be used to apply the modulation method and they are internal modulation and external modulation [60].

**Internal Modulation :** It is a mechanism that takes place within the laser resonator which relies on the modification induced by the additive components and according to the information signal, adjusts the intensity of the laser beam.

**External Modulation :** The external modulation is a process which take place outside the laser resonator. It relies on both the refractive dualism phenomenon and the polarization phenomena.

## II Laser Driver

The transmitter's laser driver circuit converts an electrical signal into an optical signal by altering the flow of current that goes via the light source.

## III Optical Source (LED or Laser)

The optical source which can be a laser diode or light emitting diode, transforms the electric signal into an optical signal.

Due to the emission of relatively narrow bandwidth of any visible light at various colored wavelengths, invisible infra-red light for remote controls or laser style light while a forward current is passing through them, light emitting diodes (LED) are commonly used today.

A laser diode is a type of semiconductor device that generates optical radiation from atoms or molecules in a lasing medium by the process of stimulated emission. Also a laser diode emits light that is very directional and extremely monochromatic. This implies that the output of the LD has a small output beam angle divergence and a narrow spectral width. With a fixed phase interaction between points on the electromagnetic wave, LDs emit light waves. These aspects may be used to choose a suitable source for a specific application. To understand the source performance descriptions for a particular application, it is important to understand these detector aspects. The aspects that influence the use of a particular light source are as follows [96]:

- Price and availability of elements.
- Transmit Power
- Lifetime
- Eye Safety
- Capabilities of Modulation

## IV Transmit Telescope

The transmitter telescope of the channel collects, collimates and directs the optical radiation towards the other end of the receiver telescope.

### 2. Atmospheric Channel :

The propagation medium is the atmosphere for FSO links. It is possible to view the atmosphere as a collection of concentric gas clouds around the planet. In the homosphere [69], the troposphere, stratosphere and mesosphere, three principal atmospheric layers

are described. With regard to height, these layers are distinguished by their temperature gradient. We are mainly interested in the troposphere layer , in FSO communication . As troposphere is where most weather events exist and FSO connections work at the bottom of this layer [69].

The atmosphere contains mainly of nitrogen (  $N_2$ , 78 percent), oxygen ( $O_2$ , 21 percent) and argon ( $Ar$ , 1 percent), but there are also a variety of other elements found in smaller concentrations, such as water ( $H_2O$ , 0 to 7 percent) and carbon dioxide ( $CO_2$ , 0.01 to 0.1 percent). Small particles are also detected. This involve particles (aerosols) including haze, soil, dust and fog that contribute to the composition of the atmosphere [79].

Because of the communication atmosphere, the propagation properties of FSO through the atmosphere change drastically, particularly, the impact of weather conditions is substantial. Atmospheric barriers, such as rain, cloud, haze and turbulence in the channel of propagation, fluctuate and attenuate the received signal power. Atmospheric attenuation occurs from the laser beam's interaction with air molecules and aerosols during the propagation. Absorption, scattering, and scintillation are the primary effects on optical wireless communication [16] (They have been described in the limitation of FSO in 1.4).

### **3. Receiver :**

The receiver part of the FSO block diagram consist of mainly five parts, as shown in figure 3.1: telescope receiver telescope , optical filter, Photo-detector, amplifier and demodulator.

#### **I Receiver Telescope**

The receiver telescope of receiver part of the block diagram captures the incoming optical radiation and directs it on the photo-detector. It should be remembered that since it absorbs multiple uncorrelated radiation and focuses its average on the photo detector, a wide receiver telescope aperture is preferable [101].

#### **II Optical Filter**

By installing optical filters, which mainly allow energy, at the wavelength of interest that influences the detector and reject unwanted wavelength energy, the nature of solar illumination is necessary to greatly decrease [79].

#### **III Photo Detector**

A semiconductor device that transforms the photon energy of light into an electrical signal by releasing and accelerating current conducting carriers inside the semiconductors is also known as the photodiode (PD) detector. Depending on photoconductivity rules, photodiodes work, which is an increase in the conductivity of

p-n semiconductor junctions due to electromagnetic radiation absorption. Generally, diodes are capacitive charged and reverse-biased [65]. The pin photodiode and the avalanche photodiode (APD) are the two most frequently used photodiodes because they have strong quantum efficiency and are constructed from semiconductors that are readily available commercially [42].

#### Features of detector:

The characteristics of output show how a detector responds to an input of light energy signal. They may be used by a specific program to pick an appropriate detector. To know the output descriptions of the detector and to be able to select a detector for a basic use, one should consider certain features of the detector. The following properties are the desired properties of detector:

- At the wavelength to be detected, a high response is needed.
- The detector introduced a small value for the additional noise.
- Sufficient response time.

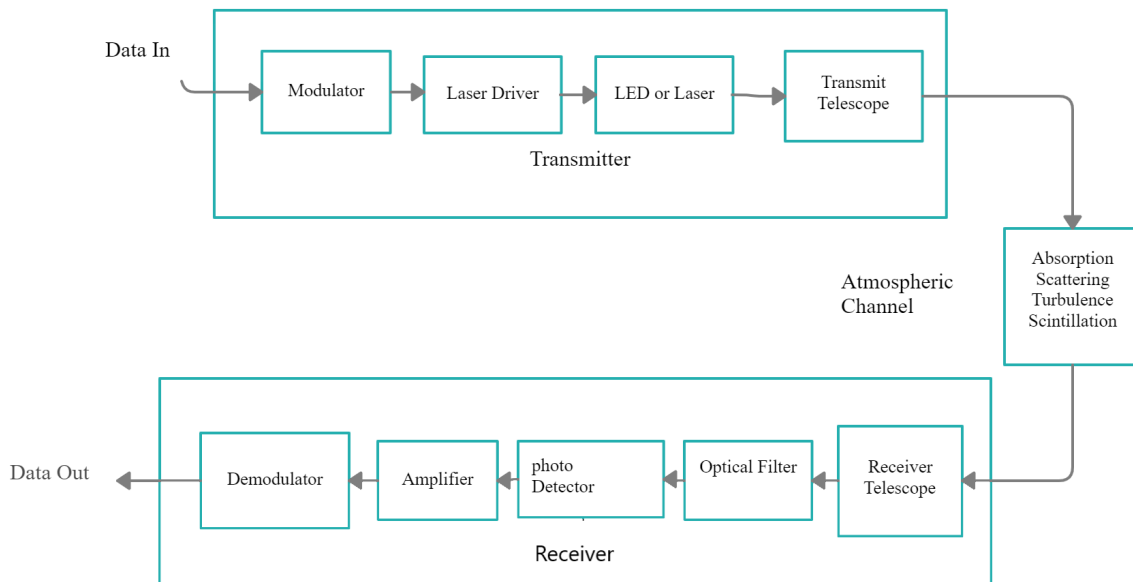


**Figure 3.1:** Block Diagram of a terrestrial FSO

### 3.3 Classification of FSO Systems Based on Detection Techniques

Depending upon on detection method, FSO systems can be divided into two main categories [36]:

- Non-coherent Optical receiver
- Coherent Optical receiver

#### **Non-coherent Optical receiver:**

In non-coherent optical receiver scheme, the receiver directly detects the instantaneous power of the collected optical field. So, they are also known as direct or power detection receivers. Such receivers represent the simplest type of implementation which might be used if the information transmitted occurs in the optical field's power variance (i.e. IM). Throughout that method, no local oscillator (LO) is used. Mainly because of its simplicity and low cost, it is used in FSO connections. The IM/DD technique is seen in figure 3.2.

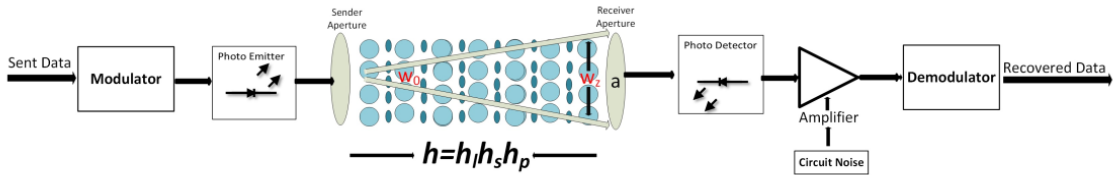


**Figure 3.2:** Block diagram of a non-coherent or direct detection optical receiver.

#### **Coherent Optical receiver:**

From the figure 3.3 it is shown that the incoming optical signal is mixed with a locally produced light wave signal. In terms of reducing higher receiver sensitivity, turbulence-induced fading and background noise rejection, it provides improved performance than IM/DD at the expense of difficulty in the implementation of coherent receivers. It is also further classified into two types : I) heterodyne and ii) homodyne. The only variation between them is the local oscillator's frequency and phase. Such optical receivers are used when data is modulated using AM, FM, or PM on the optical carrier, and are important for FM or PM detection.

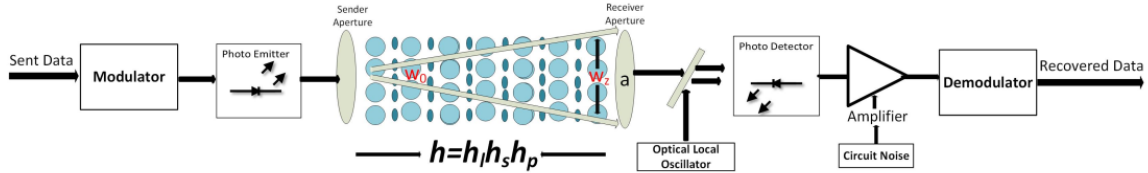


**Figure 3.3:** Block diagram of a coherent detection optical receiver.

Numerous noise sources present at the receiver effects the detection of optical fields. In FSO communications, the three primary sources are: induced noise photo detector, background ambient light, and electronic thermal noise in circuits. While the use of optical filters may minimize the background radiation, it also creates substantial interference in the process of detection.

### 3.4 Atmospheric Turbulence Statistical Fading Models

The biggest impediment to communication among the transmitter and the receiver of the FSO communication system is atmospheric turbulence. Mainly as a result of turbulence, both the phase of the received light signal and the intensity fluctuate randomly, and thereby the efficiency of the model is intensively influenced [55]. It is possible to view uniformities caused by turbulence as discrete cells or eddies of various temperatures, behaving like refractive prisms of various sizes and refractive indices. The relationship between the turbulent medium and the laser beam results in random amplitude variations(scintillation) and random phases of the information-bearing optical beam that eventually lead to FSO links performance degradation. Due to the fluctuations of the refractive index of the air, atmospheric turbulence is actuated. In a sunny day, attributed to solar radiance, the air above the earth's surface region gets warmer than the air at a higher altitude. Such a surface of warm air becomes even less dense and then rises from the earth to interact with the colder air encompassing it and the air temperature fluctuates spontaneously because of that. Severe combinations of the refractive index  $n$  of the atmosphere occur in the optical ray transmission path generated by atmospheric turbulence. The direct end product of spontaneous fluctuations in atmospheric temperature from point to point is this refractive index fluctuation [75]. This refractive index fluctuation is coming about from the irregular changes in atmospheric temperature that is a function of the elevation, atmospheric air pressure and time of the day and even the speed of wind movement. These feeble lens-like eddies, graphically seen in Figure 3.4 tends to result in a randomized impact of interaction between various regions of the propagating pulse, allowing the mechanism to distort the wavefront.

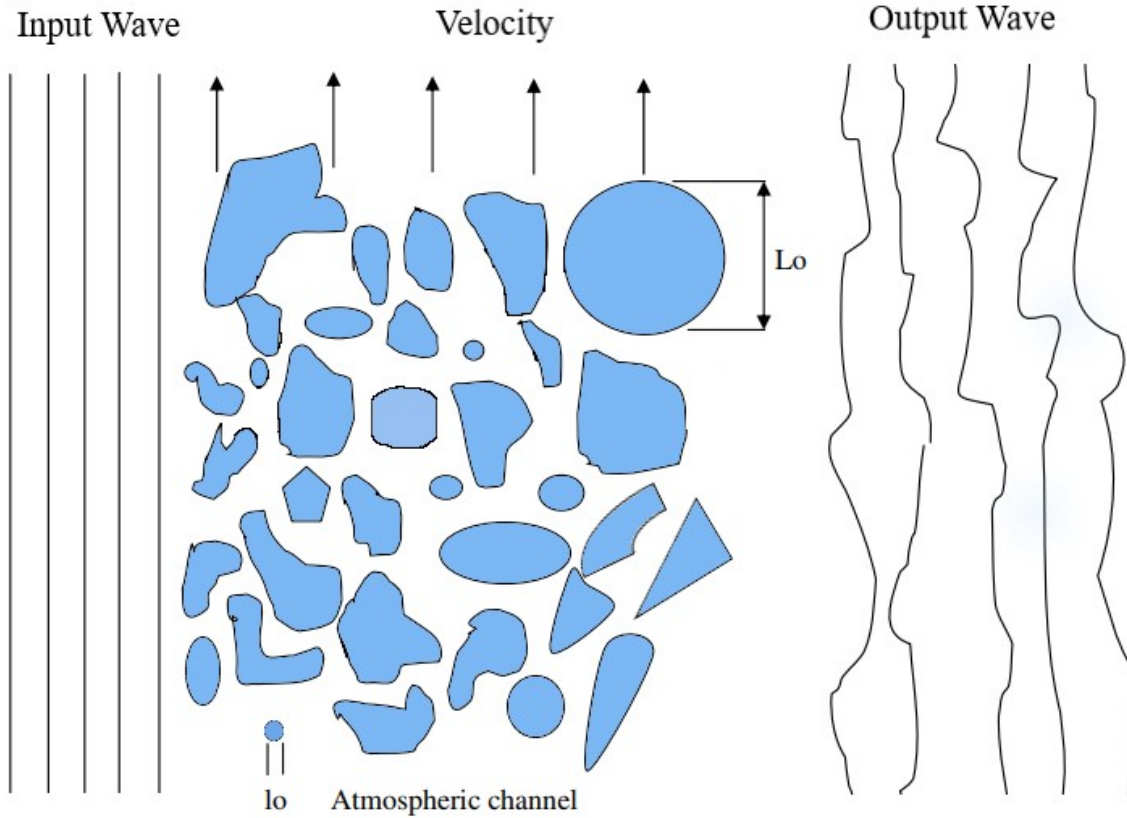


**Figure 3.4:** Atmospheric Channels with turbulent eddies

The smallest of the turbulence eddies are defined as the inner size  $l_0$ , while the biggest of the turbulence eddies are defined as the turbulence outer size  $L_0$ . Typically,  $l_0$  is just a few millimeters in order, whereas  $L_0$  is usually a few millimeters in order [67] [60]. The interaction between the temperature of the atmosphere and its refractive index is established by [60] which is given below:

$$\eta = 1 + 77.6 \left( 1 + 7.52 \times 10^{-3} \lambda^{-2} \right) \frac{P}{T_e} \times 10^{-6} \quad (3.1)$$

Where  $P$  is the atmospheric pressure in millibars,  $\lambda$  in microns is the wavelength and  $T_e$  in Kelvin is the temperature.

Due to the presence of turbulence in the propagating medium, there can exist many different models recommended to quantify the losses. As for example Gamma-Gamma, Log-normal, Nakagami, Weibull, K-distribution, and Negative Exponential and so on. Not only do these models have different probability distribution function, but because of this, they are often used in

various forms of turbulence conditions (such as weak, strong, or moderate) and their efficiency differs under different conditions as well. The concept of the lognormal model is limited to weak turbulences [30] whereas the negative exponential distribution [73] and the K-distribution [83] are for strong turbulence. And the turbulence effects from moderate to strong levels can be characterized by gamma-gamma distribution[5] and double Weibull distribution[23]. Andrews [72] proposed Gamma-Gamma PDF as a reasonable alternative to Beckmann's PDF due to its much more tractable mathematical model [51]. Lately a model, the distribution of Málaga ( $\mathcal{M}$ ), was proposed in [51] to model the fluctuation of irradiance of an unbounded optical wavefront propagating through a turbulent medium under all irradiance conditions in homogeneous, isotropic turbulence [50] . This M distribution unifies, in a closed-form expression, most of the proposed mathematical models extracted so far in the bibliography, providing an excellent alignment with reported simulation results over a wide range of (weak to strong) turbulence conditions [51]. It follows the experimental results accurately and unifies a variety of previously existing mathematical models for atmospheric turbulence effects, such as distributions of gamma-gamma, lognormal, exponential, and K.

Some of the models are described below.

- Lognormal(LN) Turbulence
- Gamma-Gamma(CC) Turbulence
- Rician-Lognormal (RLN) Turbulence

Málaga ( $\mathcal{M}$ ) atmospheric turbulence (It is a generalized distribution which used widely in designing a statistical model and vastly described in chapter 4).

### 3.4.1 Lognormal(LN) Turbulence Scenario

A continuous distribution in which in the logarithm of a variable there is a normal distribution. The normal distribution of the log results when the variable is the function of a large number of independent, identical-distributed variables in the same way as the normal distribution results when the variable is the sum of a large number of independent, identical-distributed variables. The log-normal distribution model takes account for the weak regime of the log intensity I of the optical beam traverse [90]. The probability density function (PDF) of the log-normal model is given below [100]:

$$f_I(I) = \frac{1}{I\sigma\sqrt{2\pi}} \exp\left(-\frac{(\ln(I) + \sigma^2/2)^2}{2\sigma^2}\right) \quad (3.2)$$

where  $\sigma$  is the standard deviation of the log-normal distribution, which depends on the channel's characteristic.

### 3.4.2 Gamma-Gamma(CC) Turbulence Scenario

The distribution of Gamma-gamma shows excellent compatibility with all turbulence ranges if there are no spatial diversity techniques applied to it. The gamma-gamma turbulence model is based on such a modulation mechanism, which implies that the small-scale and large-scale effects are responsible for the changes in the direction of the turbulent atmosphere moving radiated light signal [41]. If spatial diversity techniques have no association between sub-channels, the gamma-gamma distribution shows substantial effects, and it can be easily adjusted in such scenarios. The independent gamma-gamma random variables are modelled within the gamma-gamma distribution. The other instance of this technique has been seen in the simulation of independent gamma-gamma variables using alpha- $\mu$  distribution (generalized gamma). The other instance of this technique has been seen in the simulation of independent gamma-gamma variables using alpha- $\mu$  distribution (generalized gamma). Even so the fading connection between sub-channels is unavoidable in realistic circumstances. The model of Gamma-gamma scintillation based on the Doubly Stochastic theory is commonly used. As we know, the Gamma-gamma model has a weak to high turbulence state, so its strength I PDF (Probability Density Function) is the product of two gamma random variables representing small and large turbulence fluctuations [54]. Therefore the irradiance obtained is shown to be the product of two statistically independent random processes I-X and I-Y below [37]:

$$I = I_X I_Y \quad (3.3)$$

$I_X$  and  $I_Y$  arise from the large scale and the small-scale turbulence eddies respectively. Assume that both the large scale and small-scale effects are controlled by the gamma distribution. The gamma-gamma model for the probability density function (pdf) of obtained irradiance fluctuation is given below:

$$p(I) = \frac{2(\alpha\beta)^{(\alpha+\beta)/2}}{\Gamma(\alpha)\Gamma(\beta)} I^{\left(\frac{\alpha+\beta}{2}\right)-1} K_{\alpha-\beta}(2\sqrt{\alpha\beta I}) \quad (3.4)$$

Where,  $I$  is the irradiance

$\Gamma(\cdot)$  is gamma function

$K(\alpha, \beta)$  is a Bessel function of second order

### 3.4.3 Rician-Lognormal (RLN) Turbulence Scenario

Inherently, FSO communication has a line-of-sight (LOS) connection; thus, an effective channel model is a Rician model with shadowing. The optical wave amplitude PDF at the receiver can be defined as  $p_Z(Z) = \int_0^\infty p(Z|S) p_S(S) dS$ , where  $p(Z|S)$  represents the Rician PDF centered on a shadowing  $S$  that is assumed to be distributed lognormally. It can be shown mathematically that  $Z = RS$ , where the Rician and lognormal random variables (RVs) are, respectively,  $R$  and  $S$ .  $R = |U_C + U_G|$  and  $S = \exp(\alpha\chi)$ , where  $U_C$  is a true deterministic quantity representing the part of LOS,  $U_G$  is a circular Gaussian RV complex with zero mean, and  $\alpha\chi$  is a real Gaussian RV. The optical irradiance is given by  $I = Z^2$  or  $I = |U_C + U_G|^2 \exp(2\chi)$ , where  $\exp(2\chi)$  is another lognormal RV, and  $|U_C + U_G|^2$  is a non-central chi-square RV with two degrees of freedom. The resulting PDF of the irradiance  $I$  is known to be lognormal-Rician [98]:

$$f_I(I) = \int_0^\infty dz \frac{1+r}{z} \exp\left(-r - \frac{(1+r)I}{z}\right) I_0\left(2\sqrt{I} \sqrt{\frac{r(r+1)}{z}}\right) \times \frac{1}{\sqrt{2\pi} \sigma_z z} \exp\left[-\frac{1}{2} \left(\frac{\ln z + \frac{1}{2}\sigma_z^2}{\sigma_z}\right)^2\right] \quad (3.5)$$

where,

$r = |U_c|^2 / E[|U_c|^2]$  is the coherence parameter and  $E[.]$  denotes the expectation operation

# Chapter 4

## System and Channel Models

### 4.1 Introduction

In this chapter we have firstly describe the system model in section 4.2. Then in section 4.3 discussing details about the Málaga ( $\mathcal{M}$ ) atmospheric turbulence model and its probability distribution function. In section 4.4 described the pointing error model both zero boresight and non-zero boresight model. In section 4.5 discussing about different atmospheric effects of FSO communication. Finally in last section 4.6 describing channel statical model.

### 4.2 System Model

In FSO communication system, a source produces information waveforms and then this information superposed onto an optical signal by modulation process. The resultant optical signal or laser beams propagate through air along a horizontal path through a Málaga ( $\mathcal{M}$ ) turbulence channel in the presence of pointing error. Then the received optical signal is converted into an electrical signal through intensity-modulation/direct detection (IM/DD) at the photodetector.

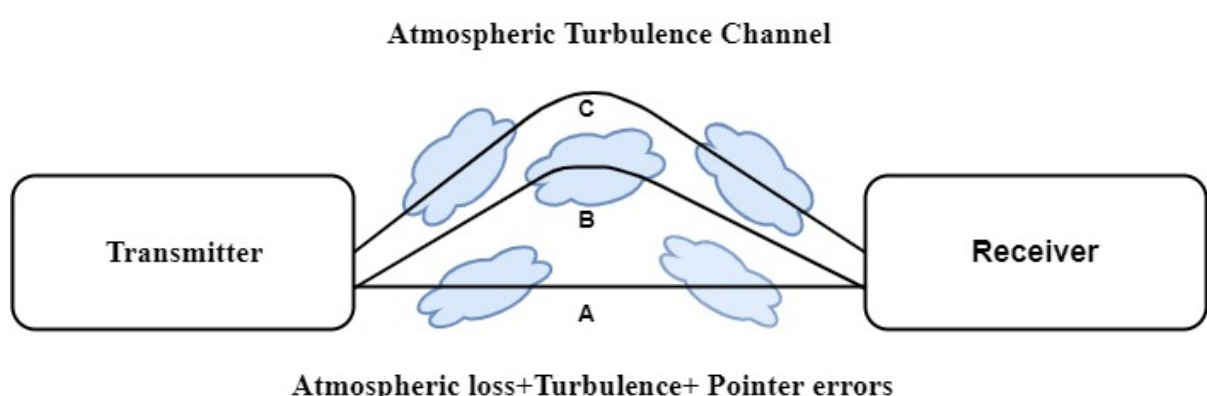


**Figure 4.1:** Practical propagation of laser beams in Málaga ( $\mathcal{M}$ ) atmospheric turbulence

Due to atmospheric turbulence and misalignment, this received signal intensity become fluctuated as well as additive noise. At the receiver end, the receiver processes the detected electrical signal to recover the original transmitted information from which we can obtain the bit error rate (BER). Now The received signal suffered from atmospheric turbulence  $Y$  at the receiver can be expressed as,

$$Y = IRx + n \quad (4.1)$$

Where  $x$  is transmitted signal and  $R$  is optoelectronic conversion factor. Whereas  $n$  is the Additive white Gaussian noise (AWGN) with zero mean and variance  $\sigma_s^2$ .  $I$  is the normalized channel fading coefficient representing the effect of the intensity fluctuations on the transmitted signal due to the combined actions of scintillation and misalignment, in the way explained in [105]. The atmospheric turbulence and the pointing error are independent. The channel gain can be expressed as

$$I = I_1 I_a I_p \quad (4.2)$$

where  $I_1$  is the path loss that is a constant in a given weather condition and propagation distance,  $I_a$  is a random variable that denotes the atmospheric turbulence loss factor and  $I_p$  is another random variable that represents the pointing error loss factor. This three factor are explained in detail next Sections.

### 4.3 Málaga ( $\mathcal{M}$ ) Atmospheric Turbulence Model

We know that FSO links can fade because of atmosphere turbulent. Even in clear sky conditions, FSO link can experience fading due to atmospheric turbulent, and in that situation, inhomogeneities in the temperature and because of atmospheric pressure refractive index can be changes along the transmission path. So on because of change in refractive index that cause power losses at the receiver or can fluctuations in both the intensity and the phase of an optical wave propagating through the medium. Causes of rapid fluctuations and turbulence-induced fading in the transmitted signal known as scintillation, these fluctuations can increase FSO link error probability also. In order to evaluate the performance of FSO system, an accurate mathematical model to describe the optical channel characteristics with respect to the atmospheric turbulence is required [67]. Numerous irradiance PDF or channel models have been proposed over the past decades to model the randomly fading FSO signal due to the atmospheric turbulence. Details of different atmospheric turbulence statistical fading models is already describe in section 3.4.

Here we use a well-known Málaga ( $\mathcal{M}$ ) turbulence model with general properties that is used for modeling transmission under the influence of atmospheric turbulence. A generalized statistical model, the Málaga ( $\mathcal{M}$ ) distribution, Which is proposed by Jurado-Navas in [51] to model the irradiance fluctuation of an unbounded optical wavefront (plane or spherical waves) propagating through a turbulent medium under all irradiance conditions and under the homogeneous isotropic turbulence [51]. This  $\mathcal{M}$  distribution unifies most of the proposed statistical models derived until now in the Literature in a closed-form expression providing an excellent agreement with published simulation data over a wide range of weak turbulence to strong turbulence conditions [4]. In all cases tested, the Málaga ( $\mathcal{M}$ ) distribution model accurately matches to the experimental data and simulation results and unifies a number of previously existing statistical models for atmospheric turbulence effects such as lognormal, K distributions, gamma-gamma, negative exponential distributions. Many researchers said that for improvement of performance of FSO links Málaga ( $\mathcal{M}$ ) distribution is very useful for communication system designing. This distribution of Málaga ( $\mathcal{M}$ ) is based on a physical model of the scattering processes that is seen as an extension of the previous work generated by Churnside and Clifford [27]. The key advantage of the Málaga ( $\mathcal{M}$ ) distribution associated with the proposed physical model is that it can decreases from every turbulence regime to a simple closed-form analytical formula. Now are define atmospheric turbulence channel.

Let's consider an electromagnetic wave is propagating with a random refractive index via a turbulent atmosphere. Since this wave moves through this medium, portion of the energy is scattered and the structure of the distribution of irradiance probability is determined by the form of scattering included. Now The Málaga ( $\mathcal{M}$ ) turbulence model is based on a physical model that involves line-of-sight (LOS) contribution,  $U_L$  the second one is the component which is quasi-forward scattered by the eddies on the propagation axis,  $U_S^C$  and coupled to the LOS contribution; whereas the third term,  $U_S^G$  is because of energy which is scattered to the receiver by off-axis eddies, the latter contribution is statistically independent compare to the previous two alternative terms[15]. The inclusion of this coupled to the LOS scatter portion is the key concept of the model and can be explained by the high divergency and narrow beam width of the laser beams in atmospheric optical communication [51]. We can see the model below in figure 4.2.

Mathematically we can write the total observed field:

$$U = \left( U_L + U_S^C + U_S^G \right) \exp(\chi + jS) \quad (4.3)$$

Where  $\chi$  and  $S$  being real random variables representing the log-amplitude and phase fluc-

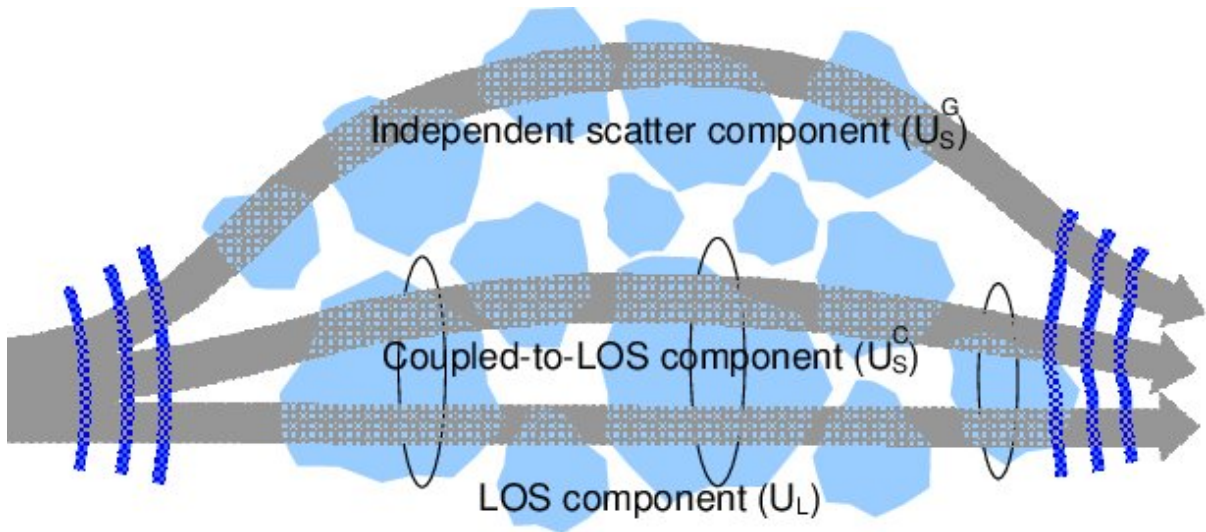


**Figure 4.2:** Laser beam propagation scheme under a Málaga ( $\mathcal{M}$ ) distributed FSO link.[51]

tuations of the optical field induced by the atmospheric turbulence,  $U_L = \sqrt{G} \sqrt{\Omega} \exp(j\phi_A)$ ,  $U_S^C = \sqrt{\rho} \sqrt{G} \sqrt{2b_0} \exp(j\phi_B)$ ,  $U_S^G = \sqrt{(1-\rho)} U'_S$ , being  $U_S^C$  and  $U_S^G$  statistically independent stationary random processes and  $U_L$  and  $U_S^G$  are also independent random processes.  $G$  is a real variable following a gamma distribution with  $E[G]=1$ . It represents the slow fluctuation of the LOS component. Following [4], this parameter  $\Omega = E[|U_L|^2]$  represents the average power of the LOS component where the average power of the total scatter components it is denoted by  $2b_0 = E[|U_S^C|^2 + |U_S^G|^2]$ .  $\phi_A$  and  $\phi_B$  are the deterministic phases of the LOS and the coupled-to-LOS scatter components. Parameter  $0 \leq \rho \leq 1$  denotes the factor expressing the amount of scattering power coupled to the LOS component and it depends on spread path distance  $Z$ , turbulence strength, optical wavelength, diameter, beam divergence due to atmospheric-induced beam spread, and distance between different spread pathways LOS component and scattering components, because if the spacing between such paths is greater than the fading correlation length, then turbulence-induced fading is not associated. While  $U'_S$  denotes a circular Gaussian complex variable and  $G$  denotes gamma random process with a unit mean value.

As an advance, this proposed model, with the presence of a random nature in the LOS component in addition to a new scattering contribution coupled to the LOS component, Offers a highly positive mathematical conditioning due to its found irradiance pdf can be expressed in a closed-form expression. Moreover, it has a high level of generality due to it includes as special cases most of the distribution models proposed in the bibliography until now[51]. A plausible justification for the coupled-to-LOS scattering component,  $U_S^C$ , is shown in [56]. Now it is said that the multipath delays of the scattered radiation received by a diffraction-limited receiver would typically be small compared to the signal bandwidth if the turbulent medium is so thin that multiple scattering can be neglected. Then the scattered field will mix coherently with the unscattered field and there'll be no-interfering signal element of the field, during a similar means as  $U_S^C$  combines with  $U_L$  in our proposed model. The unscattered portion of the field can be

ignored when the turbulent medium becomes too dense.[49]

### 4.3.1 Málaga ( $\mathcal{M}$ ) Probability Density Function

From Equation 4.3 the irradiance is given below:

$$\begin{aligned} I &= |U_L + U_S^C + U_S^G|^2 \exp(2\chi) \\ &= \left| \sqrt{G} \sqrt{\Omega} \exp(j\phi_A) + \sqrt{\rho} \sqrt{G} \sqrt{2b_0} \exp(j\phi_B) + \sqrt{(1-\rho)} U'_S \right|^2 \exp(2\chi) \end{aligned} \quad (4.4)$$

From Equation 4.4 we can write observed irradiance of our proposed propagation model:

$$\begin{aligned} I &= |U_L + U_S^C + U_S^G|^2 \exp(2\chi) = YX \\ \begin{cases} Y \triangleq |U_L + U_S^C + U_S^G|^2 & (\text{small-scale fluctuations}) \\ X \triangleq \exp(2\chi) & (\text{large-scale fluctuations}) \end{cases} \end{aligned} \quad (4.5)$$

where the small-scale fluctuations denotes the small-scale contributions to scintillation related with turbulent cells smaller than either the first Fresnel zone or the transverse spatial coherence radius whichever is smallest.and large-scale fluctuations of the irradiance are generated by turbulent cells larger than that of any the Fresnel zone or the so-called “scattering disk”, whichever is largest [49].

From Equation 4.3 we can rewrite the lowpass-equivalent complex envelope as:

$$\begin{aligned} R(t) &= (U_L + U_S^C + U_S^G) \\ &= \sqrt{G} \left( \sqrt{\Omega} \exp(j\phi_A) + \sqrt{\rho} \sqrt{2b_0} \exp(j\phi_B) \right) + \sqrt{(1-\rho)} U'_S \end{aligned} \quad (4.6)$$

We have the identical shadowed Rice single model employed in [4], composed by the sum of a Rayleigh random phasor (the independent scatter component,  $U'_S$ ) and a Nakagami distribution  $\sqrt{G}$  used for both the LOS component and the coupled-to-LOS scatter component).We also can introduce the same process as seen in[4] and determining the expectation of the Rayleigh component regarding the Nakagami distribution and afterwards deriving the pdf of the instantaneous power. The  $Y$  pdf is thus generated by:

$$f_Y(y) = \frac{1}{\gamma} \left[ \frac{\gamma\beta}{\gamma\beta + \Omega'} \right]^\beta \exp \left[ -\frac{y}{\gamma} \right] {}_1F_1 \left( \beta; 1; \frac{1}{\gamma} \frac{\Omega'}{(\gamma\beta + \Omega')} y \right) \quad (4.7)$$

Where  $\beta \triangleq (E[G])^2/\text{Var}[G]$  is a amount of fading parameter with  $\text{Var}[\cdot]$  as the variance operator. Now we denote  $\Omega' = \Omega + \rho 2b_0 + 2\sqrt{2b_0\Omega\rho} \cos(\phi_A - \phi_B)$  and  $\gamma = 2b_0(1 - \rho)$ .  ${}_1F_1(a; c; x)$  this is the Kummer confluent hypergeometric function of the first kind. Otherwise, the large-scale fluctuations,  $X \triangleq \exp(2\chi)$  is widely accepted to be a lognormal amplitude [27] but but in [4, 5] The gamma one latter with a more desirable analytical structure, follows this distribution.

$$f_X(x) = \frac{\alpha^\alpha}{\Gamma(\alpha)} x^{\alpha-1} \exp(-\alpha x) \quad (4.8)$$

We already know that  $I=XY$  and can be obtained from the statistical characterization model present in Equation (4.3). It said  $I$  that follows a Málaga ( $\mathcal{M}$ ) distribution if  $X$  and  $Y$  be a random variable according to 4.7 and 4.8 respectively, and representing the irradiance fluctuations for a propagating optical wave. The distribution of  $I$  is a generalized Málaga ( $\mathcal{M}$ ) distribution can be written in the following way  $I \sim \mathcal{M}(\alpha, \beta, \gamma, \rho, \Omega')$ , here  $\alpha, \beta, \gamma, \rho, \Omega'$  they are real and positive parameters of this generalized ( $\mathcal{M}$ ) distribution. The parameter  $\alpha$  represents the effective number of large-scale cells of the scattering process[5], while the parameter  $\beta$  is a natural number and represents the effective number of small-scale effects, a generalized expression for  $\beta$  being a real number can be also derived [51] with an infinite sum, but because of its high degree it is less interesting freedom.

So the Málaga ( $\mathcal{M}$ ) distribution Pdf is given by :

$$f_{I_a}(I_a) = A \sum_{k=1}^{\beta} a_k I_a^{\frac{\alpha+k}{2}-1} K_{\alpha-k} \left( 2 \sqrt{\frac{\alpha\beta I_a}{\gamma\beta + \Omega'}} \right) \quad (4.9)$$

Where

$$\left\{ \begin{array}{l} A \triangleq \frac{2\alpha^{\frac{\alpha}{2}}}{\gamma^{1+\frac{\alpha}{2}}\Gamma(\alpha)} \left( \frac{\gamma\beta}{\gamma\beta + \Omega'} \right)^{\beta + \frac{\alpha}{2}} \\ a_k \triangleq \binom{\beta - 1}{k - 1} \frac{(\gamma\beta + \Omega')^{1-\frac{k}{2}}}{(k-1)!} \left( \frac{\Omega'}{\gamma} \right)^{k-1} \left( \frac{\alpha}{\beta} \right)^{\frac{k}{2}} \end{array} \right. \quad (4.10)$$

Here  $K_v(\cdot)$  denotes the modified Bessel function of the second kind,  $\Gamma(\cdot)$  is the gamma function and  $\binom{\cdot}{\cdot}$  represents the binomial coefficient. Here some characteristics about large-scale and small-scale fluctuations discuss. In [12] said that under weak fluctuations, Scintillation of weak turbulence is mainly a small-scale effect. Generally, Fluctuations of small-scale amplitude are related to small-scale (diffractive) eddies and Fluctuations of Large-scale amplitude directly related to large-scale (refractive) eddies.

In Table (4.1), we can see that A Generalized turbulence model, Málaga ( $\mathcal{M}$ ) distribution model can be reduced to other most of the existing distribution models for FSO communications.

**Table 4.1:** List of most popular existing distribution models for FOS communications that can generation by using the proposed Málaga ( $\mathcal{M}$ )distribution model.

Distribution model	Generation
Rice-Nakagami	$\rho = 0, \text{Var}[ U_L ] = 0$
Lognormal	$\rho = 0, \text{Var}[ U_L ] = 0, \gamma \rightarrow 0$
Gamma	$\rho = 0, \gamma = 0$
Shadowed-Rician distribution	$\text{Var}[ X ] = 0$
K distribution	$\Omega = 0 \text{ and } \rho = 0 \text{ or } \beta = 1$
HK (Homodyned K) distribution	$\Omega = 0, \rho = 0, X = \gamma$
Exponential distribution	$\Omega = 0, \rho = 0, \alpha \rightarrow \infty$
Gamma-gamma distribution	$\rho = 1, \text{then } \gamma = 0 \text{and} \Omega' = 1$
Gamma-Rician distribution	$\beta \rightarrow \infty$

## 4.4 Pointing Error

In line-of-sight FSO communication links, pointing accuracy is an important issue in determining link performance and reliability [33] and In FSO communication performance is highly dependent on the pointing errors. In terrestrial FSO communication systems, the transmitters and receivers are positioned at the top of high-rise buildings to obtain a (LOS) line of sight. Moreover, accurate laser beam pointing is critical in and free-space optical communications. Pointing errors is one of the key factors influencing the performance of the communication

system. It generated on the transmitter side when the line of sight to receiver is not strictly maintained. There are numerous sources of pointing errors, such as noise, structural manufacturing, in the electronic and mechanical telescope apparatus cause, what is called, boresight errors. The uncertainties in the line-of-sight direction due to the errors in the reference frame and the inability to compensate for the motion of the transmitter and receiver contributes to the pointing errors [66].

Thermal expansion, dynamic wind loads, and weak earthquakes result in the building sway phenomenon that causes vibration of the transmitter beam leading to a misalignment between transmitter and receiver known as pointing error [13]. A misalignment between the transmitter, signal fading at the receiver can lead to pointing errors and additional performance degradation. These pointing errors may lead to significant performance degradation and are a serious issue in urban areas, where the FSO equipments are placed on high-rise buildings [84].

Ponting errors are not always happed due to misalignments at the time of the installation process, but it can also happen possibly due to mechanical vibration of the transmitter beam causes a misalignment between the transmitter and the receiver. For horizontal FSO links, the vibration comes from transceiver stage oscillations and the building sway because of wind, building vibration and thermal expansion of building and for vertical FSO links for example ground-satellite links, satellite-vibrating oscillations can result in pointing errors [22]. Pointing errors result from the displacement of the laser beam along vertical (elevation) and horizontal (azimuth) directions that are typically assumed to be independent Gaussian random variables, as shown in Figure [4.3]. The pointing errors are widely considered as a combination of two fundamental pointing errors components that arise in most laser control systems: a fixed error called boresight, and a random error called jitter.

The boresight is the fixed displacement between beam center and center of the detector plane. In typical terrestrial FSO communication systems is initially installed near zero boresight error but the boresight error is still considerable due caused by thermal expansion of the laser beam. Where the jitter is the random offset of the beam center at detector plane, which is mainly caused by building sway and building vibration [99].

In FSO links, the assumption of negligible detector aperture size with respect to the beam width at the receivers made due to the large distances. The effect of pointing error and atmospheric turbulence has also been considered in terrestrial links of shorter range [33].

All over the literature, for the modeling of a pointing error model effectively, various statistical models were proposed based on its values as well as the precision characterization form of the laser beam and jitter. Farid and Hranilovic proposed a model in [33] for zero boresight and same jitter effect for both displacement directions.

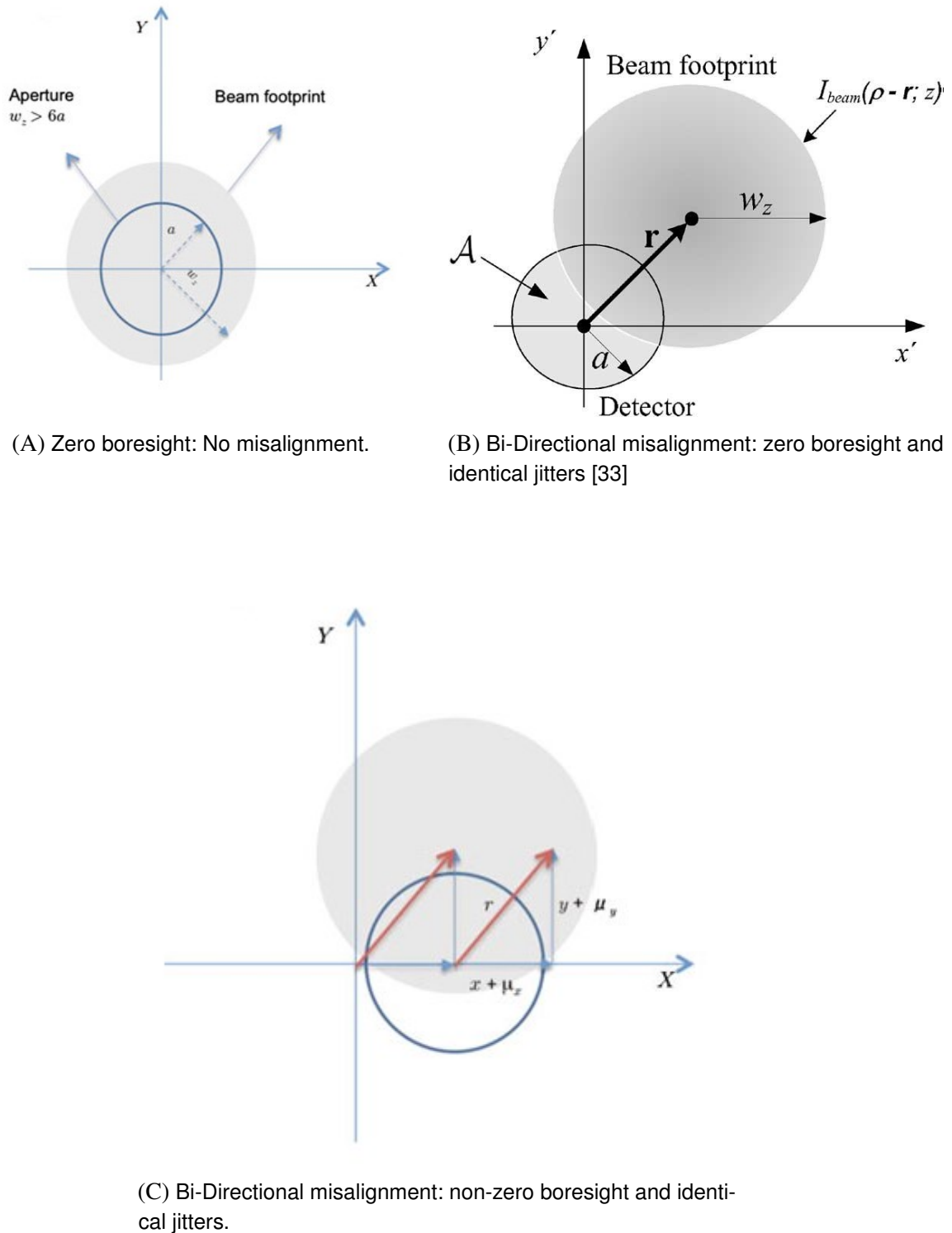


**Figure 4.3:** Beam footprint with misalignment on the detector plane [7]

Fan Yang proposed in [99] Nonzero Boresight Pointing Errors model by generalizing the model in [33].

To investigate the effect of pointing error on the performance of our FSO link, we taking statistical model for pointing error with zero Boresight and non-zero Boresight error, which takes into account the laser beam width, finite size circular detector, detector aperture size, and jitter variance. One things that this [99] proposed Non zero pointing error PDF can specializes to Zero boresight pointing when the boresight error  $S$  is zero. Now the Zero and Non-Zero Boresight pointing Error model describe below.

#### 4.4.1 Zero Boresight Pointing Error Model

Here We are showing statistical model that drive in [33] for Zero Boresight pointing error loss due to misalignment, which considers detector aperture size, beam width, and jitter variance. For a Gaussian beam, the normalized spatial distribution of the transmitted intensity at distance from the transmitter is given by [19].

$$I_{\text{beam}}(\rho; z) = \frac{2}{\pi w_z^2} \exp\left(-\frac{2\|\rho\|^2}{w_z^2}\right) \quad (4.11)$$

Where  $\rho$  is is the radial vector from the beam center, $w_z$  is beam width at distance  $z$ ,  $a$  is circular detection aperture of radius can see in figure(4.3B) and Gaussian beam profile at the receiver Ibeam. So the attenuation due to geometric spread with pointing error  $r$  is writing as

$$I_p(r : z) = \int_{\mathcal{A}} I_{\text{beam}}(\rho - r; z) d\rho \quad (4.12)$$

where  $I_p(\cdot)$  is the fraction of the collected power at receiver by the detector and  $\mathcal{A}$  is the detector area. When a pointing error of  $r$  is present  $I_p$  is a function of the radial displacement and angle.Because of the beam shape symmetry and the detector area, the resulting  $I_p(r : z)$  depends only on the radial distance  $r = \|\mathbf{r}\|$ .Therefore, without loss of generality we can claim that the radial distance is located along the  $x'$ -axis.The fraction of the collected power at a receiver of radius  $a$  in the transverse plane of the incident wave can be Writing as [33]

$$I_p(r : z) = \int_{-a}^a \int_{-\zeta}^{\zeta} \frac{2}{\pi w_z^2} \exp\left(-2\frac{(x' - r)^2 + y'^2}{w_z^2}\right) dy' dx' \quad (4.13)$$

Here  $\zeta = \sqrt{a^2 - x'^2}$ . As shown in [33] paper this integration can be writing approximated as the Gaussian form

$$I_p(r : z) \approx A_0 \exp\left(-\frac{2r^2}{w_{zeq}^2}\right) \quad (4.14)$$

Where  $w_{zeq}$  is the equivalent beamwidth defined as  $w_{zeq}^2 = w_z^2 \frac{\sqrt{\pi} \operatorname{erf}(v)}{2v \exp(-v^2)}$ , such that  $A_0 = [\operatorname{erf}(v)]^2$  is the maximum fraction of the collected power at  $r = 0$ , and  $v = (\sqrt{\pi}a)/(\sqrt{2}w_z)$  is the ratio between the aperture radius  $a$  and the beamwidth  $w_z$ ,  $\operatorname{erf}()$  denoting the error function. It is important to note that the approximation in 4.14 is valid when  $w_z > 6a$ [33] which is satisfied in typical terrestrial FSO communication systems.

Consider independent identical Gaussian distributions for the elevation and the horizontal displacement sway as was done in [17] previous work. The radial displacement  $r$  at the receiver is modeled by a Rayleigh distribution

$$f_r(r) = \frac{r}{\sigma_s^2} \exp\left(-\frac{r^2}{2\sigma_s^2}\right), \quad r > 0 \quad (4.15)$$

The fading due to pointing errors  $I_p$  has been modeled as the result of considering independent identical Gaussian distributions, where  $\sigma_s^2$  is the jitter variance at the receiver. Now after Combining equation 4.14 and 4.15 the Probability distribution function(PDF) of zero boresight pointing error as

$$f_{I_p}(I_p) = \frac{g^2}{A_0^{g^2}} I_p^{g^2-1}, \quad 0 \leq I_p \leq A_0 \quad (4.16)$$

Here  $g = \omega_{zeq}/(2\sigma_s)$  is the ratio between the equivalent beam radius at the receiver  $\omega_{zeq}$  and the pointing error displacement standard deviation at the receiver  $\sigma_s$ .

#### 4.4.2 Non-Zero Boresight Pointing Error Model

Here we are showing statistical model that drive in [99] for Non-Zero Boresight pointing error loss due to misalignment, which considers detector aperture size, beam width, and jitter variance. We assume that When a Gaussian beam propagates from transmitter to circular photodetector with aperture radius  $a$  as showing in figure(4.3). An instantaneous radial displacement

between the beam centroid and the detector center is  $r$ , at distance  $z$  the fraction of collected power at the receiver we already see in Equation(4.14).

At the receiver aperture plane, the radial displacement vector can be expressed as  $r = [xy]^T$ , where  $x$  and  $y$  represent the horizontal and vertical(elevation) displacement of the beam in the detector plane. Therefore, the distribution of  $r = |r| = \sqrt{x^2 + y^2}$  depends on the distribution of  $x$  and  $y$ , and they are assumed to be independent Gaussian displacements along the horizontal axis and the elevation axis, then  $r$  can be allocated according to the Beckman distribution. The Beckmann distribution is used to describe the PDF of fading channels in general. It is a versatile model which applies to a variety of distributions as special cases. It is a four-parameter distribution modeling the envelope of two independent Gaussian random variables (RVs) [7]. Here consider in [99] a nonzero boresight error in addition to the random jitters, now if both displacements  $X$  and  $Y$  are nonzero-mean Gaussian RVs with different variances, i.e.,  $x \sim \mathcal{N}(\mu_x, \sigma_x)$  and  $y \sim \mathcal{N}(\mu_y, \sigma_y)$ , then radial displacement  $r = |r| = \sqrt{x^2 + y^2}$  follows the Beckmann distribution [88].

$$f_r(r) = \frac{r}{2\pi\sigma_x\sigma_y} \times \int_0^{2\pi} \exp\left(-\frac{(r \cos \phi - \mu_x)^2}{2\sigma_x^2} - \frac{(r \sin \phi - \mu_y)^2}{2\sigma_y^2}\right) d\phi \quad (4.17)$$

The jitter is primarily caused by turbulence and building motion in terrestrial FSO systems. Since the turbulence cells randomly appear on the beam path, and the building could be considered to sway in orthogonal and parallel directions to the beam path with equal probabilities [99]. If both displacements have different mean and common non-zero variance, as seen in Figure (4.3C) (i.e.  $\mu_x \neq \mu_y$  and  $\sigma_x^2 = \sigma_y^2 = \sigma_s^2$ ) as a result, the PDF of radial displacement  $r$  in 4.17 becomes Rician distributed RV

$$f_r(r) = \frac{r}{\sigma^2} \exp\left(-\frac{(r^2 + s^2)}{2\sigma^2}\right) I_0\left(\frac{rs}{\sigma^2}\right) \quad (4.18)$$

where  $s$  is the boresight displacement,  $s = \sqrt{\mu_x^2 + \mu_y^2}$  and  $I_0(\cdot)$  is the modified Bessel function of the first kind with order zero. By combining Equation (4.14) and (4.18) the Probability distribution function(PDF) of nonzero boresight pointing error can writing as

$$f_{I_p}(I_p) \approx \frac{g^2 \exp(-s^2/(2\sigma_s^2))}{A_0^{g^2}} I_p^{g^2-1} I_0\left(\frac{s}{\sigma_s^2} \sqrt{\frac{-\omega_{zeq}^2 \ln(I_p/A_0)}{2}}\right), \quad 0 \leq I_p \leq A_0 \quad (4.19)$$

## 4.5 Atmospheric Effects

Different experiments are going on to develop new models based on the system's efficacy in different weather conditions. Fog, haze, rain, and snow environmental conditions are the principal targets of these studies. Action is being taken in a realistic system based on the findings of these studies [46]. Owing to the composition of the atmosphere and climate, atmospheric disruption occurs. It is induced at various temperatures by wind and convection combining the air parcels. This induces air density variations and results in a decrease in the refractive index of the air. Atmospheric attenuation is really the product of natural fog and haze. Dust and rain also depend on it. Atmospheric attenuation is expected to be dependent on the wavelength, but that is not accurate. Haze is dependent on wavelength. In haze weather, attenuation at 1550 nm is lower than other wavelengths. The attenuation in fog climatic conditions is not dependent of wavelength. The transmission medium for an FSO link is the atmospheric. The attenuation it creates depends on many circumstances. The principal cause of attenuation is environmental conditions. There are some unique weather conditions in the area in which a connection is formed so that the previous knowledge of attenuation can be gained; for instance, fog and heavy snow are the two primary weather conditions in temperate regions. Heavy rain and haze are two primary weather conditions in tropical regions and have a direct impact on the availability of FSO links in that region [61]. The following describes some of the weather conditions:

- **Fog:** Fog attenuates visible radiation significantly. The hindrance created by fog absorbs, disperses, and reflects the optical beam of light. Fog-induced scattering, also known as Mie scattering, is mainly a function of enhancing the power transmitted [1].
- **Rain:** Due to rain drops, rain attenuation occurs and is a non-selective scattering. This attenuation form is independent of wave length. Rain has the potential to generate the effects of laser transmission fluctuations. The visibility of the FSO system depends on the amount of rain involved. Water droplets have a solid structure in the event of heavy rain and may either change the characteristics of the optical beam or restrict the beam passage as the optical beam is absorbed, dispersed and reflected [77].
- **Haze:** Haze particles can remain in the air for longer periods of time and contribute to atmospheric attenuation. So, attenuation principles at that moment depend on the type of visibility. There seem to be two ways to collect attenuation information to verify the performance of the FSO system: first, by temporarily installing the system on site and testing its efficiency, and secondly, while using the model of Kim and Kruse [32].

- **Smoke:** The combustion of various compounds, such as carbon, glycerol, and household pollutants, produces smoke. The visibility of the mean of communication is affected [46].
- **Sandstorms:** The well-known issue in outdoor connection communication is sandstorms. This can be defined in two ways: first the size of the wind particles, which depends on the texture of the soil, and second, the wind speed needed to blow up the particles for a minimum period of time [35].
- **Clouds:** The dominant component of the Earth's atmosphere is the cloud layers. The creation of clouds takes place by condensing or depositing water above the surface of the earth. Fractions of the optical beam transmitted from earth to space may be absolutely blocked. Owing to the diversity and homogeneity of the cloud particles, the attenuation caused by clouds is difficult to measure [80].
- **Snow:** Snow has bigger molecules that induce geometric dispersion. For the continuous attenuation spectrum of fog and smoke conditions, the snow particles have an effect similar to the Rayleigh scattering [17] result, and results show that the disambiguation decreases linearly [47].

#### 4.5.1 Atmospheric loss

Atmospheric loss is modelled by the exponential Beers-Lambert Law and it describes the attenuation of laser power through the atmosphere as:

$$I_1(z) = \frac{P(z)}{P(0)} = \exp(-\sigma z) \quad (4.20)$$

$I_1(z)$  is atmospheric attenuation over a propagation path distance  $z$ , where  $P(z)$  is the laser power at distance  $z$ , and  $\sigma$  is the attenuation coefficient [6]. During a long period of time, the attenuation  $I_1$  is known as a specified scaling factor, and there is no randomness in its action. It depends on the size and particle size distribution that scatter and the wavelengths used. Visibility, which can be calculated directly from the atmosphere, can be expressed [57] [64]. A powerful inverse association exists between the strength of turbulence and attenuation. During a fog case, for instance, heavy turbulence is extremely unlikely to occur.

**Table 4.2:** Attenuation coefficients for different weather conditions[94]

Weather condition	Attenuation $\sigma$ (dB/KM)
Very clear air	0.0647
Haze	0.7360
Light fog	4.2850

## 4.6 Channel Statistical Model

So After defining in previous section both Zero and Non-zero boresight pointing error models, we can calculate the final probability density functions (PDFs) of Zero and Non-zero boresight pointing error with Málaga ( $\mathcal{M}$ ) turbulence. Now calculating the PDFs for zero and non-zero boresight pointing error by combining their distribution separately with the distribution of Málaga ( $\mathcal{M}$ ) turbulence which are presented above in equation (4.9) and (4.16) or equeuation (4.9) and (4.19).

$$f_I(I) = \int_0^\infty f_{I|I_a}(I | I_a) f_{I_a}(I_a) dI_a \quad (4.21)$$

where  $f_{I|I_a}(I | I_a)$  is the conditional probability given a turbulence state  $I_a$  and it is expressed for the zero boresight pointing error as

$$f_{I|I_a}(I | I_a) = \frac{g^2}{A_0^{g^2} I_a} \left( \frac{I}{I_a} \right)^{g^2-1}, \quad 0 \leq I_p \leq A_0 I_a \quad (4.22)$$

For the non-zero boresight pointing error as

$$f_{I|I_a}(I | I_a) = \frac{g^2 \exp[-s^2/(2\sigma_s^2)]}{A_0^{g^2} I_a I_1} \left( \frac{I}{I_a I_1} \right)^{g^2-1} I_0 \left( \frac{s}{\sigma_s^2} \sqrt{\frac{-\omega_{zeq}^2}{2} \ln \left( \frac{I}{A_0 I_a I_1} \right)} \right) \quad (4.23)$$

Substituting equation (4.22) in (4.21) the expression for PDF for the zero boresight pointing error which is represented as:

$$f_I(I) = \frac{g^2 A}{A_0^{g^2}} I^{g^2-1} \sum_{k=1}^{\beta} a_k \int_{I/A_0}^{\infty} I_a^{(a+k)/2-1-g^2} K_{\alpha-k} \left( 2 \sqrt{\frac{\alpha \beta I_a}{\gamma \beta + \Omega'}} \right) dI_a \quad (4.24)$$

After evaluating integral in equation (4.24) according to [2], the modified Bessel function of the second kind  $K_v(\cdot)$  can be expressed as a special case of the Meijer G-function, given by the following relationship in [76], we can write the closed form expression for PDF for a zero boresight pointing error:

$$f_I(I) = \frac{g^2 A}{2} I^{-1} \sum_{k=1}^{\beta} a_k \left( \frac{\alpha\beta}{\gamma\beta + \Omega'} \right)^{-(\alpha+k)/2} G_{1,3}^{3,0} \left( \frac{\alpha\beta}{\gamma\beta + \Omega'} \frac{I}{A_0} \middle| {}_{g^2, \alpha, k}^{g^2+1} \right) \quad (4.25)$$

Now Substituting Equation (4.23) in (4.21), we can get the expression of PDF for a non-zero boresight pointing error which is represented as:

$$\begin{aligned} f_I(I) &= \frac{g^2 A \exp[-s^2/(2\sigma_s^2)]}{(A_0 I_1)^{g^2}} I^{g^2-1} \sum_{k=1}^{\beta} a_k \\ &\times \int_{I/(A_0 I_1)}^{\infty} I_a^{(\alpha+k)/2-1-g^2} K_{\alpha-k} \left( 2\sqrt{\frac{\alpha\beta I_a}{\gamma\beta + \Omega'}} \right) I_0 \left( \frac{s}{\sigma_s^2} \sqrt{\frac{-\omega_{zeq}^2}{2} \ln \left( \frac{I}{A_0 I_a I_1} \right)} \right) dI_a \end{aligned} \quad (4.26)$$

After evaluating the integral of equation (4.26), we can write the closed form expression of PDF for non-zero boresight pointing error:

$$\begin{aligned} f_I(I) &= \frac{2\pi g^2 A \exp[-s^2/(2\sigma_s^2)]}{\omega_{zeq}^2} \sum_{k=1}^{\beta} \frac{a_k I^{(\alpha+k)/2-1}}{(A_0 I_1)^{(\alpha+k)/2} \sin[\pi(\alpha-k)]} \\ &\times \sum_{p=0}^P \left\{ \frac{\left[ \frac{\alpha\beta I}{(\gamma\beta + \Omega') A_0 I_1} \right]^{p-(\alpha-k)/2}}{\Gamma[p-(\alpha-k)+1] p!} \left[ \frac{-\omega_{zeq}^2}{4(p+k-g^2)} \exp \left( \frac{-\omega_{zeq}^2 s^2}{8(p+k-g^2)\sigma_s^4} \right) \right] \right. \\ &\left. - \frac{\left[ \frac{\alpha\beta I}{(\gamma\beta + \Omega') A_0 I_1} \right]^{p+(\alpha-k)/2}}{\Gamma[p+(\alpha-k)+1] p!} \left[ \frac{-\omega_{zeq}^2}{4(p+\alpha-g^2)} \exp \left( \frac{-\omega_{zeq}^2 s^2}{8(p+\alpha-g^2)\sigma_s^4} \right) \right] \right\} \end{aligned} \quad (4.27)$$

# **Chapter 5**

## **Modulation Techniques and BER Analysis**

### **5.1 Introduction**

Nowadays, the main aim of modulation is to cram as much data into the least possible amount of bandwidth. This goal, known as spectral efficiency, tests how fast data can be transmitted over an allocated bandwidth. In order to achieve and enhance spectral efficiency, several techniques have emerged [78]. In the field of Free Space Optical Communication, there are various modulation techniques available, including such Binary Phase Shift Keying (BPSK), Quadrature Phase Shift Keying (QPSK), On-Off Keying (OOK), Quadrature Amplitude Modulation (QAM), Pulse Amplitude Modulation (PAM), Pulse Position Modulation (PPM), Differential Phase Shift Keying(DPSK). Good BER output is given by the OOK modulation, but the data rate is poor. The need for the present moment, along with good BER results, is to get a high data rate. Since the average optical power emitted is often constrained, modulation technique output is always comparison in terms of the average optical signal needed to achieve the desired BER at a given connection speed. The power efficiency of the modulation scheme is very desirable, but this is not the only determining factor in the choice of a modulation technique [53]. The amplitude of a source is modulated in FSO communication systems to transmit signals over the tube. The signal's amplitude, frequency, phase, and polarization can be modulated. We know, there are various kinds of modulation schemes that have been compared in terms of the expected power obtained needed to achieve the desired BER from the data rate. In order to optimize the ratio of peak to average output, a power-efficient modulation scheme is desirable. Intensity modulation with direct detection is the easiest and most widely used modulation scheme in free space optics. Based on power consumption, bandwidth effectiveness, basic design criteria, low-cost implementation and tolerance to interference background radiation, the modulation scheme should be selected [53]. We are now talking about modulation techniques using their

phases to modulate the signal. The first modulation scheme in these groups is Binary Phase Shifting Keying Modulation Alteration (BPSK). The PSK is a digital modulation technique in which the signal process for modulation is used. With respect to a fixed signal, this shift in the stage takes place. The BPSK is a binary PSK where we function with two stages,  $0^\circ$  and  $180^\circ$ , respectively. We only have phases there that we use to modulate the signal, which is why we call it binary PSK. In connected devices such as Bluetooth, radio frequency recognition where the source range and destination is smaller, the BPSK is widely used. Compared to the QPSK, the demand for electricity used by the BPSK is much smaller (Quadrature Phase Shift Keying) [29]. secondly, The QPSK is a technique for modulation in which the modulation takes place across four phases. The QPSK uses two bits at a time, which increases the network's power. As compared to the QPSK to obtain the BER, the BPSK is less than the specific value of the signal - to - noise. The bandwidth efficiency of the QPSK is much more than the PSK. The power requirement is also high for modulating two bits, so the QPSK fails when we compare it to the BPSK on the parameters of power efficiency. Thirdly, we come across a modulation technique called DPSK as we step forward in the stage modulation (Differential Phase Shifting Key). DPSK is a modulation technique in which, without considering the reference signal, we adjust the signal phase. To solve the inconvenience of QPSK and PSK, DPSK is used. Fourthly, in the OOK modulation method, the data packets are translated into certain special code pulses (NRZ), pulse presence denotes bit 1 and pulse absence denotes bit 0. In that slot, the data packets are converted to particular code pulses in the OOK modulation scheme [45]. OOk, because of its easy implementation, easy design of the recipient, reliability, and cost-efficiency, is the easiest and widely adopted modulation scheme used in commercial FSO communication systems. By using pulse modulation, a number of time-basic features of the pulse carrier are used to convey information, a significant average efficiency can also be achieved [28].Nextly, QAM is the modulation technique which is the combination of the modeling of a carrier's phase and amplitude into a single channel. QAM is known as the modulation technique. In other words, by changing both the amplitude and phase of a carrier wave, QAM transmits information, thus doubling the effective bandwidth. "QAM is often referred to as "multiplexing of quadrature carrier". A strong data rate benefits QAM. Thus, the carrier signal can transport the number of bits. It is best for cellular communications networks, regardless of these benefits. It has a low chance of error. In the field of radio communications, QAM technology has wide applications because there is a probability of noise increase as the data rate increases, but this QAM approach is not influenced by noise interference, so with this QAM there is a simple mode of signal transmission. On the other hand, the basic type of modulation is pulse amplitude modulation(PAM). This modulation samples the signal periodically and makes each sample equal to the modulating signal amplitude. Other modulation signals can be produced by

PAM, and the message can be carried simultaneously. It is used for the production of control signals in many microcontrollers. It is used in the areas of photobiology, photobiology, Ethernet networking etc. The PAM scheme is a prime candidate for bandwidth quality [81]. Lastly we have discussed in our thesis is the M-PPM scheme. It is a common modulation format used in FSO communication systems, it is far more powerful than the OOK modulation but shows that bandwidth effectiveness declines rapidly and power efficiency increases. The performance of BER of M-PPM technique is better perform than the other modulation technique. We have also described the modulation schemes broadly, are given below:

## 5.2 Binary Phase Shift Keying (BPSK)

Binary Phase-Shift Keying (BPSK) is a digitally modulated device that transmits information by altering or modulating the reference signal (carrier wave) phase. BPSK is suitable for low-cost passive transmitters, and phase-shift keying (PSK) is the simplest type of BPSK. Two stages are used, which are separated by  $180^\circ$  of all the PSKs, this modulation is the most stable because it takes the maximum amount of noise or distortion to make an incorrect decision on the demodulator. On the Nakagami channel and Rician Fading channel, the efficiency of BPSK modulation is studied [41]. The BPSK modulation BER equation is as described below:

$$P_{BPSK} = Q\left(\sqrt{2SNR}\right) \quad (5.1)$$

## 5.3 Quadrature Phase Shift Keying (QPSK)

Different from BPSK and DPSK, the QPSK scheme using two bits are grouped together to form signals [104]. The Quadrature Phase Shift Keying is one of the variants of PSK modulation which uses four different points on the constellation diagram, equally spaced around a circle to represent the data bits. Those four stages allow the QPSK to encrypt, while representing the data, two bits per symbol. Compared to a BPSK system, the QPSK can be used to double the data rate while maintaining the same signal bandwidth. The QPSK can also operate in a way that preserves the BPSK data rate, but makes the requirement for bandwidth half as opposed to BPSK [58]. The QPSK modulation bit-error-rate equation is given below:

$$P_{QPSK} = 2Q\left(\sqrt{2SNR}\right) \quad (5.2)$$

BER for QPSK can therefore be viewed as a mixture of two BPSK orthogonal. Since the average

BPSK power requirement requires a factor of  $2\sqrt{2}$  more power than NRZ-OOK, the average QPSK power requirement normalized to NRZ-OOK can therefore be expressed as [104]:

$$\frac{P_{QPSK}}{P_{NRZ-00K}} = \frac{1}{2\sqrt{2}} \frac{\operatorname{erfc}^{-1}(BER)}{\operatorname{erfc}^{-1}(2BER)} \quad (5.3)$$

## 5.4 Differential Phase Shift Keying (DPSK)

DPSK is a modulation scheme that the, without taking into consideration the reference signal, we change the phase of the signal. To achieve the inconvenience of QPSK and PSK, DPSK is used. When we use the signal modulated by the DPSK, the performance of the differential encoding QPSK(DQPSK) is almost the same as compared to the DPSK, the various types of modulation effects that affect the signal decrease. As the two bits are transmitted at the same time, the data rate provided by the DQPSK is twice as high as the DPSK. As compared to the DPSK, the DQPSK has more spectral efficiency, but the DPSK is better when we talk about power. A modulating technique that is almost the same as the QAM is the carrier less amplitude and phase modulation (CAP), but the only difference is in the signal phase [78]. DPSK is a model of relative phase modulation, the transferred information defined by the phase difference between the usual term. If  $\Delta\phi$  is equal to 0, it means two adjacent symbol signals that are the same before and after. And so, with the DPSK modulation system, the inverted  $\pi$  phenomenon can be avoided. In the case of synchronous demodulation, compared to BPSK modulation, it is not necessary to know the phase and frequency of the carrier, however, the local carrier is necessary [58]. It can calculate the BER for DPSK as follows:

$$P_{DPSK} = Q\left(\sqrt{SNR}\right) \quad (5.4)$$

If differential decoding is used the information bit '1' will be transmitted by moving the modulated signal phase  $180^\circ$  relative to the previous modulated signal phase. Without shifting the modulated signal phase relative to the previous modulated signal, bit '0' is transmitted. For DPSK, the bandwidth required is equal to the  $B_{DPSK}=R_b$  bit rate. DPSK's spectrum efficiency is relatively higher, which can improve dispersion tolerance, nonlinear tolerance, and PMD tolerance [104].

## 5.5 On-Off Keying (OOK)

In the FSO, there are several modulation methods employed. The modulation technique called OOK is the most widely used (On Off Keying). The technique became prevalent because of its simplicity and BW (Bandwidth) quality. The OOK is the technique modulation based on the binary number in which 1 or real is the meaning of on' and 0 or false is the meaning of off'. 1 and o are used to reflect the presence of light in which the presence of light is represented by 1 and the absence of light is represented by 0. For better performance, the on-off keying modulation technique needs an adaptive threshold compared to the IM/DD modulation technique. The OOK modulation technique is combined to enhance the results with the line coding technique. As we can learn from the moderate signal-to-noise ratio (SNR) of the OOK NRZ, low cost where the RZ is highly sensitive. The OOK usually suffers from poor spectral and energetic efficiency. The distortion of amplitude is also the downside of this kind of system of modulation. Whenever we select the modulation technique for the FSO system, power and energy are very significant parameters. Energy efficiency is the parameter associated with the data rate, and the parameter associated with the information rate [78]. Because of their ease of implementation, bandwidth efficiency, and cost-efficiency, it is a type of modulation scheme that is widely used in commercial FSO communication systems. On-off key (OOK) modulated links are the simplest type of FSO links, which require the presence and absence of optical pulses for binary '1' and binary '0' respectively. In addition to ease of modulation and development, compared to traditional RF systems, the following features have rendered unbeatable options. For the NRZ-OOK and the RZ-OOK modulated signal, the BER and SNR relationship is as follows [31][58]:

On-off key (OOK) modulated links are the simplest type of FSO links, which require the presence and absence of optical pulses for binary '1' and binary '0' respectively. In addition to ease of modulation and development, compared to traditional RF systems, the following features have rendered unbeatable options [92]. For the NRZ-OOK modulated signal, the BER and SNR relationship is as follows:

$$P_{NRZ-OOK} = Q\left(\frac{\sqrt{SNR}}{2}\right) \quad (5.5)$$

It is also possible to use return to zero (RZ) coding in addition to NRZ, in which the 'one' logic returns to zero in the center of the sample. RZ displays greater sensitivity than NRZ. OOK is influenced by the distortion of amplitude, i.e. the fading and propagation of the signal from different roots. When the sky is bright, these problems are the least successful [92]. Here the

BER for RZ-OOK modulated signal is given by:

$$P_{RZ-OOK} = Q\left(\sqrt{\frac{SNR}{2}}\right) \quad (5.6)$$

## 5.6 Quadrature Amplitude Modulation (QAM)

QAM is a signal that modulates and combines two carriers shifted by 90° degrees (i.e. sine and cosine) in phase. They are in quadrature as a consequence of their 90° phase difference and this gives rise to the name. The In-phase or "I" signal is often called one signal, and the quadrature or "Q" signal is the other. Both amplitude and phase variations are included in the resulting total signal consisting of the combination of both I and Q carriers. It can also be regarded as a mixture of amplitude and phase modulation, since both amplitude and phase variations are present. Although QAM tends to improve the transmission efficiency of radio communications systems by using amplitude and phase variations, it has some disadvantages. First since the states are closer together to transfer the signal to a different decision point so that a lower level of noise is needed, it is more sensitive to noise. Receivers can both use small amplifiers for phase or frequency modulation use, which can eliminate some noise from the amplitude and thereby increase noise dependence. This is not the case with QAM. The second restriction is related to the amplitude portion of the signal as well. When a phase or frequency modulated signal is amplified in a radio transmitter, there is no need to use linear amplifiers, while when using QAM, which includes an amplitude portion, linearity must be retained. Unfortunately, linear amplifiers are less effective for mobile applications and use more power, which makes them less attractive. 16-QAM gives better BER performance than 64-QAM. DPSK and 8-QAM behave more or less the similar but for higher values of M (16-QAM and 64-QAM) the performance of DPSK is far better. The PDF of the QAM is given below:

$$P_{bc} = \frac{4}{\log 2M} \left(1 - \frac{1}{\sqrt{M}}\right) Q\left(\sqrt{\frac{3 \log 2M}{M-1} SNR}\right) \quad (5.7)$$

$$P_{M-QAM} = 1 - (1 - P_{bc})^{\log 2M} \quad (5.8)$$

## 5.7 Pulse Amplitude Modulation (PAM)

The modulation of the pulse amplitude is a type of signal modulation where the message information is encoded in the amplitude of a series of pulses of the signal. It is an analog pulse modulation scheme in which the amplitudes of a carrier pulse train are varied according to the message signal sample value. By detecting the amplitude level of the carrier at any single period, demodulation is carried out, and it is possible to express the BER for the M-PAM scheme as follows[58]:

$$P_{M-PAM} = Q\left(\frac{\sqrt{SNR \log_2 M}}{2(M-1)}\right) \quad (5.9)$$

## 5.8 Pulse Position Modulation (PPM)

Each pulse of a laser may be used in this modulation scheme to represent one or more bits of information by its location in time relative to the beginning of a symbol whose length is identical to that of the bits of information it contains. And the great value of the PPM scheme is the reduction of reliance on the input power of the decision threshold. Bits in block encoding are distributed one at a time rather than one in blocks. By translating each word of the "K1" bits into one of the "L=2K1" optical transmission fields, optical block encoding is achieved [92]. On the other hand In PPM, by its location in time corresponding to the start of the symbol, each pulse represents one or more information bits. M-PPM is used to display the order for "M" possible pulse location code for "K1" bit of information, with an unconditional BER equation as [58]:

$$P_{M-PPM} = Q\left(\frac{\sqrt{SNR \frac{M}{2} \log_2 M}}{2}\right) \quad (5.10)$$

We can also write for the Gaussian noise, the BER for the M-PPM scheme can be expressed as[58]:

$$P_{PPM} = \frac{1}{2} \operatorname{erfc}\left(\frac{1}{2\sqrt{2}} \sqrt{SNR \frac{M}{2} \log_2 M}\right) \quad (5.11)$$

An orthogonal modulation technique is the pulse position modulation (PPM) scheme. Pulse position modulation (PPM), where information is encoded into the position of the optical pulse rather than amplitude, provides greater turbulence tolerance [58].

## 5.9 BER Analysis In-Terms of Atmospheric Turbulence for Different modulation

Turbulence and pointing errors are the key explanation for the deteriorating efficiency of the FSO system. The fluctuation of light intensity follows the Malaga(M) distribution channel. To set up a communication system with a specific data rate and error probability lower than the appropriate BER, the FSO must be competent. For FSO Communication, the efficiency of the communication system needs to be measured. The available signal-to-noise ratio (SNR) available at the receiver is one of the standard evaluation techniques for FSO system efficiency. System output in the presence of noise is one of the essential issues in the design of a communication system. Data is normally transmitted in digital form in the case of FSO, and the actual performance evaluation in digital communications is not provided directly by the SNR, but is given in terms of the probability of error, also given as bit error rate (BER). BER is the probability that an error can occur in digital data transmission.

The SNR of the signal received is given below:

$$\text{SNR} = \left( \frac{PIR}{\sigma_N} \right)^2 \quad (5.12)$$

In our model, we are analyzing bit-error-rate (BER) performance to take into account Zero boresight and nonzero boresight pointing errors in the presence of Málaga( $\mathcal{M}$ ) atmospheric turbulence Channel. Now the expression for probability of average bit-error rate (ABER) for BPSK, QPSK, DPSK, NRZ-OOK, RZ-OOK, QAM, PAM, and PPM modulation with Equation 4.25 for zero boresight pointing error and Equation 4.27 for non-zero boresight pointing error with Málaga( $\mathcal{M}$ ) distribution can be obtained by using the following integral calculation.

### Calculation for BPSK:

$$\begin{aligned} P_{e,BPSK} &= \int_0^{\infty} f_I(I) p_{e,BPSK}(I) dI \\ &= \int_0^{\infty} f_I(I) \left[ Q(\sqrt{2\text{SNR}}) \right] dI \end{aligned} \quad (5.13)$$

**Calculation for QPSK:**

$$\begin{aligned} P_{e,QPSK} &= \int_0^\infty f_I(I) p_{e,QPSK}(I) dI \\ &= \int_0^\infty f_I(I) \left[ 2Q(\sqrt{2SNR}) \right] dI \end{aligned} \quad (5.14)$$

**Calculation for DPSK:**

$$\begin{aligned} P_{e,DPSK} &= \int_0^\infty f_I(I) p_{e,DPSK}(I) dI \\ &= \int_0^\infty f_I(I) \left[ Q(\sqrt{SNR}) \right] dI \end{aligned} \quad (5.15)$$

**Calculation NRZ-OOK:**

$$\begin{aligned} P_{e,NRZ-OOK} &= \int_0^\infty f_I(I) p_{e,NRZ-OOK}(I) dI \\ &= \int_0^\infty f_I(I) \left[ Q\left(\frac{\sqrt{SNR}}{2}\right) \right] dI \end{aligned} \quad (5.16)$$

**Calculation For RZ-OOK:**

$$\begin{aligned} P_{e,NRZ-OOK} &= \int_0^\infty f_I(I) p_{e,NRZ-OOK}(I) dI \\ &= \int_0^\infty f_I(I) \left[ Q\left(\sqrt{\frac{SNR}{2}}\right) \right] dI \end{aligned} \quad (5.17)$$

**Calculation for QAM:**

$$P_{bc} = \frac{4}{\log 2M} \left(1 - \frac{1}{\sqrt{M}}\right) Q\left(\sqrt{\frac{3\log 2M}{M-1} SNR}\right) \quad (5.18)$$

$$P_{M-QAM} = 1 - (1 - P_{bc})^{\log 2M} \quad (5.19)$$

$$\begin{aligned}
 P_{e,QAM} &= \int_0^{\infty} f_I(I) p_{e,QAM}(I) dI \\
 &= \int_0^{\infty} f_I(I) [1 - (1 - P_{bc})^{\log_2 M}] dI
 \end{aligned} \tag{5.20}$$

**Calculation for PAM:**

$$\begin{aligned}
 P_{e,PAM} &= \int_0^{\infty} f_I(I) p_{e,PAM}(I) dI \\
 &= \int_0^{\infty} f_I(I) \left[ Q\left(\frac{\sqrt{SNR \log_2 M}}{2(M-1)}\right) \right] dI
 \end{aligned} \tag{5.21}$$

**Calculation for PPM:**

$$\begin{aligned}
 P_{e,PPM} &= \int_0^{\infty} f_I(I) p_{e,PPM}(I) dI \\
 &= \int_0^{\infty} f_I(I) \left[ Q\left(\frac{\sqrt{SNR \log_2 M}}{2}\right) \right] dI
 \end{aligned} \tag{5.22}$$

In this thesis paper, we have evaluated the performance of the ABER by considering zero-boresight and non-zero-boresight pointing errors in the performance of the atmospheric turbulence channel of Málaga ( $\mathcal{M}$ ) distribution.

# Chapter 6

## Simulation output

### 6.1 Simulation Parameters

The simulation parameters that we have used throughout our simulation for this thesis are given in table 6.1. We have tune effective number of large-scale cells of the scattering process, amount of fading parameter, propagation distance and Beam width for four different situations.

**Table 6.1:** Simulation parameters [59]

Parameter	Value
Optoelectronic conversion factor $R$ ( A / W)	0.5
Noise standard deviation $\sigma_n$ (A/Hz)	$10^{-7}$
Atmospheric attenuation coefficient $\sigma$ (dB/km)	8
Jitter standard deviation $\sigma_s$ (m)	0.2
Beam width $w_z$ (m)	2.5
Effective number of large-scale cells of the scattering process $\alpha$	3.5,3.7,3.99
Amount of fading parameter $\beta$	2,4,6
Average optical power of classic scattering component received by off-axis eddies $\gamma$	0.2
Average optical power of coherent contributions $\Omega'$	0.8
Boresight error $s$ (m)	0.3
Aperture radius $a$ (m)	0.1
Propagation distance $z$ (km)	1, 2, 3, 4

## 6.2 Model Validation

In this paper [9] named as “Performance analysis of subcarrier intensity modulation using rectangular QAM over Malaga turbulence channels with integer and non-integer beta” by Wael G. Alheadary\*, Ki-Hong Park and Mohamad-Slim Alouini, we have observed that they have worked (one part) with ABER vs Average SNR of quadrature amplitude modulation-based non-adaptive subcarrier intensity modulation with integer beta over the Málaga ( $\mathcal{M}$ ) turbulence channels for different turbulence conditions (turbulence conditions for integer beta Málaga ( $\mathcal{M}$ ) channels with alpha = 2.04, beta = 1 as strong; alpha = 2.296, beta = 2 as moderate; and alpha = 2.4, beta = 3 as light turbulence.) . The primary observation from figure 1 is that with the increasing value of SNR, the value of BER is decreasing. Also, with the increasing value of beta, the BER is decreasing. So, we can say the performance of BER is getting better with the increasing beta. On the other hand, in our paper we have worked(one part) with ABER vs transmit power of different modulation schemes with integer beta over the Malaga turbulence channels for different turbulence conditions (weak turbulence when, ( $=3.99$  and  $\beta=6$ ); ( $=3.99$ ,  $\beta=4$ ) it consider as moderate turbulence; and stronger turbulence when , ( $=3.50$  and  $\beta=2$  ). our figure 6.1 inferred that with the increasing value of transmit power, the value of ABER is decreasing that means performance of ABER is increasing and with the increasing beta, the ABER performance is increasing. Again, we know that SNR is proportional to transmit power and that is why there impacts on BER will be same. So, we can say that our observation is reliable based on the result of the attached paper.

## 6.3 Result and Discussion

In this chapter, we have explained all the Simulation output regarding the average bit error rate (ABER) performance of different modulation schemes over Málaga ( $\mathcal{M}$ ) atmospheric turbulence channel by varying four different parameters and they are divided into four sections as follows:

### 6.3.1 ABER Performance of Zero and Non-zero Boresight Pointing Errors for Different Turbulence Condition

The simulation results of average bit error rate (ABER) versus transmit power performance of different modulation schemes for zero and non-zero boresight pointing errors over Málaga ( $\mathcal{M}$ ) Turbulence channel is given below: The below figures (6.1 to 6.14) represents the ABER performance of different modulation scheme by varying different values of  $\alpha$  and  $\beta$  when, z

$= 4\text{Km}$ ,  $a = 0.1\text{m}$ ,  $s = 0.3\text{m}$   $\sigma = 8 \text{ dB/Km}$  over Málaga ( $\mathcal{M}$ ) atmospheric turbulence channel by considering the effect of zero and non-zero boresight pointing error. Here we have used Eight different modulation schemes and they are BPSK, QPSK, DPSK, RZ-OOK, NRZ-OOK, M-PPM, M-PAM and M-QAM (Where,  $M = 4, 8, 16$ ). Firstly, in Figure 6.1 we have compared the ABER performance of BPSK modulation by considering two cases, zero boresight pointing error and Non-zero boresight pointing error respectively. Generally, we know that for larger values of  $\alpha$  and  $\beta$ , less severe fading conditions is consider as weak turbulence ( $\alpha = 3.99, \beta = 6$ ) and at this condition values of ABER is lower and performances become improve. Also, when ( $\alpha = 3.99, \beta = 4$ ), it considers as moderate turbulence and smaller values of  $\alpha$  and  $\beta$ , which is consider as stronger turbulence when ( $\alpha, \beta = (3.50, 2)$ ).

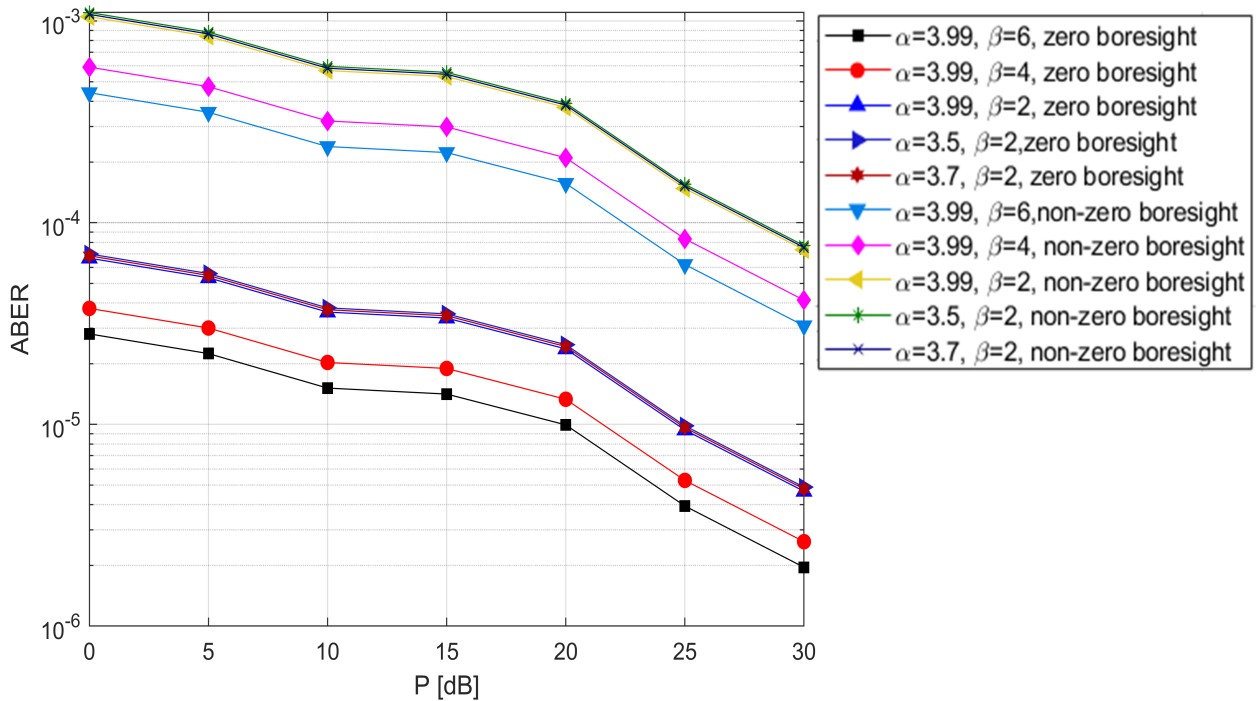
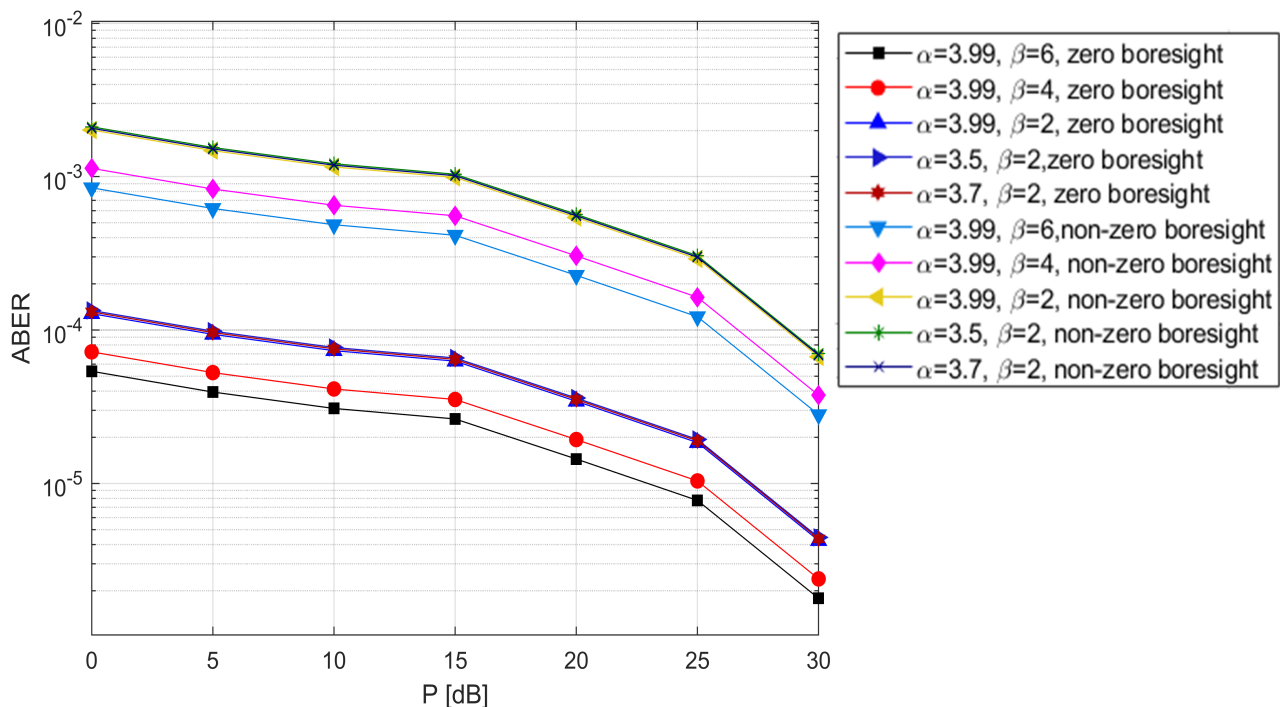


**Figure 6.1:** ABER performance of BPSK for zero and non-zero boresight pointing errors.

Now in Figure 6.1, we can see the ABER performance by varying the values of  $\alpha$  and  $\beta$  for zero boresight case. Where firstly we have set constant values of  $\alpha$  as 3.99 and varied the values of ( $\beta = 6, 4, 2$ ) respectively, then we can see when value of  $\beta$  is higher, ABER is low and with the decreasing values of  $\beta$ , we can see that ABER value is increasing. Then we have set constant values of  $\beta = 2$  and changed the values of  $\alpha$  and observe that ABER performance for ( $\alpha = 3.99, \beta = 2$ ) is same as the ABER for ( $\alpha = 3.5, 3.7, \beta = 2$ ). Also, there is no change in ABER when  $\beta$  is constant. On the other hand, for non-zero boresight case we can see that the ABER is higher than zero boresight case but the effect of varying values of  $\alpha$  and  $\beta$  is same as zero boresight case. Now it can be clearly seen that with the increasing value of power, the

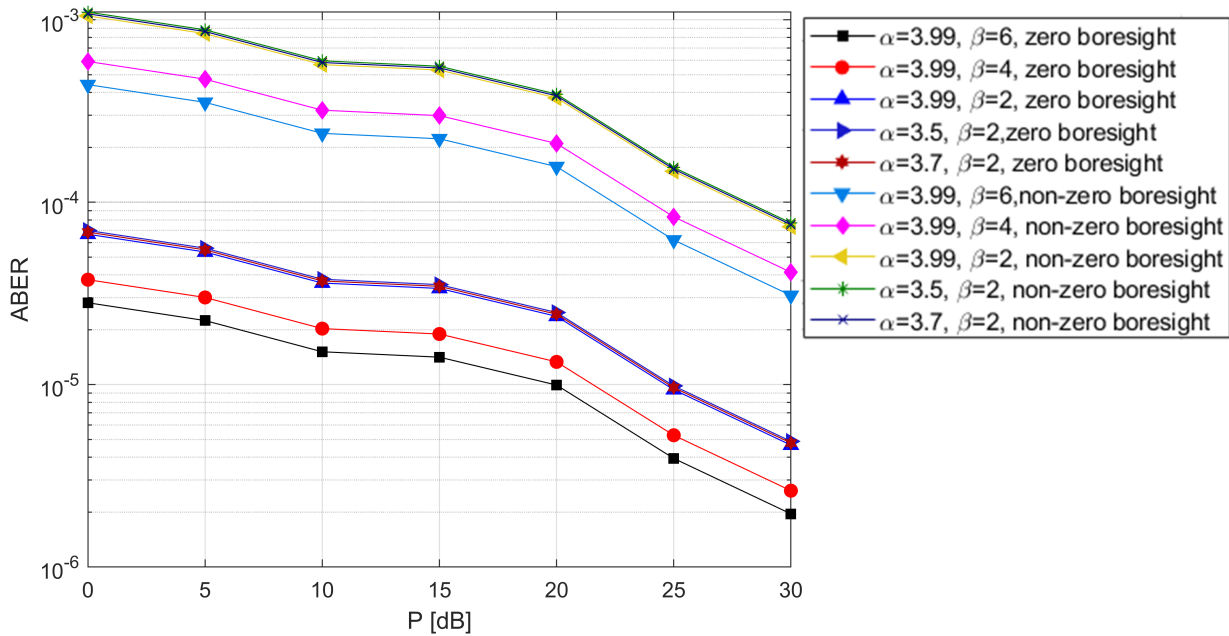
ABER is decreasing. At 30dB power, the ABER is within  $10^{-7}$  for zero boresight at ( $\alpha = 3.99$ ,  $\beta = 6$ ) and at ( $\alpha = 3.99$ ,  $\beta = 4, 2$ ) and ( $\alpha = 3.5, 3.7, \beta = 2$ ), ABER is within  $10^{-6}$ . Where for non-zero boresight case ABER is within  $10^{-5}$  at ( $\alpha = 3.99$ ,  $\beta = 6, 4, 2$ ), ( $\alpha = 3.5, 3.7, \beta = 2$ ). So, it is proved from the results that for larger values of parameters  $\alpha$  and  $\beta$ , ABER values is smaller and for small and moderate values of parameters  $\alpha$  and  $\beta$ , the ABER is higher. And also, we can said from figure 6.1 result that for varying values of  $\alpha$  (is large-scale scattering) there is no effect on ABER performance for BPSK when pointing error is considering under Málaga ( $\mathcal{M}$ ) atmospheric turbulence channel. On the other hand, when we are varying the values of  $\beta$  (effective number of small-scale effects), we have observed that it has effect on ABER performance. So finally, it can be seen that for a zero-boresight pointing error case, when boresight displacement is zero, system gives better performance but for a non-zero boresight pointing error, when boresight displacement is greater than zero ( $s = 0.3m$ ), the ABER is higher and system gives lower performance.

Figure 6.2 compared the ABER performance of QPSK modulation by considering two cases, zero boresight pointing error and Non-zero boresight pointing error respectively. So, we can see in result that the ABER is within  $10^{-6}$  for zero boresight and ABER is within  $10^{-5}$  for non-zero boresight at ( $\alpha = 3.99, \beta = 6, 4, 2$ ) and ( $\alpha = 3.5, 3.7, \beta = 2$ ).



**Figure 6.2:** ABER performance of QPSK for zero and non-zero boresight pointing errors.

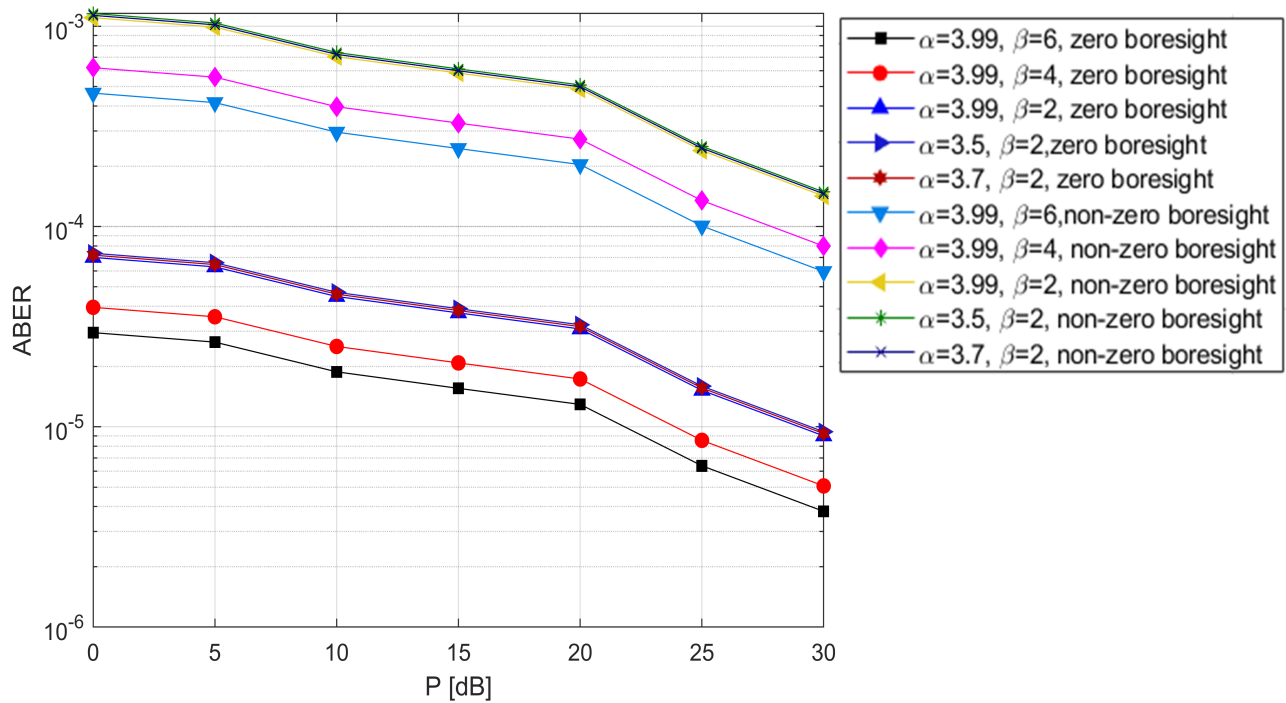
Figure 6.3 shows ABER performance of DPSK modulation for zero boresight pointing error and Non-zero boresight pointing error respectively. We can observe that for non-zero boresight case, ABER value is within  $10^{-5}$  and for zero boresight case, ABER value is less than  $10^{-5}$  at  $(\alpha = 3.99, \beta = 6, 4, 2)$  and  $(\alpha = 3.5, 3.7, \beta = 2)$ . Also, we can see that the performance of QPSK and DPSK is quite similar.



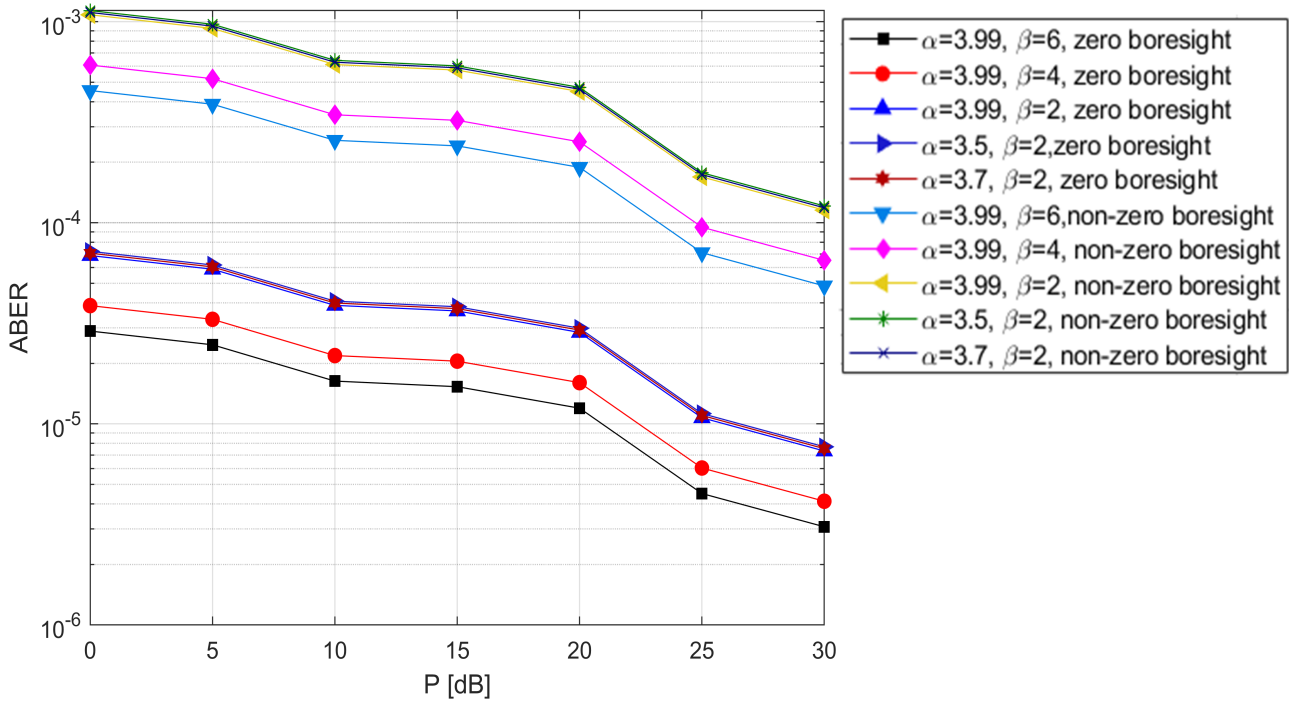
**Figure 6.3:** ABER performance of DPSK for zero and non-zero boresight pointing errors.

From figure 6.4 and 6.5, we can depict the ABER versus transmit power of NRZ-OOK and RZ-OOK modulation for zero boresight pointing error and Non-zero boresight pointing error respectively. By comparing them, we can see that the ABER value is less in case of RZ-OOK. So, we can conclude that the ABER performance of RZ-OOK is better than NRZ-OOK.

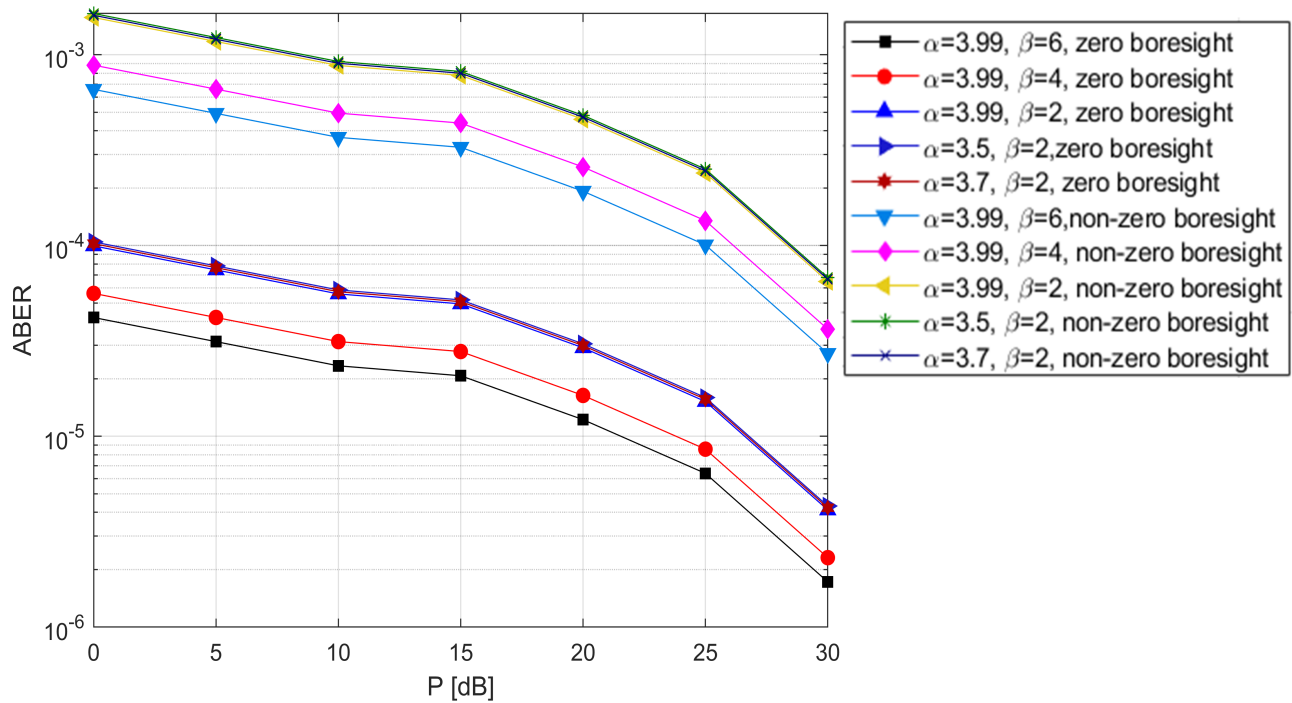
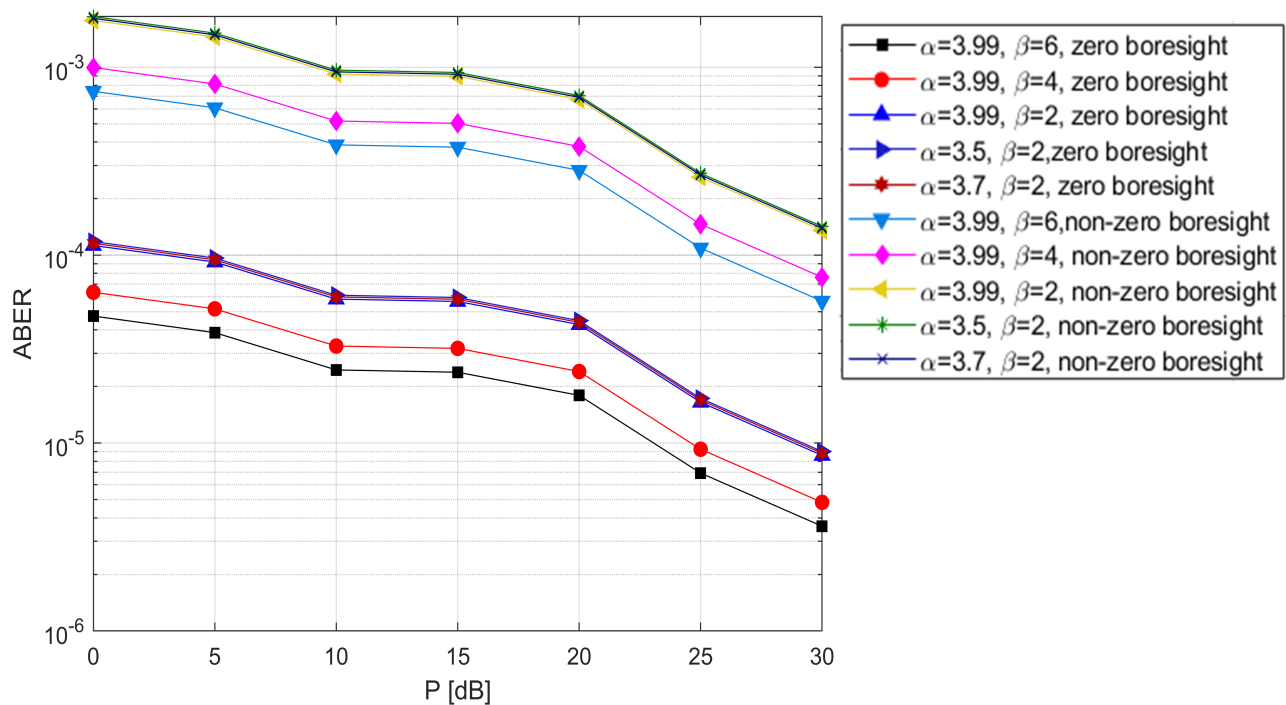
We can see the change of ABER against the transmit power of 4-QAM, 8-QAM and 16-QAM modulation respectively for zero boresight pointing error and Non-zero boresight pointing error in figures 6.6, 6.7 and 6.8. Where we can see that in figure 6.6 the ABER performance of 4-QAM is better than 8-QAM and 16-QAM. It can be said that with the increasing value of M, the value of ABER is increasing that means the performance of ABER is degrading.



**Figure 6.4:** ABER performance of NRZ-OOK for zero and non-zero boresight pointing errors.



**Figure 6.5:** ABER performance of RZ-OOK for zero and non-zero boresight pointing errors.

**Figure 6.6:** ABER performance of 4-QAM for zero and non-zero boresight pointing errors.**Figure 6.7:** ABER performance of 8-QAM for zero and non-zero boresight pointing errors.

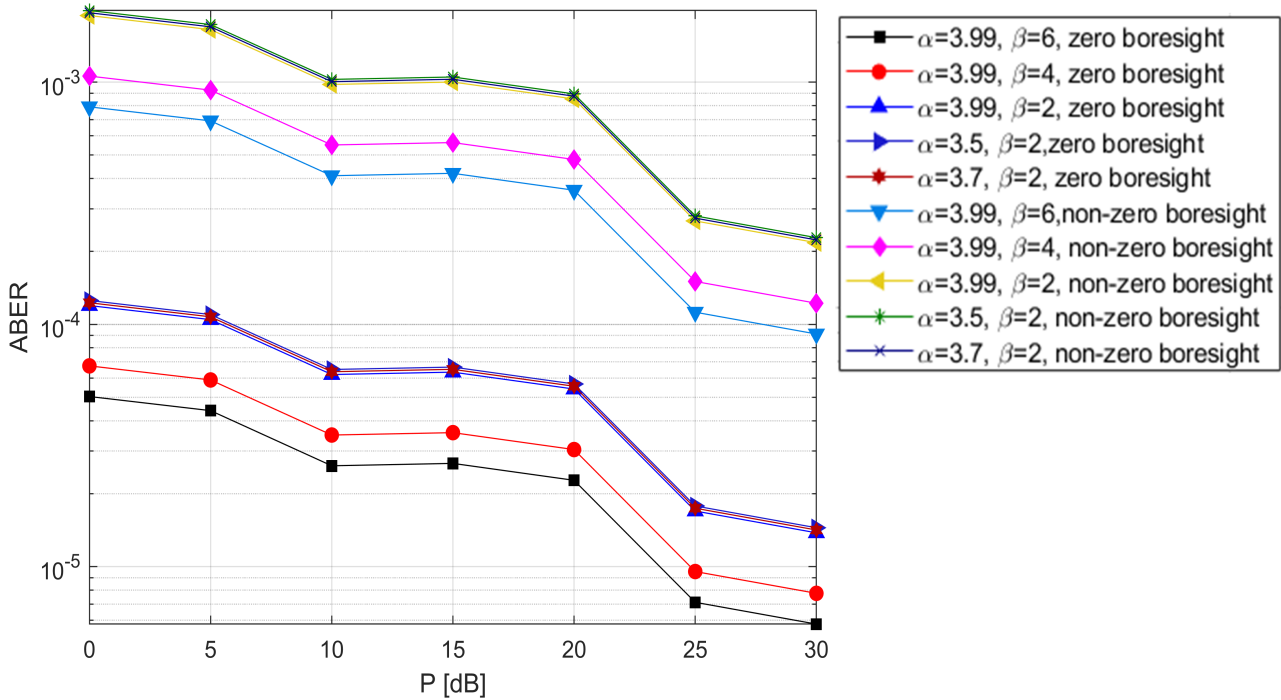


**Figure 6.8:** ABER performance of 16-QAM for zero and non-zero boresight pointing errors.

In figures 6.9, 6.10 and 6.11 we can observe the relation between the ABER and transmit power of 4-PAM, 8-PAM and 16-PAM modulation respectively for zero boresight pointing error and Non-zero boresight pointing error. Now from these results we can observe that the 4-PAM gives lowest ABER values compared to 8 and 16 PAM. In addition, one thing we can clearly see that that the ABER performance gap between zero boresight Non-zero boresight pointing error for 4-8-16 PAM is very higher compare to other modulation schema that till now we discuss. So it can be said that in M-PAM modulation zero boresight and Non-zero boresight pointing error is higher domination each other.

From figures 6.12, 6.13 and 6.14, we can see that the performance of ABER of 4-PPM, 8-PPM and 16-PPM modulation respectively for zero boresight pointing error and Non-zero boresight pointing error. Where we can see that from mentioned figures, that with the increasing value of M, the performance of ABER is getting better. Now for 8-PPM at 30 dB power we can see that for non-zero boresight case, ABER values is within  $(10^{-5}-10^{-4})$  at  $(\alpha = 3.99, \beta = 6, 4, 2)$  and  $(\alpha = 3.5, 3.7, \beta = 2)$ . Where for zero boresight case, ABER is  $10^{-6}$  at  $(\alpha = 3.5, 3.7, \beta = 2)$ ) and ABER is within  $10^{-7}$  at  $(\alpha = 3.99, \beta = 6, 4)$ . On the other hand we can see that the ABER performance of 16-PPM at 30 dB power is very well compare to 4-PPM and 8-PPM. ABER is greater and  $10^{-9}$  at  $(\alpha = 3.99, \beta = 6, 4, 2)$  and around  $10^{-8}$  at  $(\alpha = 3.99, 3.5, 3.7, \beta = 2)$  for zero boresight case, Where for non-zero boresight case at  $(\alpha = 3.99, \beta = 6, 4, 2)$  ABER is  $10^{-7}$  and at  $(\alpha = 3.99, 3.5, 3.7, \beta = 2)$  ABER is greater than  $10^{-7}$ .

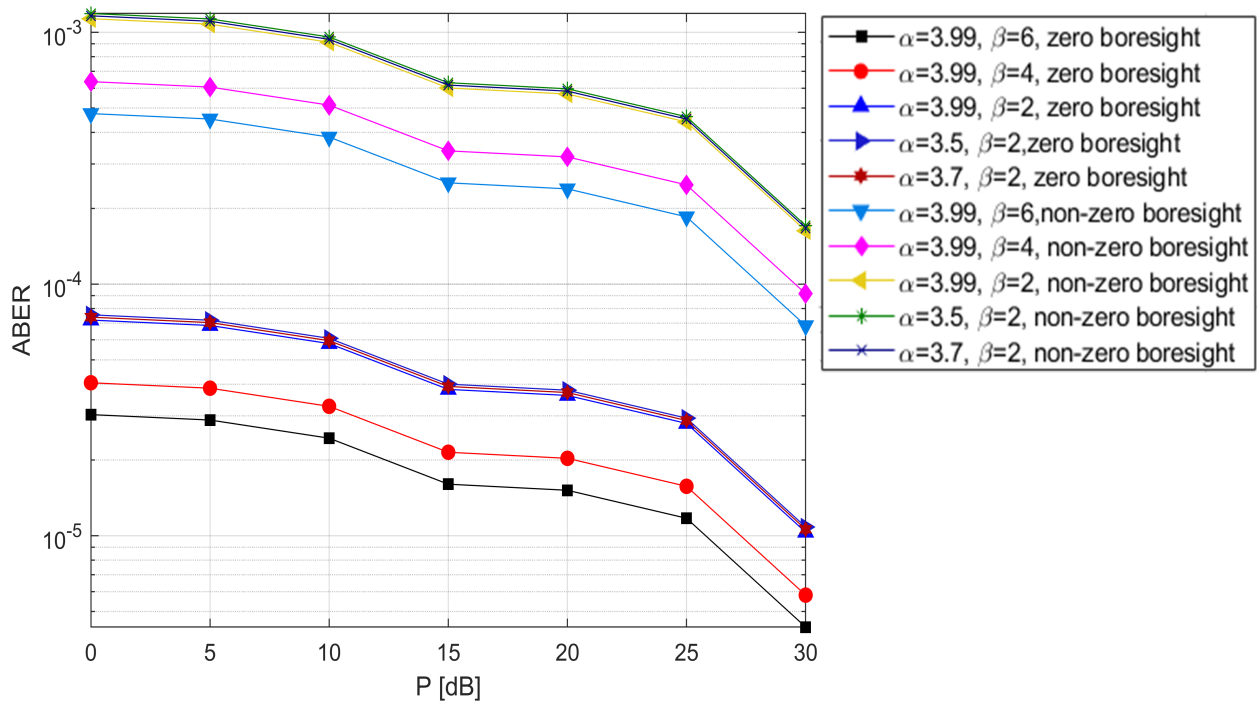


**Figure 6.9:** ABER performance of 4-PAM for zero and non-zero boresight pointing errors.

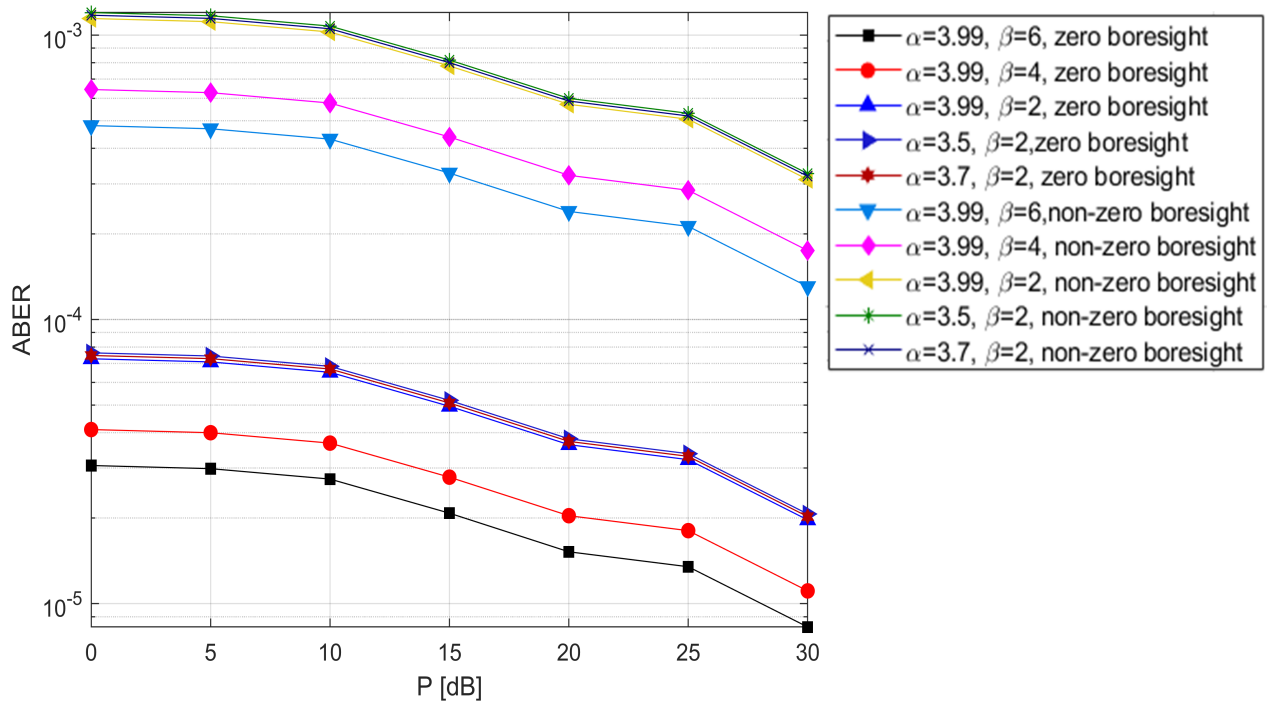


**Figure 6.10:** ABER performance of 8-PAM for zero and non-zero boresight pointing errors.

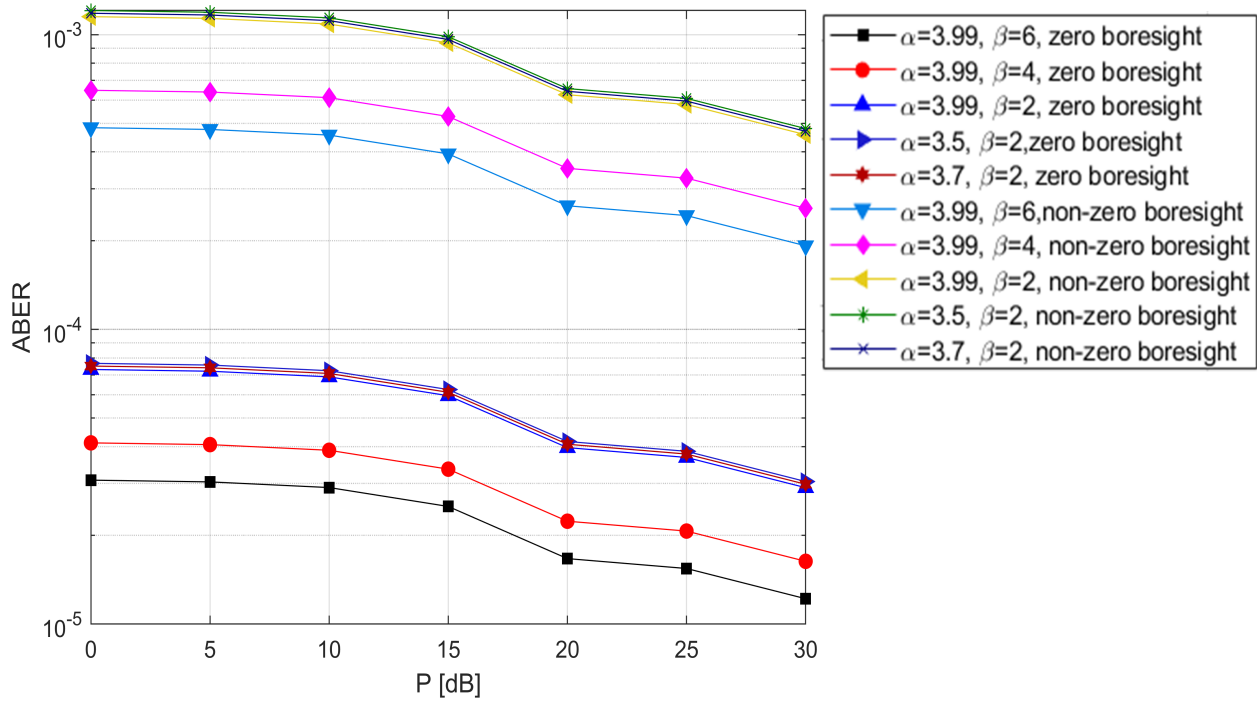


Figure 6.11: ABER performance of 16-PAM for zero and non-zero boresight pointing errors.

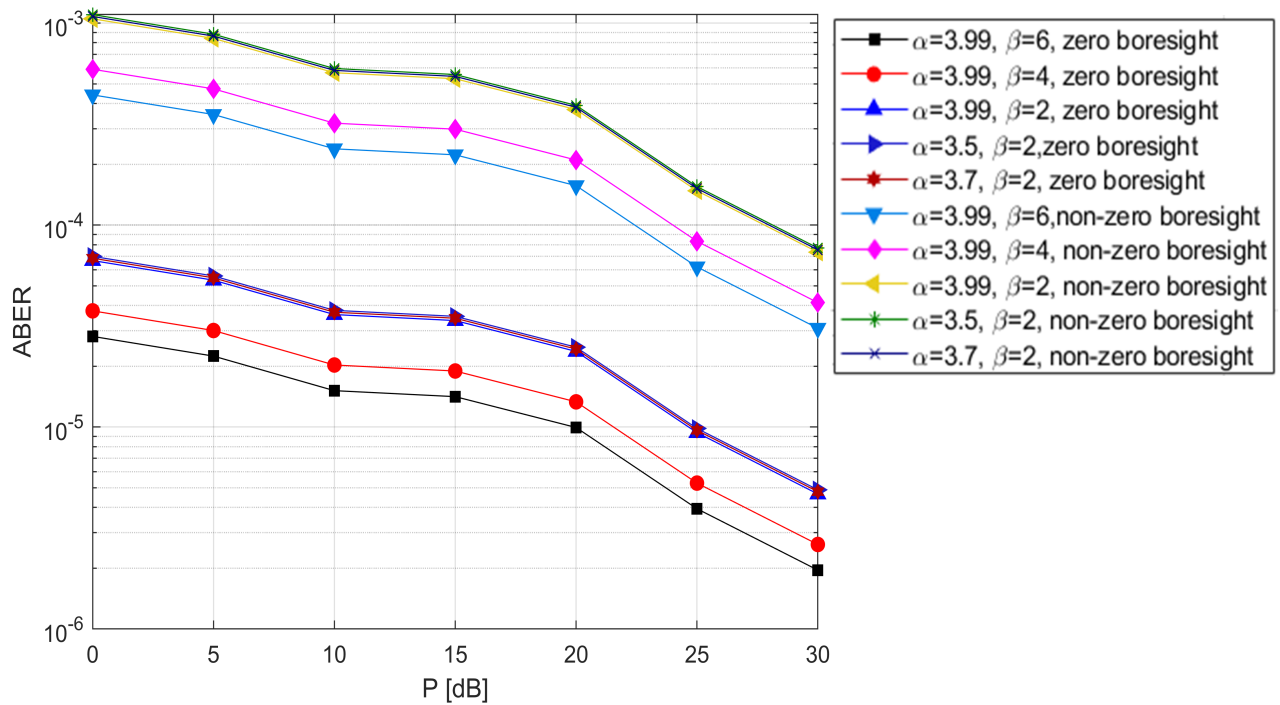
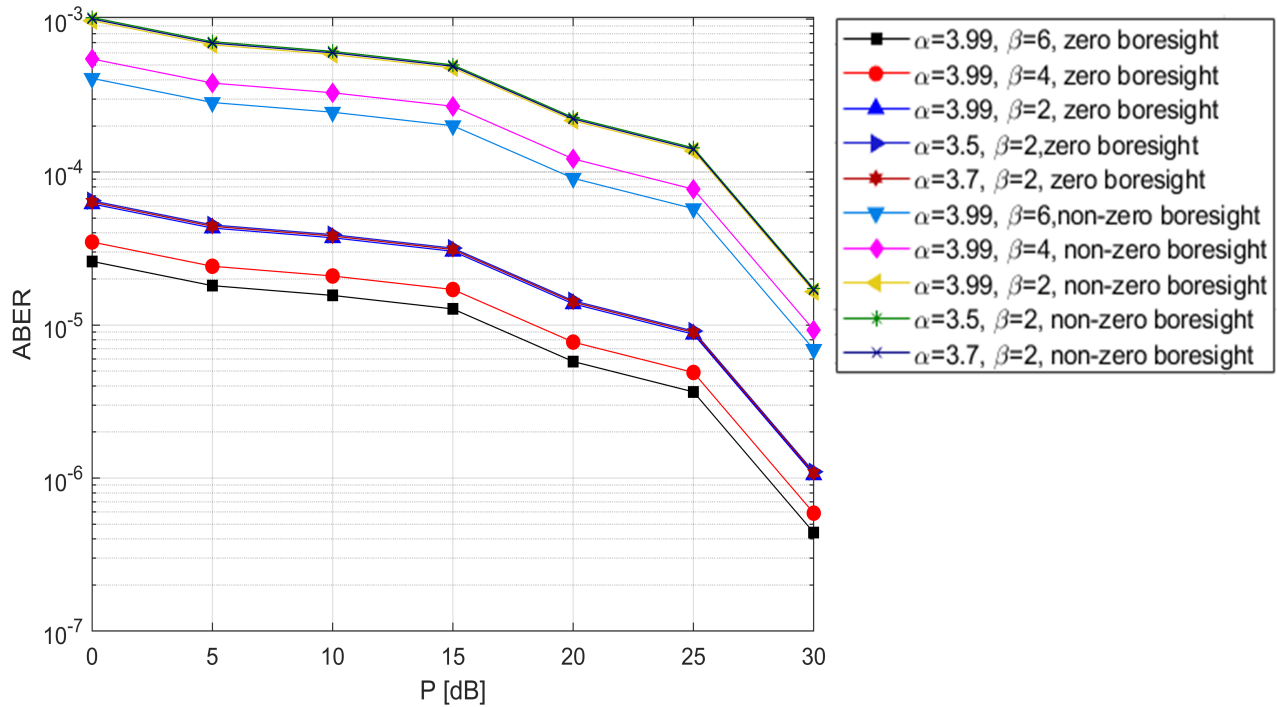
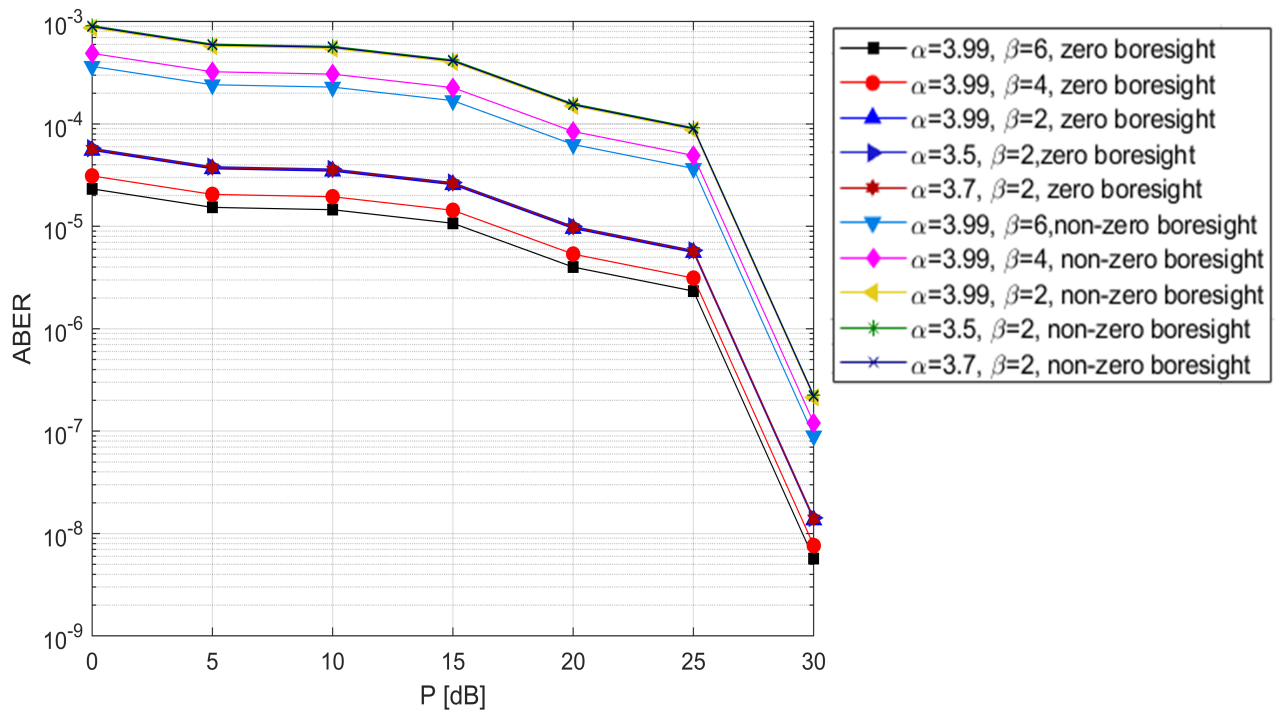


Figure 6.12: ABER performance of 4-PPM for zero and non-zero boresight pointing errors.



**Figure 6.13:** ABER performance of 8-PPM for zero and non-zero boresight pointing errors.



**Figure 6.14:** ABER performance of 16-PPM for zero and non-zero boresight pointing errors.

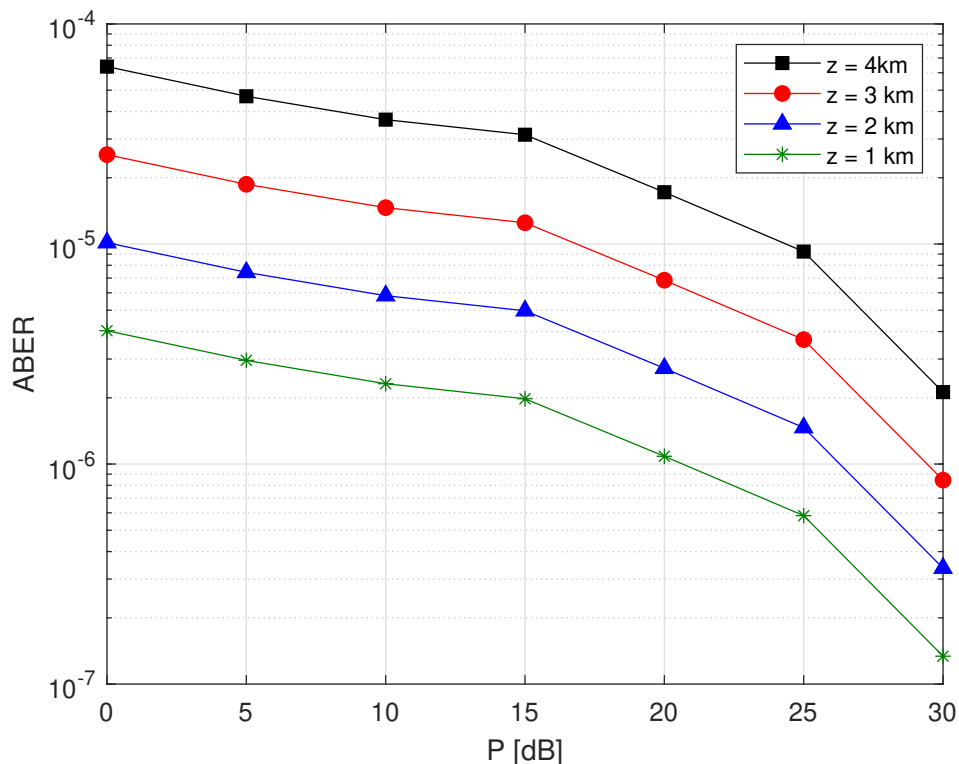
Finally after observing all the simulation results we observe that 16-PPM, 8-PPM, BPSK, 4-PPM, DPSK, QPSK, 4-QAM this 7 modulation schemes giving the best results to achieving lowest ABER value when we consider zero boresight pointing error and Non-zero boresight pointing error at 30 dB power. Moreover, 16-PPM is giving the best ABER performance compare to rest of the modulation scheme used here.

### 6.3.2 ABER Performance for Different Propagation link Distance

The simulation results on ABER performance of different modulation schemes for different propagation link distance over Málaga ( $\mathcal{M}$ ) Turbulence channel is given below:

The below figures (6.15 to 6.26) represents the ABER performance of different modulation scheme for different propagation link distance ( $Z = 1, 2, 3, 4$  Km) over Málaga ( $\mathcal{M}$ ) atmospheric turbulence channel by considering the effect of non-zero boresight pointing error. Here we have used Eight different modulation schemes and they are BPSK, QPSK, DPSK, RZ-OOK, NRZ-OOK, M-PPM, M-PAM and M-QAM (Where,  $M = 4, 8, 16$ ).

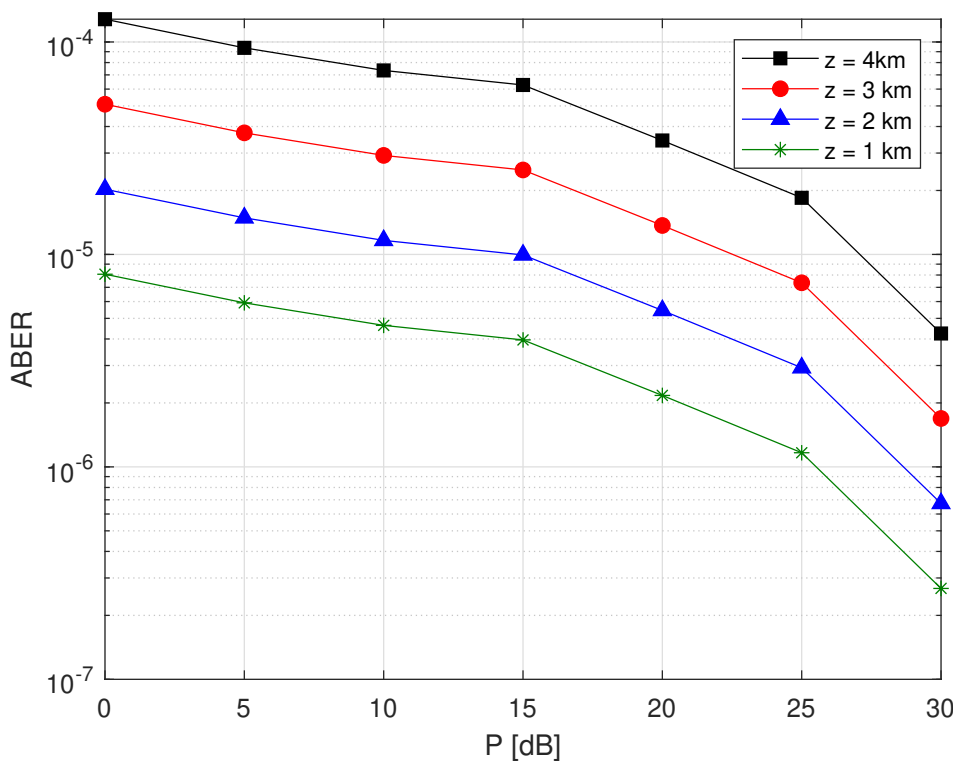
So firstly, in figure 6.15 we can see that the ABER performance of BPSK modulation for different link distance.



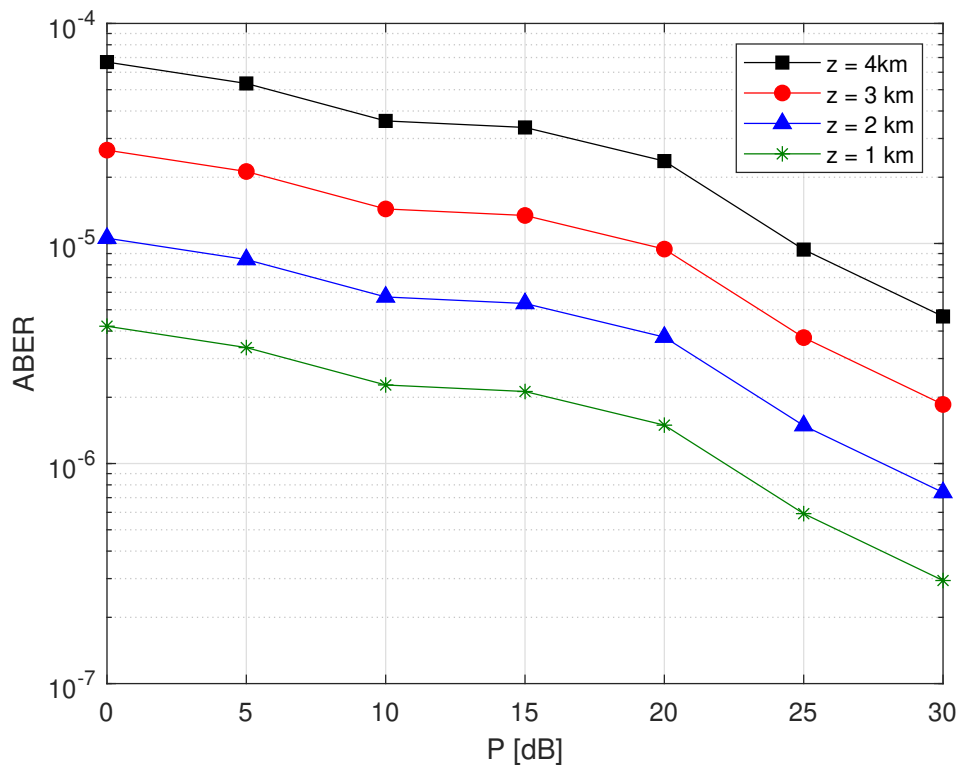
**Figure 6.15:** ABER performance of BPSK for different propagation link distance

Here, it can be observed that ABER of BPSK is increasing with the increasing value of the propagation link distance from 1Km to 4Km. As we know that when the propagation link distance is small, less bit error occurs and for larger link distance, possibility of bit error will rise. Again, we can observe that for specific value of transmit power the BER is increasing with distance, the cause behind this scenario is laser power depends on link distance and due to this reason path loss can vary as path loss is also depends on link distance. Therefore, we can say that with the increasing value of link distance due to path loss the bit error is increasing. Now the most noticeable thing is with the increase of transmit power the average bit error rate (ABER) decreased which means that ABER performance is becoming well with the increasing value of transmit power. Now At 30 dB power we can see that the BER performance is much better. That means when power become high, we will get better performance.

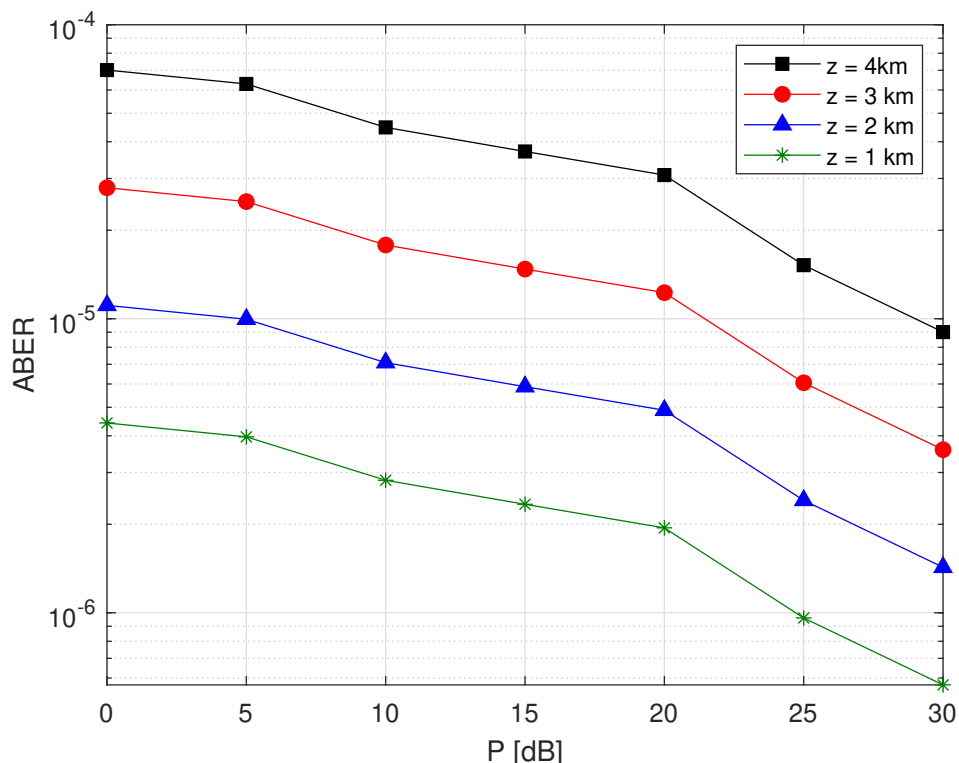
In figure 6.16 and 6.17, we can notice the ABER performance of QPSK and DPSK modulation respectively for different link distances. By comparing them with figure 6.15 which represent the ABER performance of BPSK modulation, we can say that for BPSK modulation we are getting far better result for ABER. As we can see clearly that in BPSK, for a specific propagation link distance such as 4km, the value of ABER is smaller than compare to QPSK and DPSK modulation scheme.



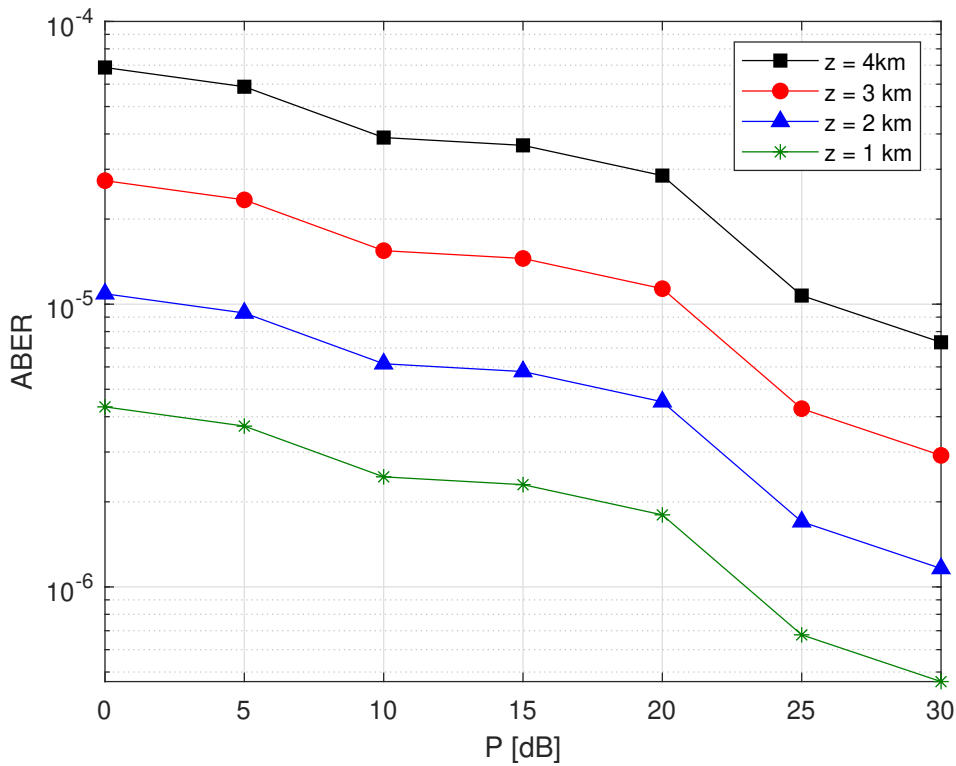
**Figure 6.16:** ABER performance of QPSK for different propagation link distance



**Figure 6.17:** ABER performance of DPSK for different propagation link distance



**Figure 6.18:** ABER performance of NRZ-OOK for different propagation link distance



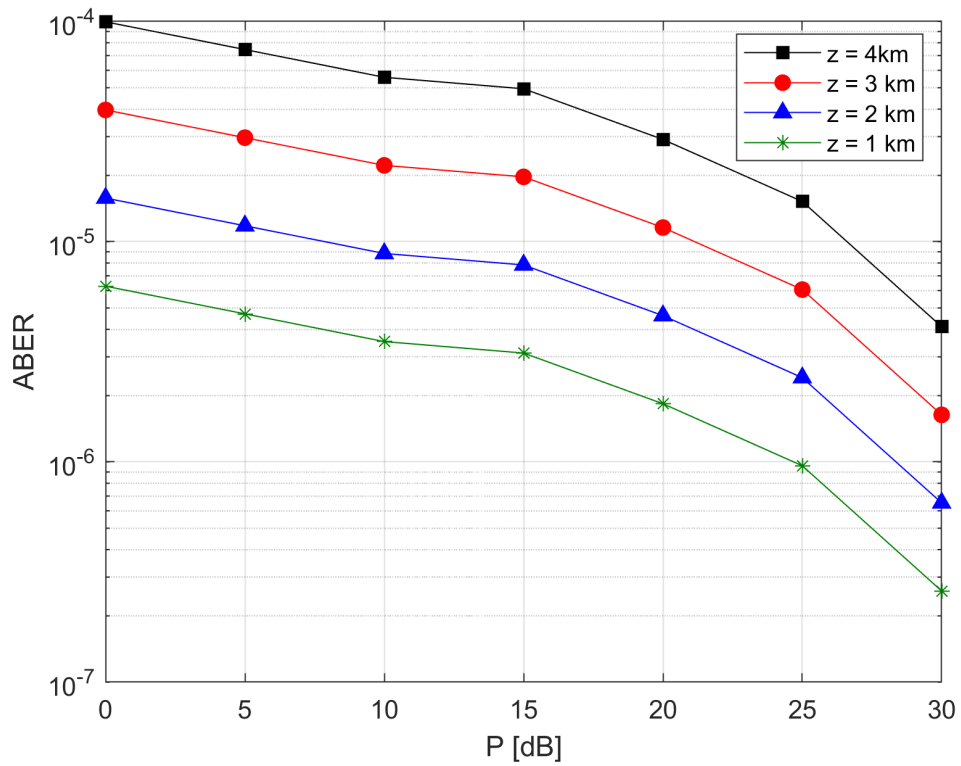
**Figure 6.19:** ABER performance of RZ-OOK for different propagation link distance

Figure 6.19 and 6.18 Shows the relation between the ABER and transmit power of RZ-OOK and NRZ-OOK modulation for different link distances. It can be observed that the graphs for different propagation link distances in NRZ-OOK is more linear than the graphs in RZ-OOK. But for RZ-OOK the value of ABER is smaller than compare to NRZ-OOK.

Figure 6.20, 6.21 and 6.22 depicts the ABER vs transmit power of 4-QAM, 8-QAM and 16-QAM for different propagation link distances. It can be observed from these figures that with the increasing value of M, the performance of ABER is degrading in the scenario for different propagation link distance.

In figure 6.23, we can see the performance of ABER of 4-PAM modulation scheme for different propagation link distances. From the figure we can observe that simply with the increasing value of transmit power the ABER is decreasing and the figure is quite linear. We also have tried to plot figures of 8-PAM and 16-PAM but got disappointing value for ABER.

Figures 6.24, 6.25 and 6.26 represents the change in ABER against the transmit power of 4-PPM, 8-PPM and 16-PPM for different propagation link distances. It is clearly demonstrated from these figures that, with the increasing value of M, the performance of ABER is improving. But the figure for 16-PPM is noticeably proves to be the best compared to the 4-PPM and 8-PPM.



**Figure 6.20:** ABER performance of 4-QAM for different propagation link distance

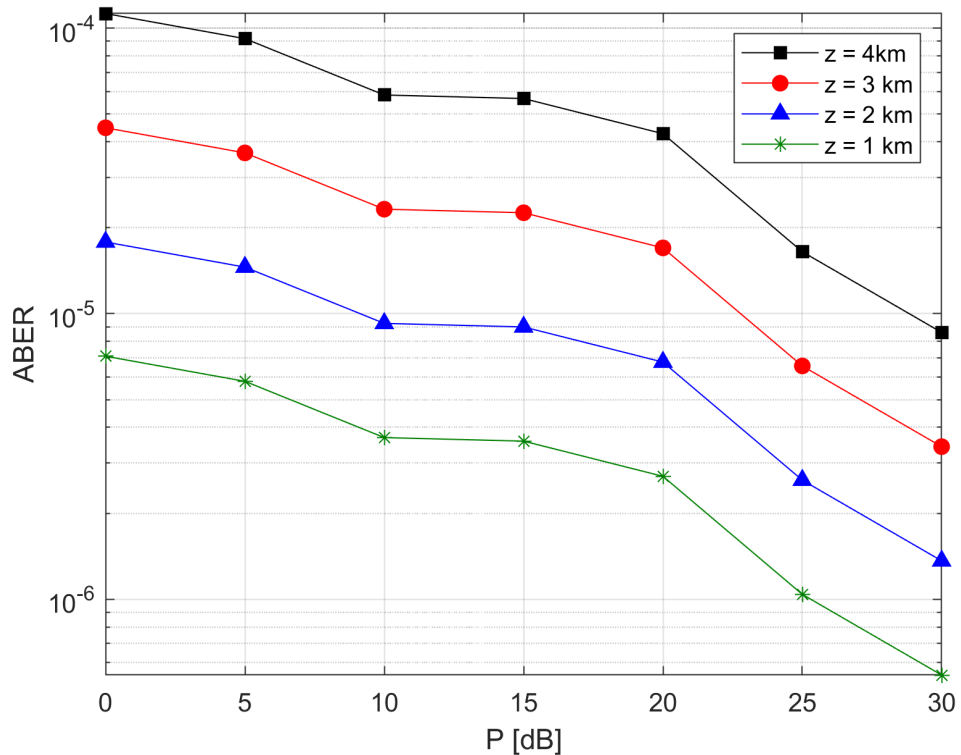


**Figure 6.21:** ABER performance of 8-QAM for different propagation link distance

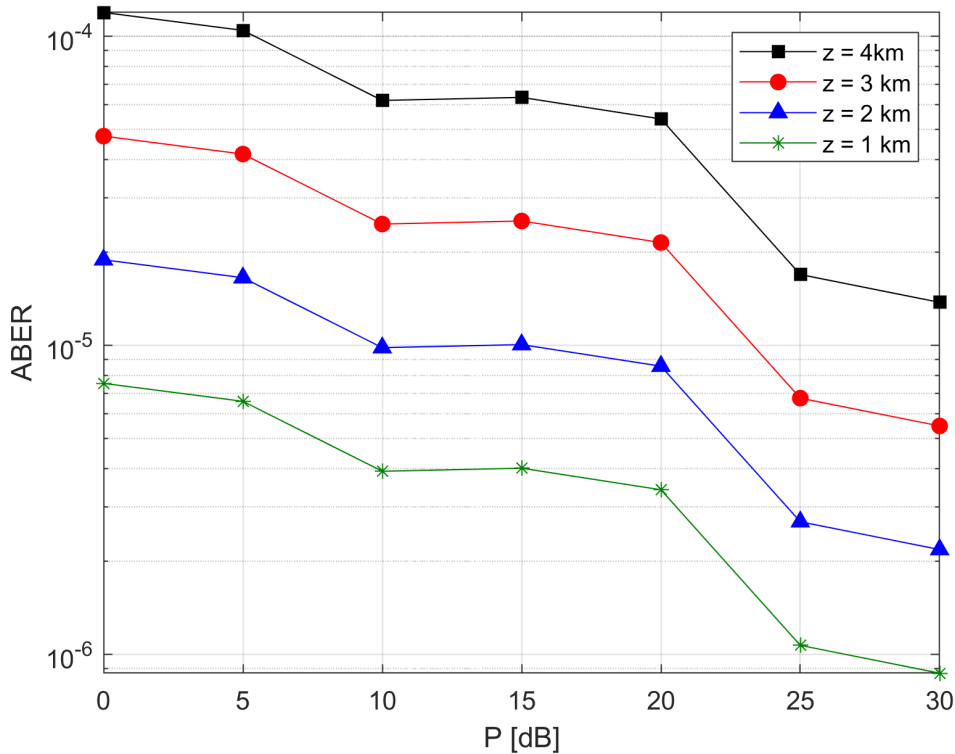


**Figure 6.22:** ABER performance of 16-QAM for different propagation link distance

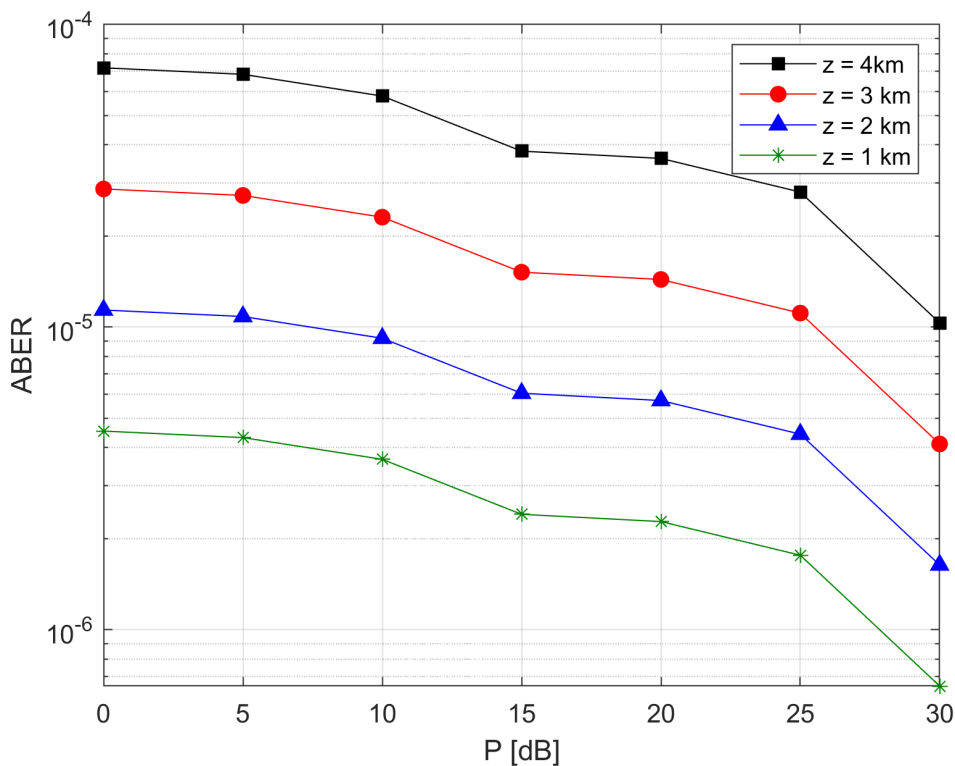


**Figure 6.23:** ABER performance of 4-PAM for different propagation link distance

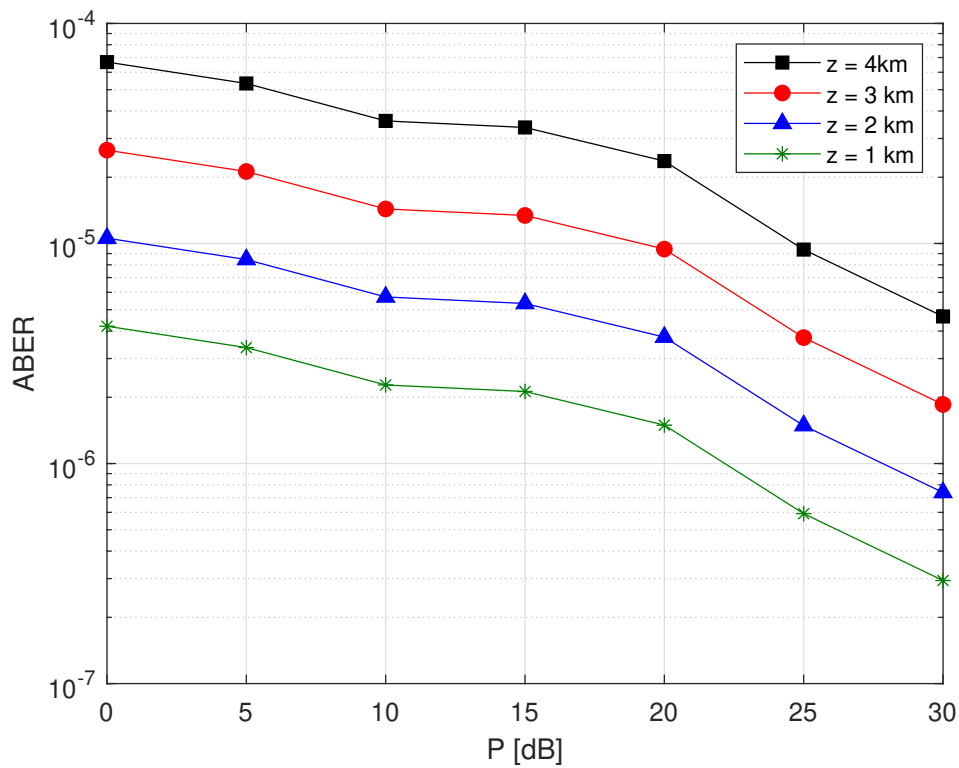


Figure 6.24: ABER performance of 4-PPM for different propagation link distance

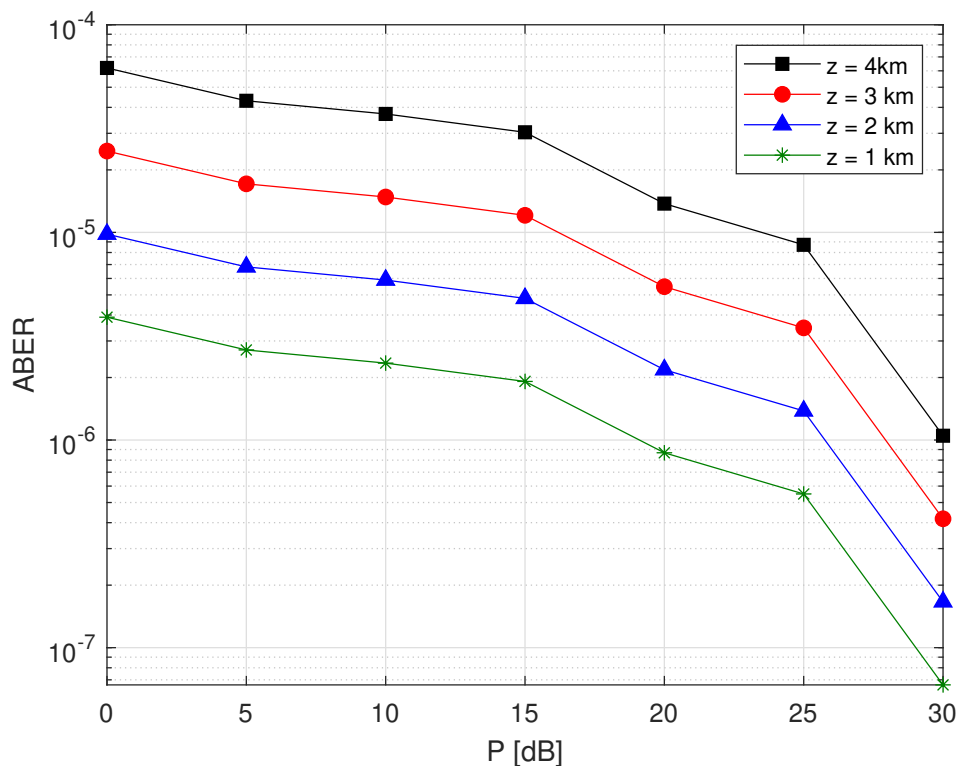
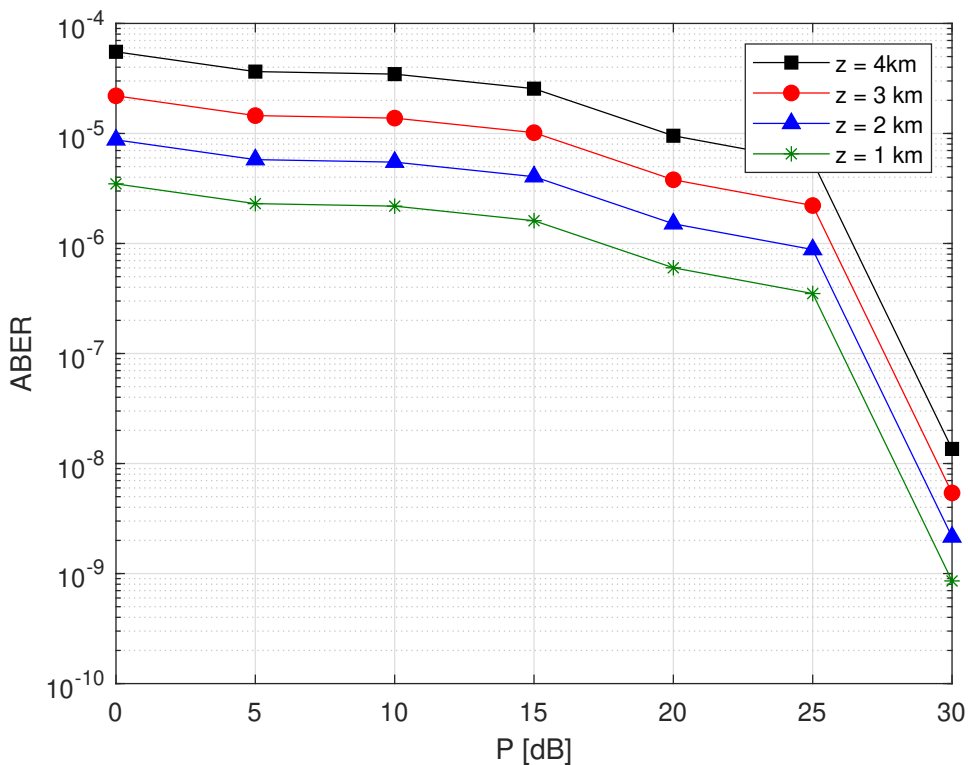
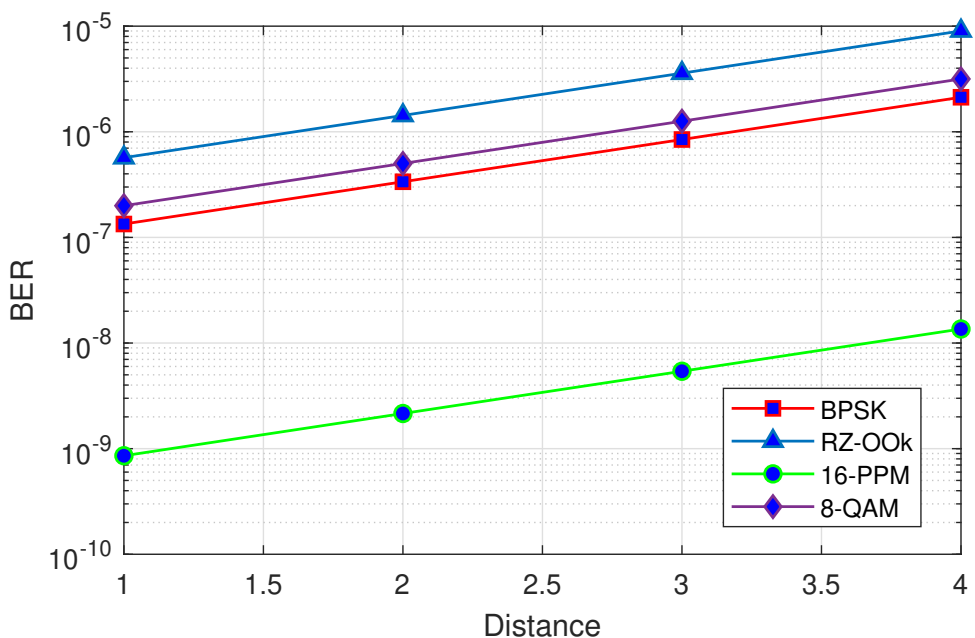


Figure 6.25: ABER performance of 8-PPM for different propagation link distance



**Figure 6.26:** ABER performance of 16-PPM for different propagation link distance



**Figure 6.27:** Comparison between four different modulationn for different propagation link distance

Again, from figure 6.15 to 6.26, it can be inferred that the difference between the four propagation link distances (1km, 2km, 3km and 4km), BER performance is not same all time, and difference between the path performances is decreasing with the increasing value of power.

Now finally to identify which modulation gives the best result, we are plotting a new graph BER vs Distance that can be seen in figure 6.27. Here in our result, some modulation gives the same result. Therefore, by considering those modulations, we are choosing the four modulation scheme such 16-PPM, BPSK, 8-QAM, RZ-OOK. We can see that at figure 6.27 among this four-modulation and the rest of the modulation 16-PPM gives the lowest ABER result for low to high distance (1Km-4Km) and other 3 modulations and the rest of the modulation gives a fairly good ABER performance compare to 16-PPM. Overall 16-PPM,4-PAM, BPSK, 4-QAM, 8-QAM gives the best results of all the modulation schemes listed above.

### 6.3.3 ABER Performance for Different Weather Conditions

The simulation results of average bit error rate (ABER) versus transmit power of different modulation schemes for different weather condition over Málaga ( $\mathcal{M}$ ) Turbulence channel is given below: The below figures (6.28 to 6.55) represents the ABER performance of different modulation scheme by varying the attenuation coefficient for different weather (Very clear, Haze, light fog) conditions over Málaga ( $\mathcal{M}$ ) atmospheric turbulence channel by considering the effect of non-zero boresight pointing error and taking two turbulence condition Weak turbulence( $\alpha = 3.99, \beta = 6$ ) and strong turbulence( $\alpha = 3.5, \beta = 2$ ) with fixed distance ( $Z = 4\text{Km}$ ). Here we have used eight different modulation schemes and they are BPSK, QPSK, DPSK, RZ-OOK, NRZ-OOK, M-PPM, M-PAM and M-QAM (Where,  $M = 4, 8, 16$ ).

Firstly, in figure (6.28 & 6.29), we have compared the ABER performance of BPSK modulation for different weather conditions such as Very clear, Haze, and light fog under Weak and strong turbulence respectively. As we know, in FSO system, ABER performance becomes degraded when the weather condition change from very clear air -haze-light fog and one important thing is ABER performance is always low for light fog condition compare to other weather condition. Moreover, it can be confirm from figure (6.28 & 6.29).

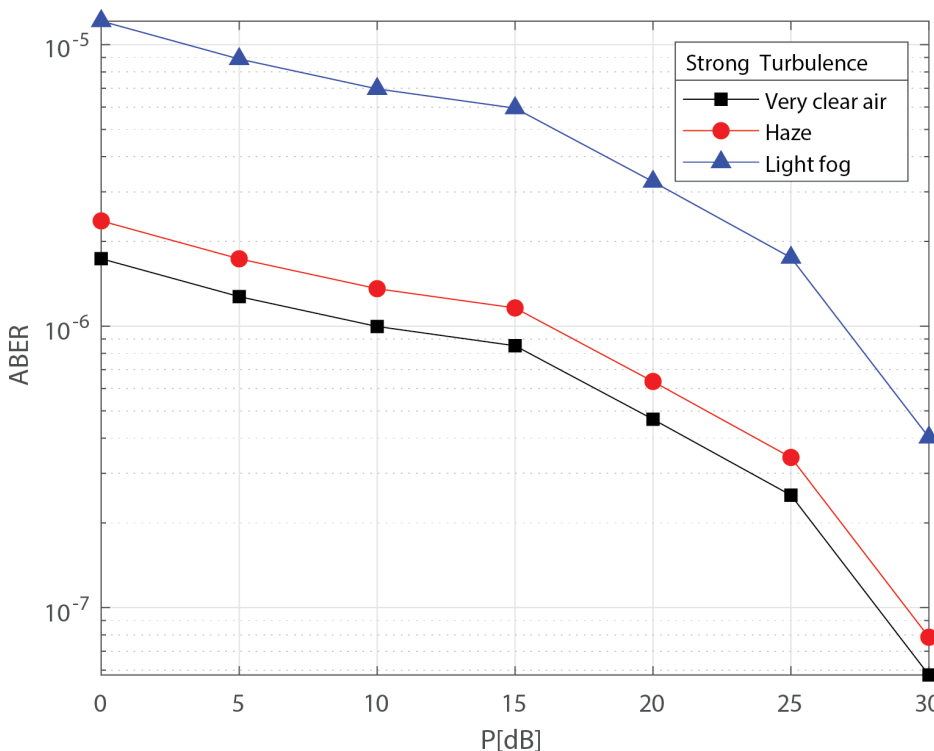


**Figure 6.28:** ABER performance of BPSK for different weather condition under strong turbulence.

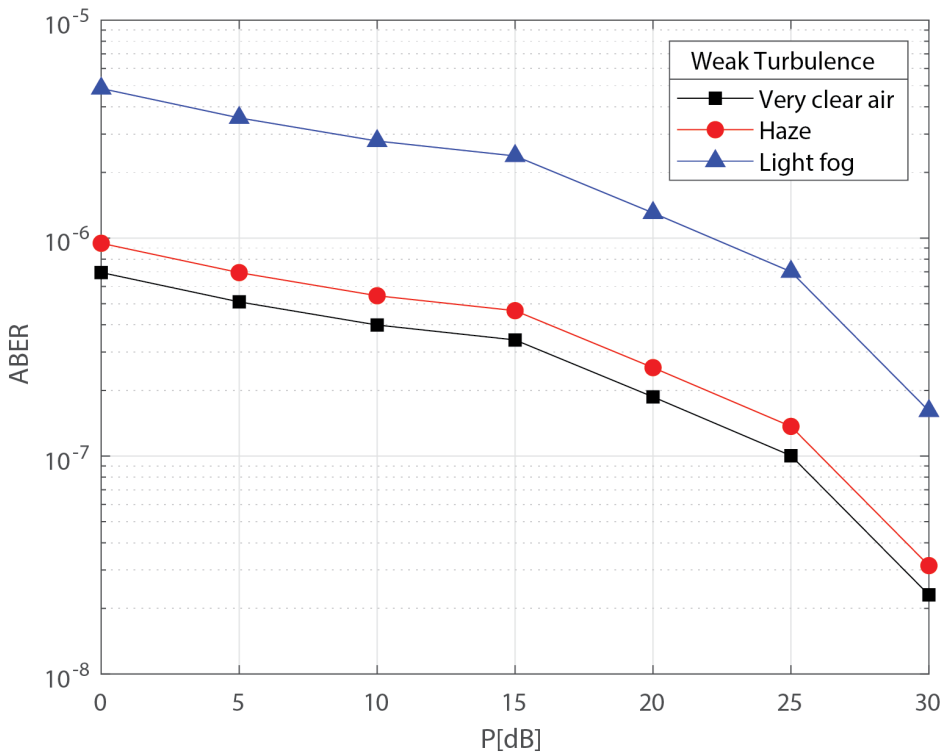


**Figure 6.29:** ABER performance of BPSK for different weather condition under weak turbulence.

In addition, we also know that in weak turbulence ABER shows better performance compares to strong turbulence condition. Therefore, it can be clearly observed in Figure 6.29 that the ABER performance for weak turbulence is better than the ABER performance of strong turbulence for BPSK modulation that is shown in Figure 6.28 . Also from Figure 6.28 for strong turbulence, it can be observed that the ABER is high at low transmit power but when the transmit power is 30 dB ABER is around  $10^{-7}$  for very clear air and for light fog ABER is less than  $10^{-6}$ ). So it can be justified that as weather conditions change from very clear air to light fog ABER increased. Now in figure 6.29 for weak turbulence, ABER is greater than  $10^{-8}$  and less than  $10^{-7}$  at 30 dB power for very clear and haze condition where for light fog ABER is around  $10^{-7}$ .

In Figurer 6.30 & 6.31, we can notice that for QPSK modulation the value of ABER is less than compare to BPSK for both weak and strong turbulence. In Figure 6.31, can be seen that ABER performance of QPSK modulation under weak turbulence is quite same as the ABER performance of BPSK under strong turbulence.

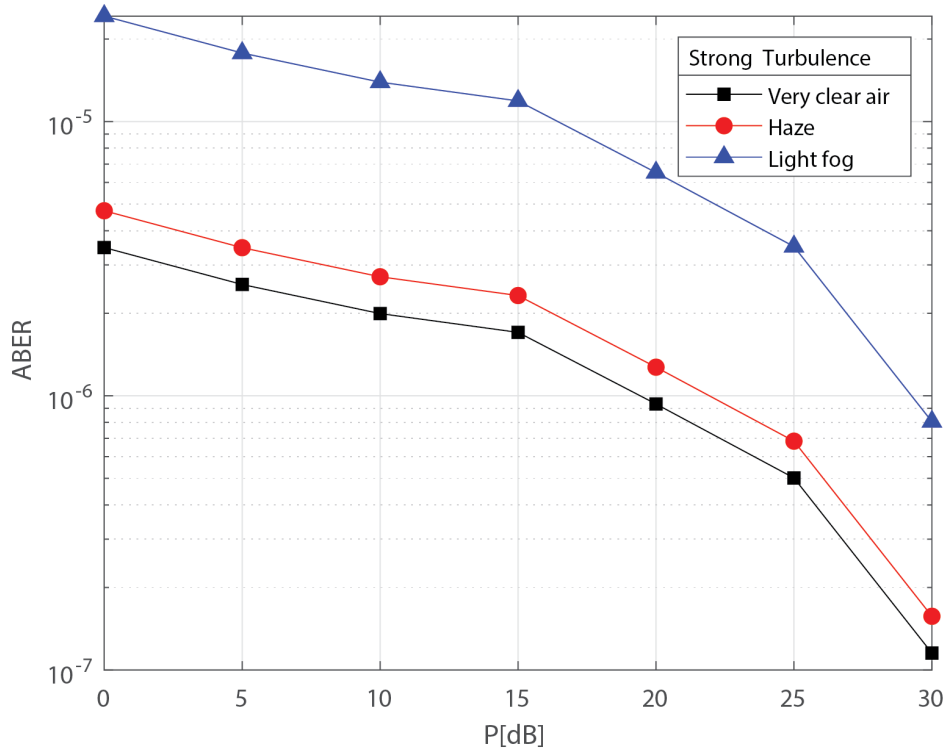


**Figure 6.30:** ABER performance of QPSK for different weather condition under strong turbulence.

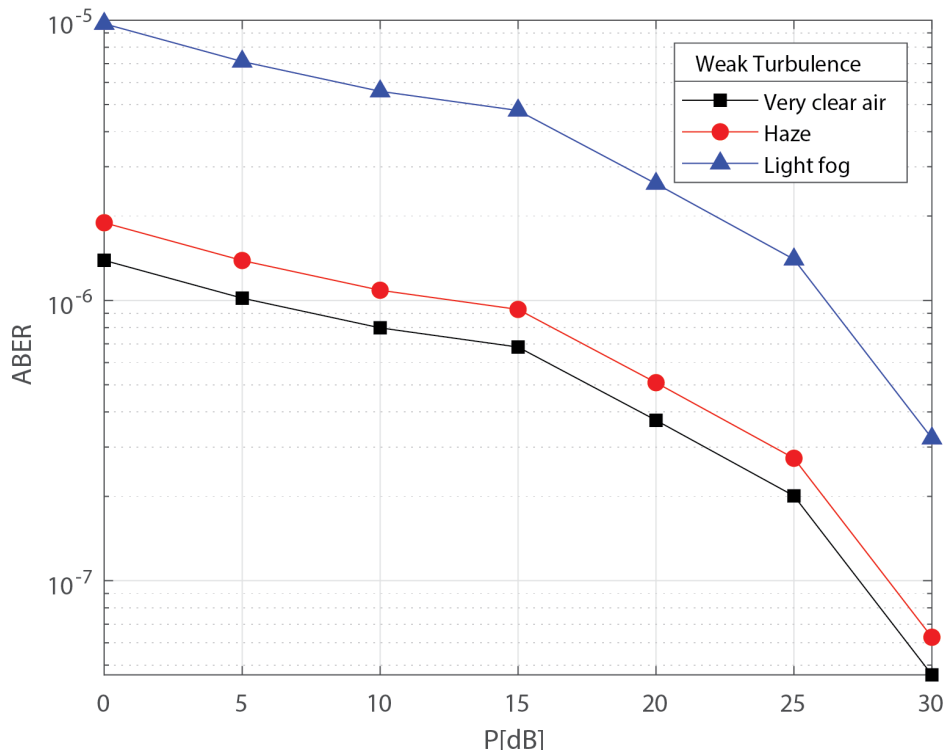


**Figure 6.31:** ABER performance of QPSK for different weather condition under weak turbulence.

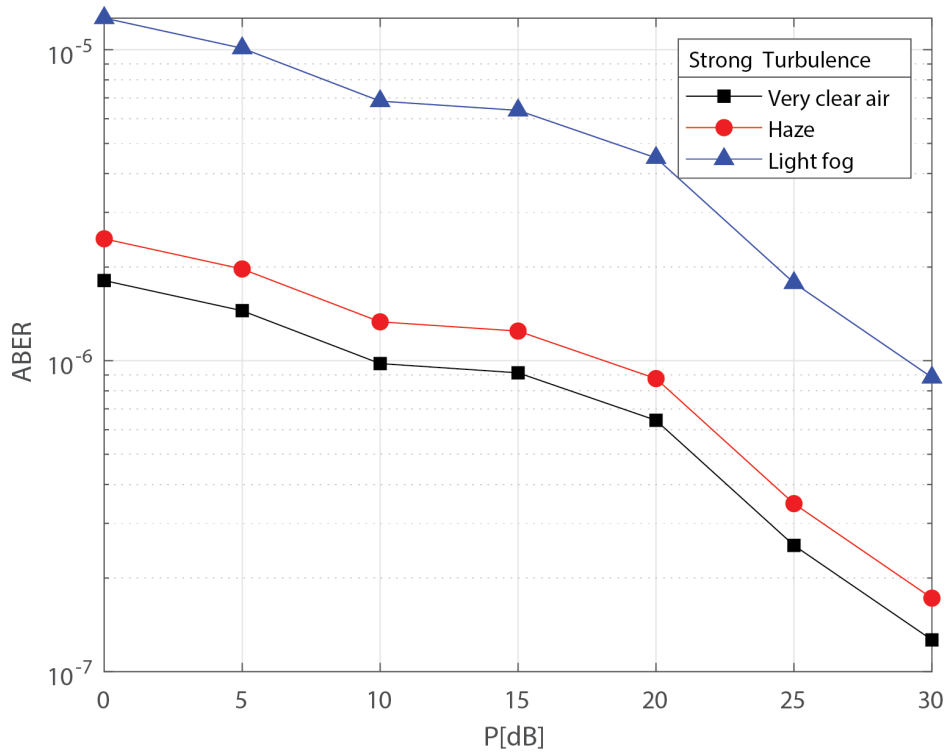


**Figure 6.32:** ABER performance of DPSK for different weather condition under strong turbulence.

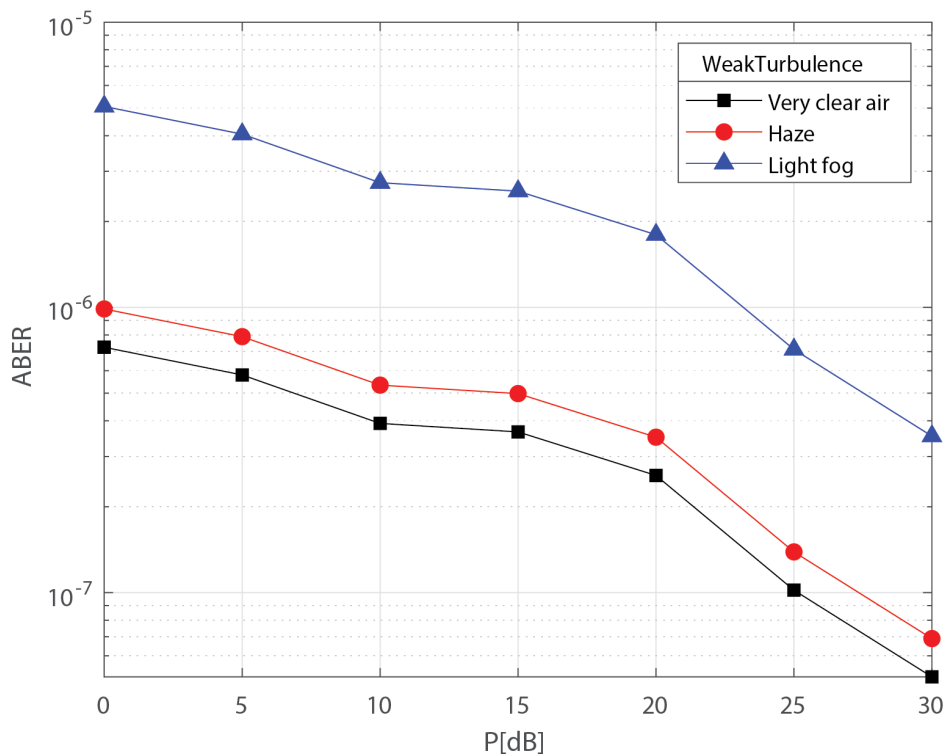


**Figure 6.33:** ABER performance of DPSK for different weather condition under weak turbulence.

On the other hand, it can be inferred from Figure 6.32 that at transmit power 30 dB the value of ABER for DPSK modulation is  $10^{-7}$  for very clear air and around  $10^{-6}$  for light fog under strong turbulence. Moreover, in figure 6.33 under weak turbulence, value of ABER for haze and clear air is around  $10^{-8}$  and for light fog, ABER is  $10^{-7}$ .

From Figure, 6.34 and 6.35 we can see that for NRZ-OOK modulation at 30dB power the value of ABER is respectively  $10^{-7}$ ,  $10^{-7}$  and  $10^{-6}$  for strong turbulence and for weak turbulence, the value of ABER is around  $10^{-8}$ ,  $10^{-8}$  and  $10^{-7}$  for clear air, haze and light fog condition. Now we can see in Figure 6.36 and 6.37 that the ABER performance of RZ-OOK under strong and weak turbulence for clear air, haze and light fog condition is very similar at 30 dB power but the only difference in RZ-OOK is that the ABER is suddenly fall when power increase from 20dB to 25 dB.

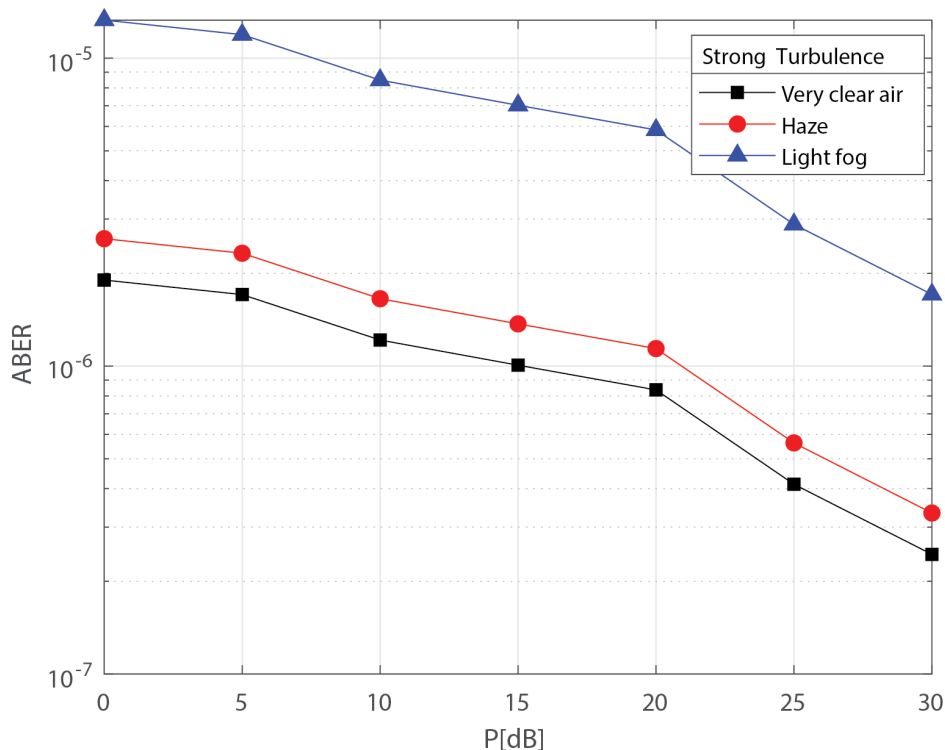


**Figure 6.34:** ABER performance of NRZ-OOK for different weather condition under stong turbulence.

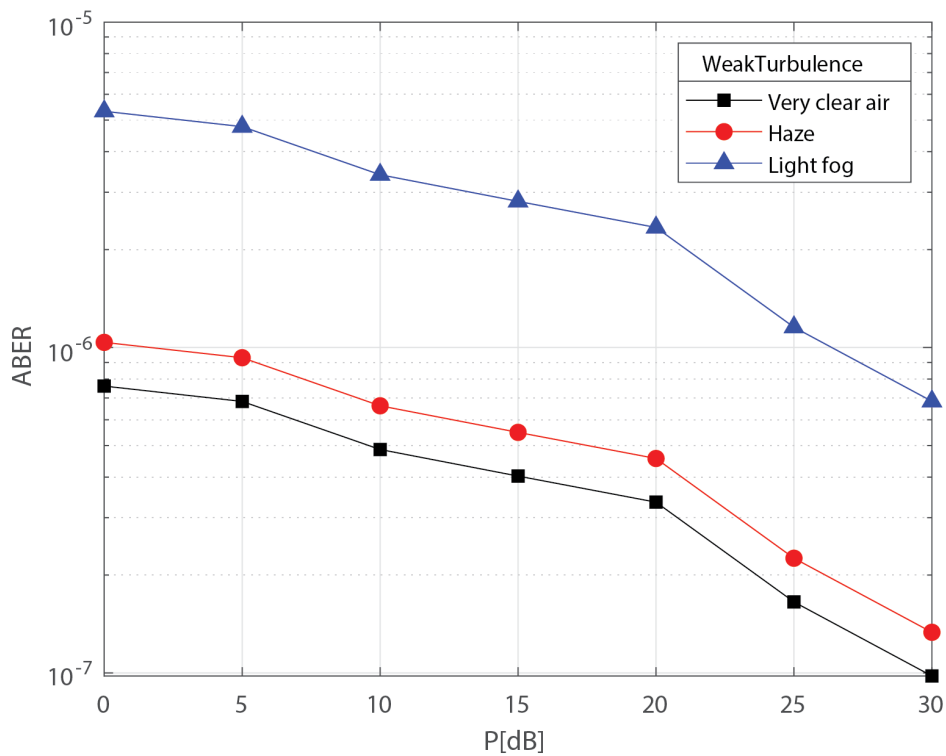


**Figure 6.35:** ABER performance of NRZ-OOK for different weather condition under weak turbulence.

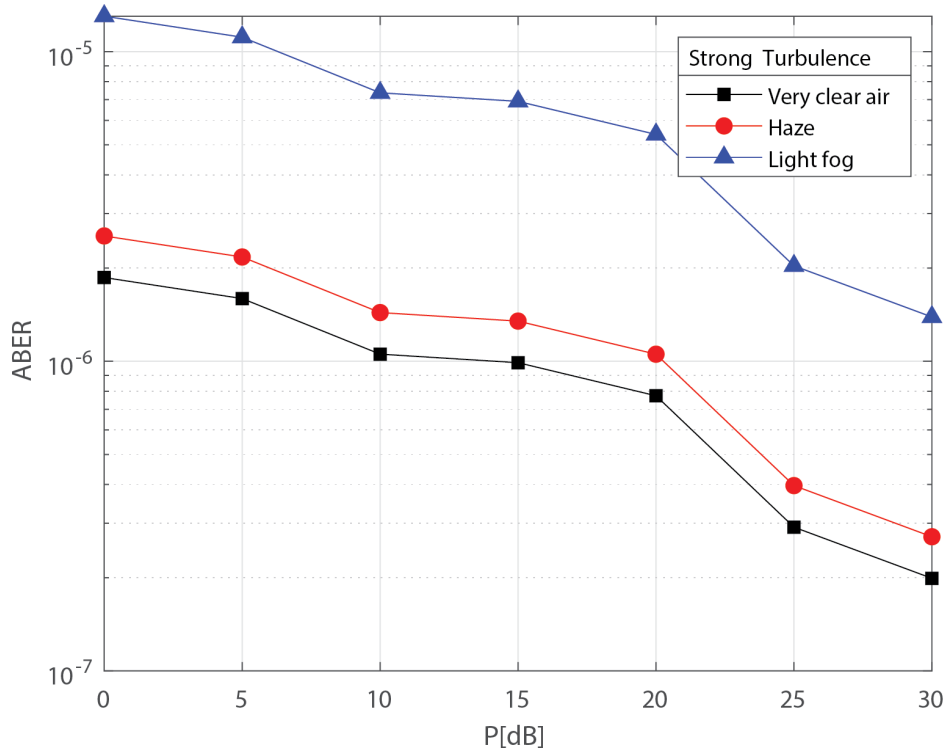


**Figure 6.36:** ABER performance of RZ-OOK for different weather condition under strong turbulence.

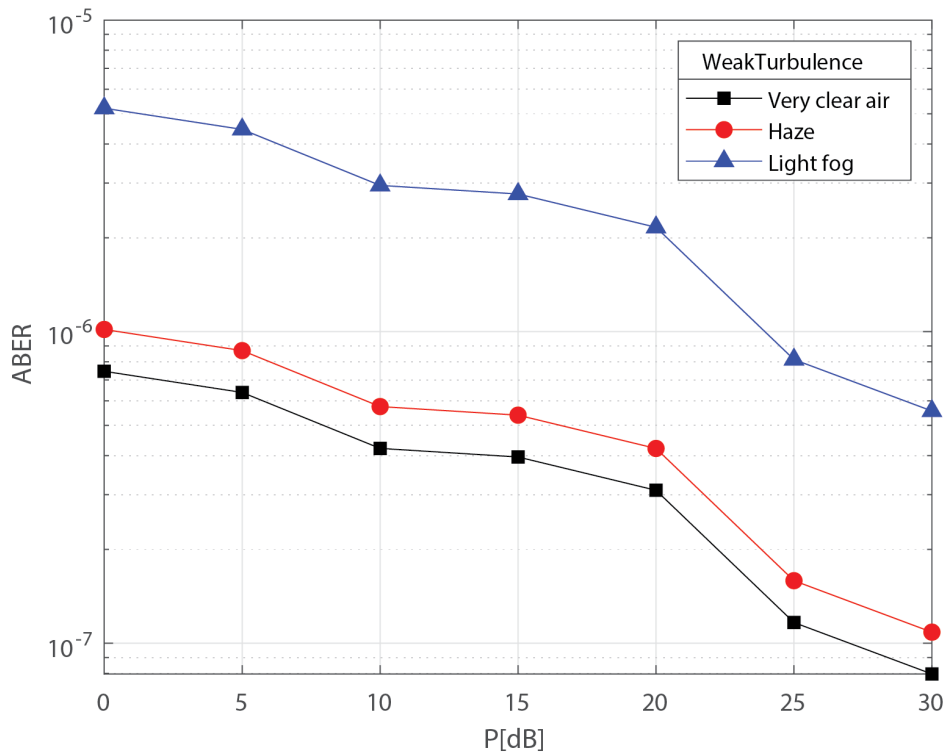


**Figure 6.37:** ABER performance of RZ-OOK for different weather condition under weak turbulence.

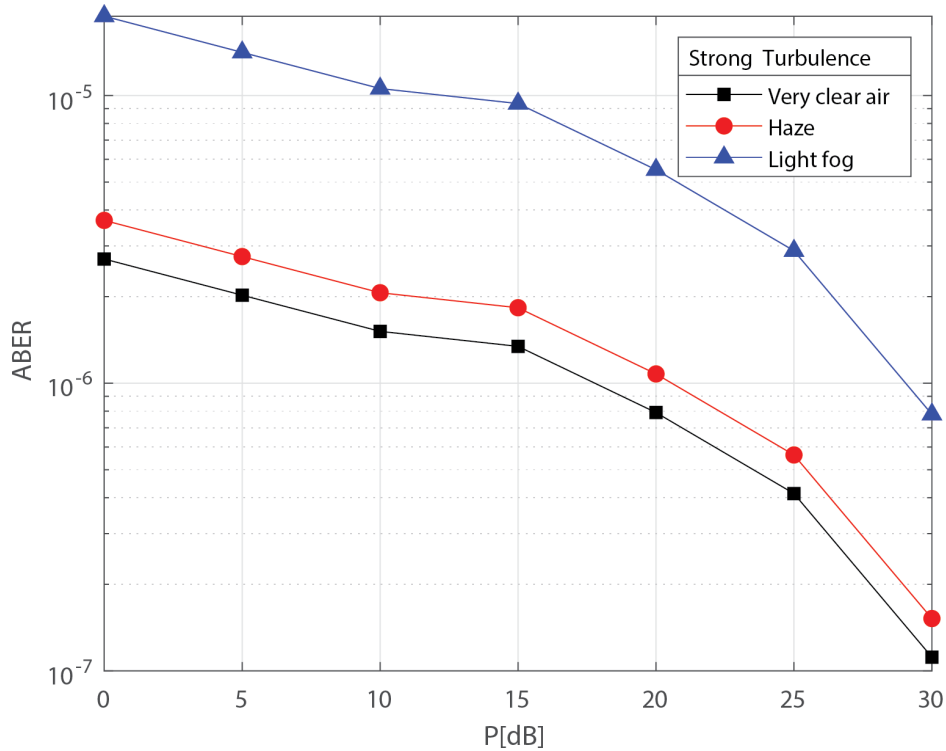


**Figure 6.38:** ABER performance of 4-QAM for different weather condition under strong turbulence.

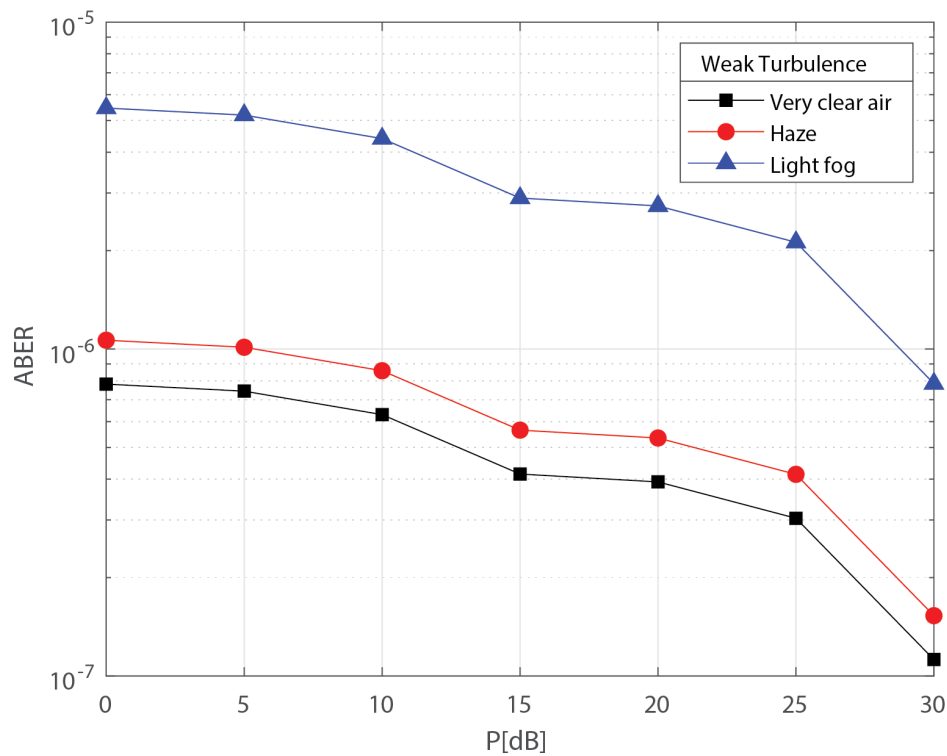


**Figure 6.39:** ABER performance of 4-QAM for different weather condition under weak turbulence.

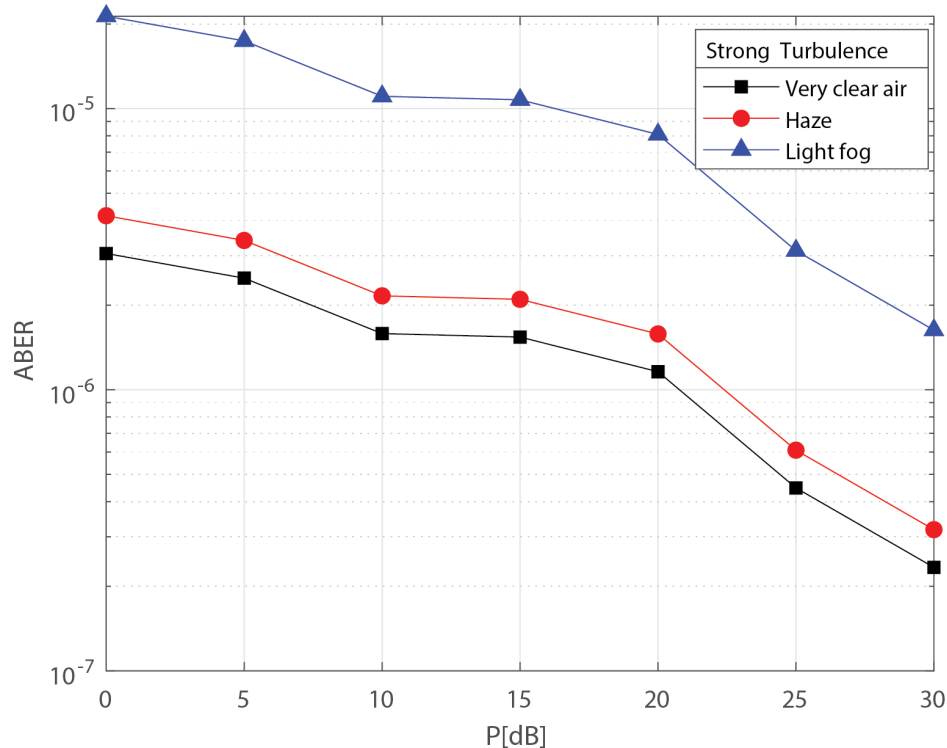


**Figure 6.40:** ABER performance of 8-QAM for different weather condition under weak turbulence.

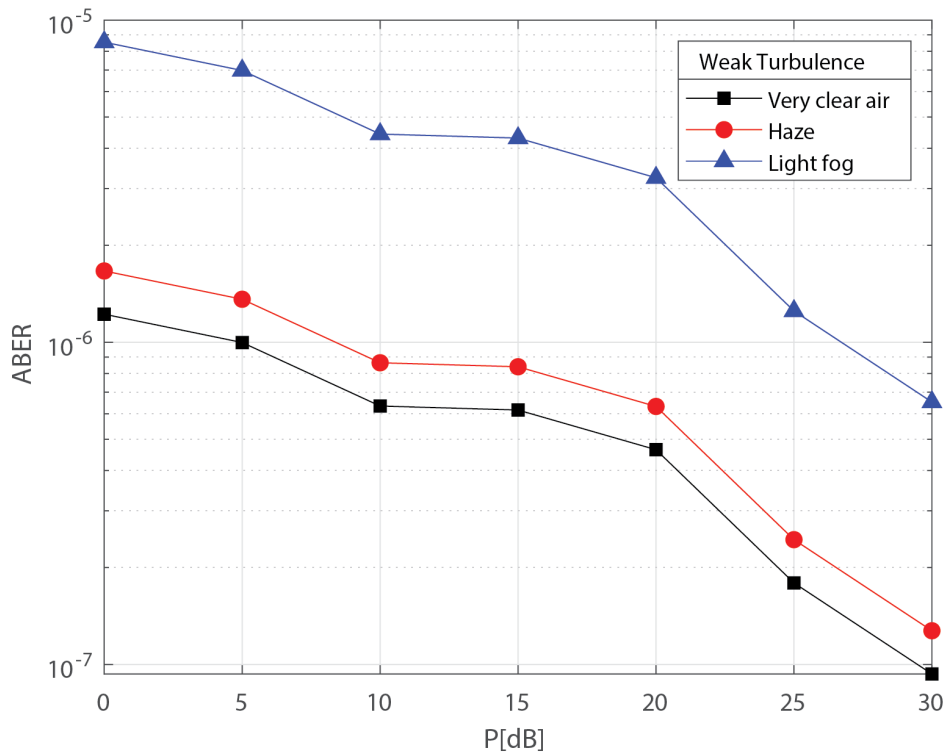


**Figure 6.41:** ABER performance of 8-QAM for different weather condition under strong turbulence.

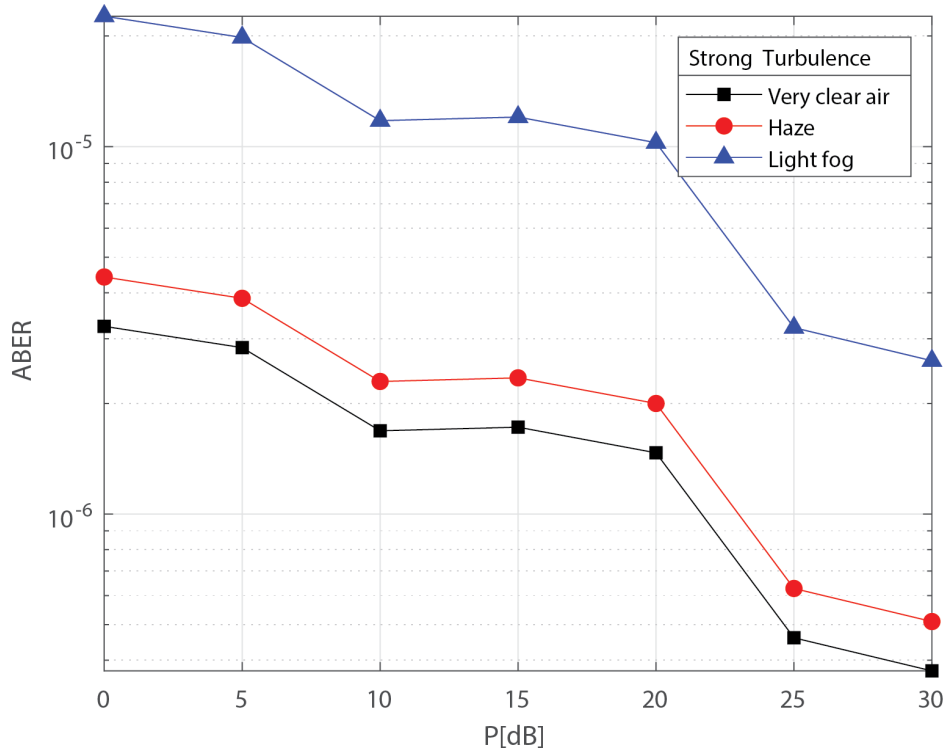


**Figure 6.42:** ABER performance of 16-QAM for different weather condition under strong turbulence.

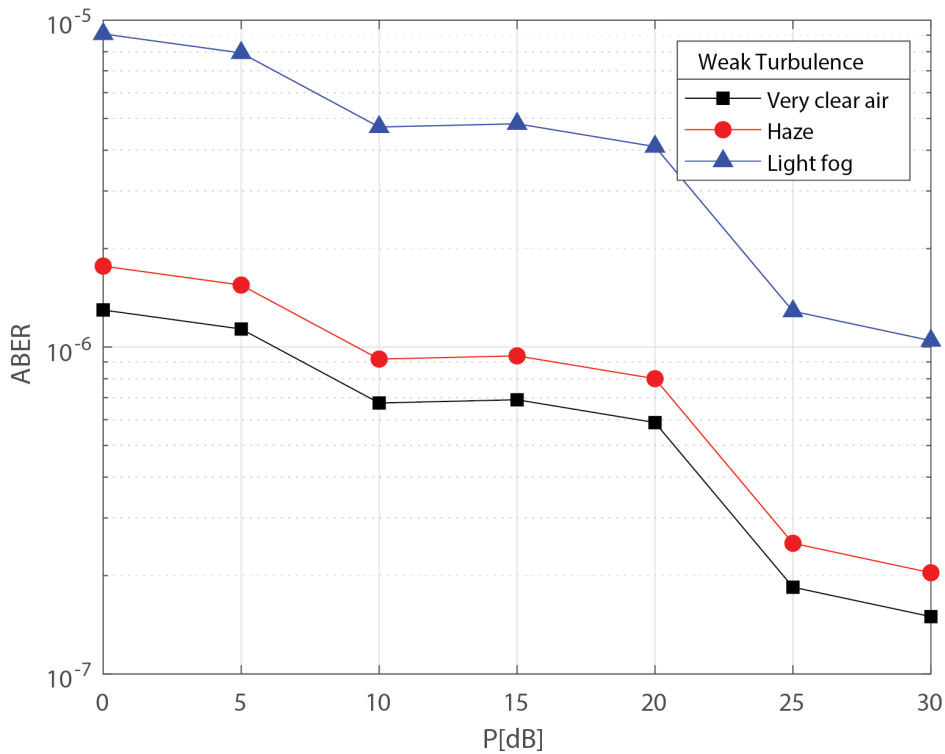


**Figure 6.43:** ABER performance of 16-QAM for different weather condition under weak turbulence.

In figures (6.38- 6.43) we are analyzing the ABER performance for M-QAM for different weather condition under Strong and weak turbulence where ( $M = 4, 8, 16$ ). Under strong turbulence condition in Fig 6.38 for 4-QAM the value of ABER for clear, haze and light fog condition respectively  $10^{-8}$ ,  $10^{-8}$  and  $10^{-7}$  and for 8-QAM ABER is around  $10^{-7}$  for clear air haze condition and  $10^{-6}$  for light fog. At 16-QAM the ABER performance is become degraded than 8-QAM can be seen in Figure 6.42, when power is 30dB.

At 30 dB transmit power Under Weak turbulence in Figure 6.39, 6.41 and 6.43 we can seen that for 4-QAM and 8-QAM the ABER performance is near to same for different weather condition but in 16-QAM ABER performance is bad compare to 4-QAM and 8-QAM.

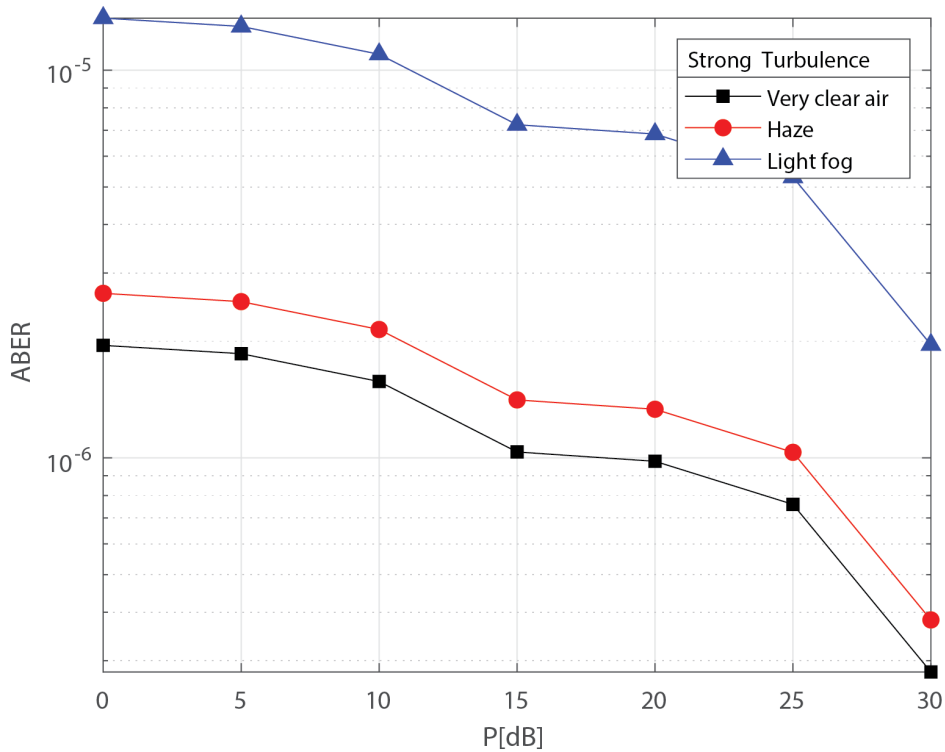


**Figure 6.44:** ABER performance of 4-PAM for different weather condition under strong turbulence.

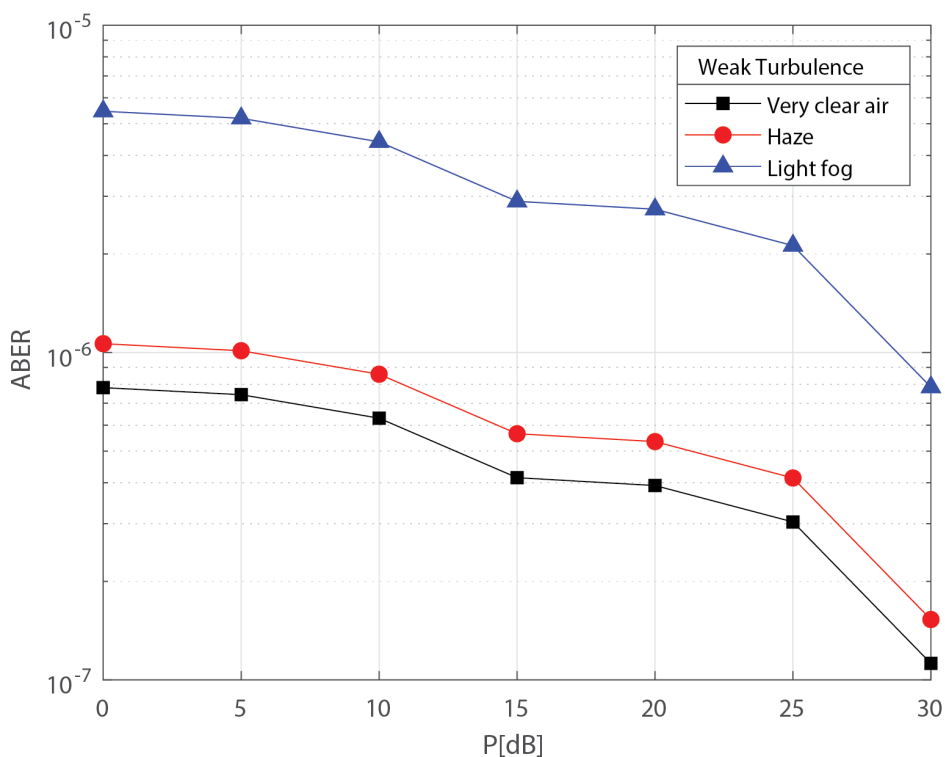


**Figure 6.45:** ABER performance of 4-PAM for different weather condition under weak turbulence.

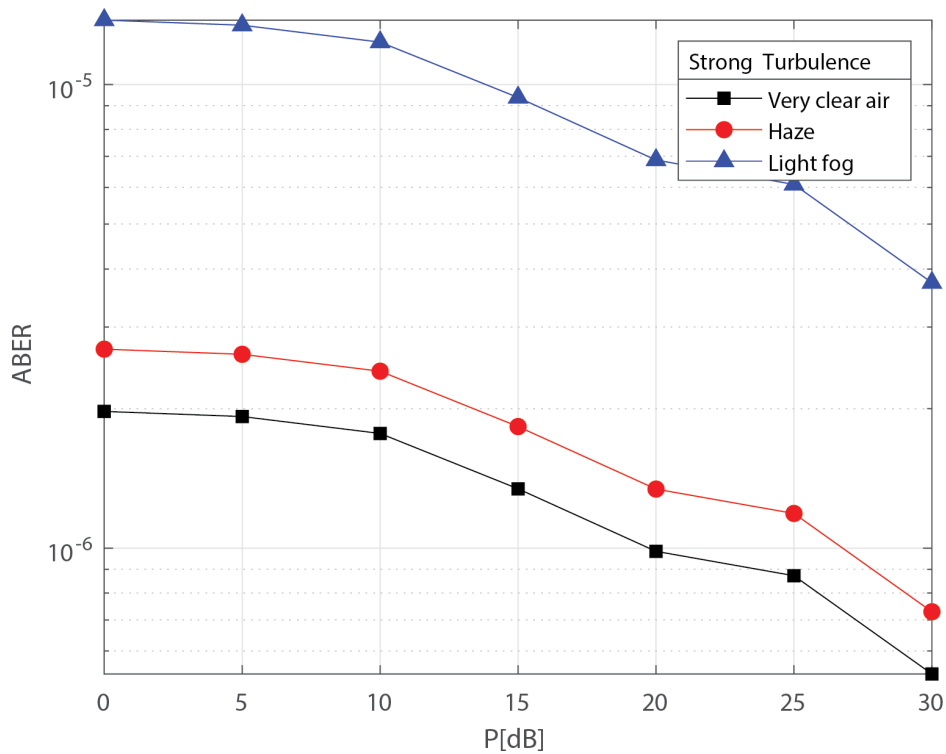


**Figure 6.46:** ABER performance of 8-PAM for different weather condition under strong turbulence.

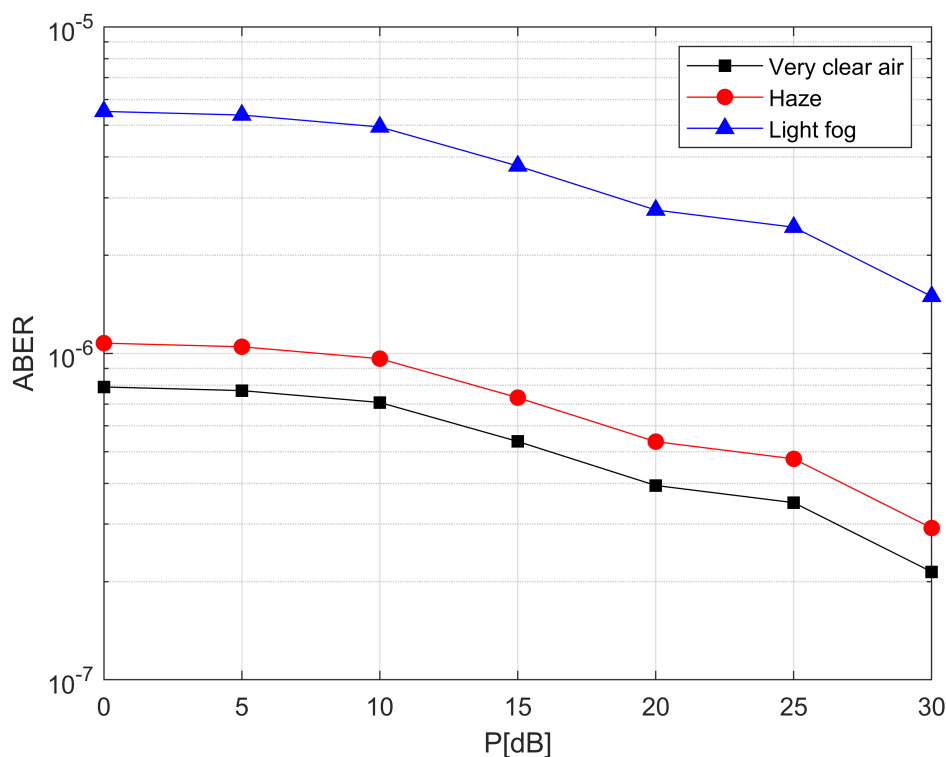


**Figure 6.47:** ABER performance of 8-PAM for different weather condition under weak turbulence.

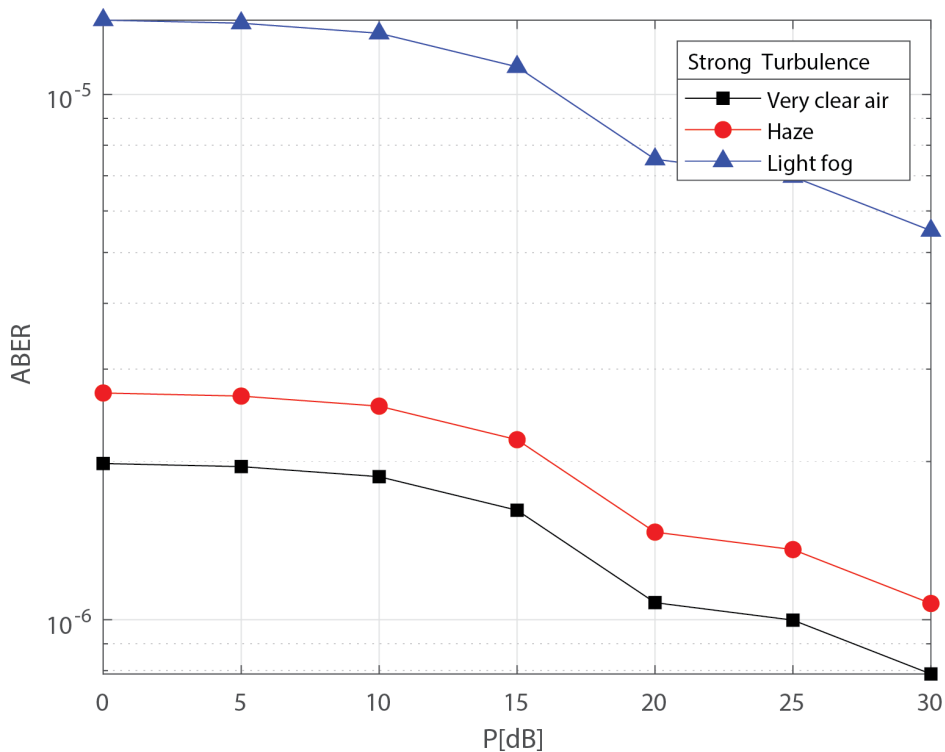


**Figure 6.48:** ABER performance of 16-PAM for different weather condition under strong turbulence.

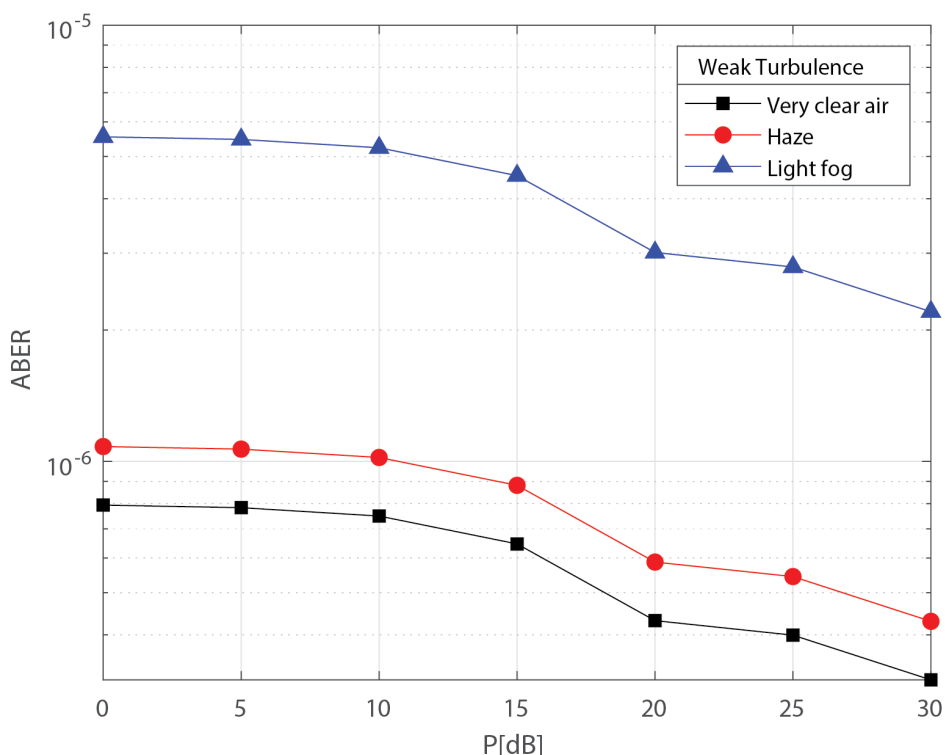


**Figure 6.49:** ABER performance of 16-PAM for different weather condition under weak turbulence.

In figures (6.44 to 6.49) we are analyzing the ABER performance for M-PAM for different weather condition under Strong and weak turbulence where ( $M = 4, 8, 16$ ). Under strong and weak turbulence condition in figures (6.44 to 6.49) we observe that 4-PAM and 8-PAM gives similar ABER performance but 16-PAM gives lower ABER is performance than 4-PAM and 8-PAM. During the observation most noticeable things is in M-PAM, value of ABER for light fog condition is more dominating than haze and clear air condition at 30 dB power.

In figures (6.50 to 6.55) we are analyzing the ABER performance for M-PPM for different weather condition under Strong and weak turbulence where ( $M = 4, 8, 16$ ). Under strong turbulence at 30 dB power in figure 6.50 we can see that the ABER performance for 4-PPM where the ABER for very clear air and haze is respectively  $10^{-7}$  for light fog  $10^{-6}$ . In figure 6.53 where for 8-PPM the ABER is greater than  $10^{-8}$  for very clear air and haze condition and  $10^{-7}$  for light fog. In addition, In figure 6.54 we can that the ABER performance for 16-PPM where ABER for very clear and haze condition is more than  $10^{-10}$  and for light fog condition ABER is greater than  $10^{-9}$ .

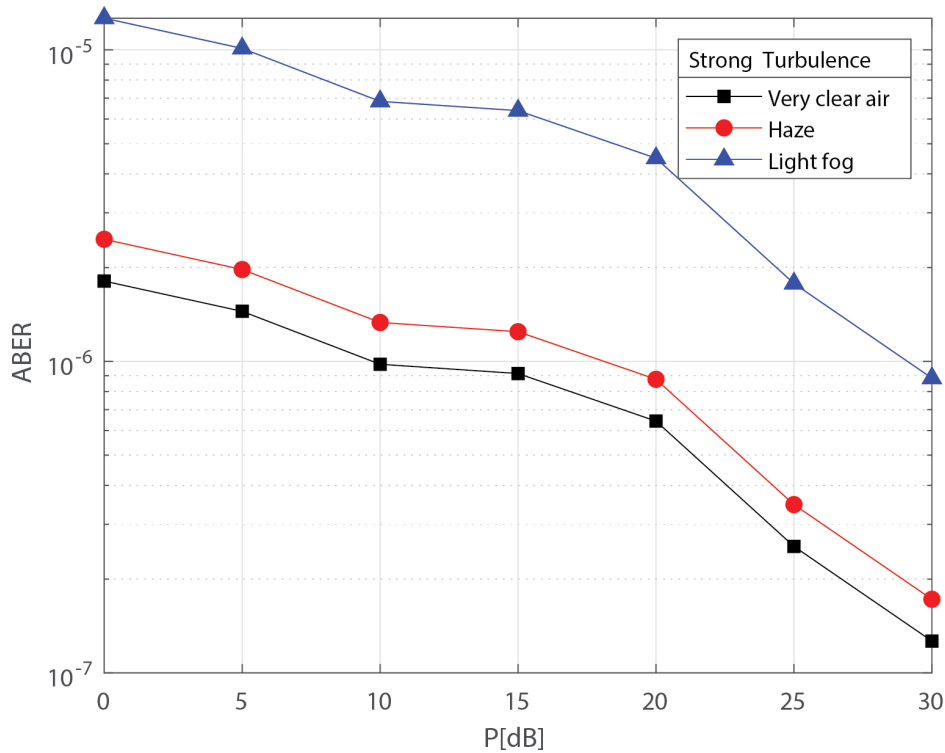


**Figure 6.50:** ABER performance of 4-PPM for different weather condition under strong turbulence.

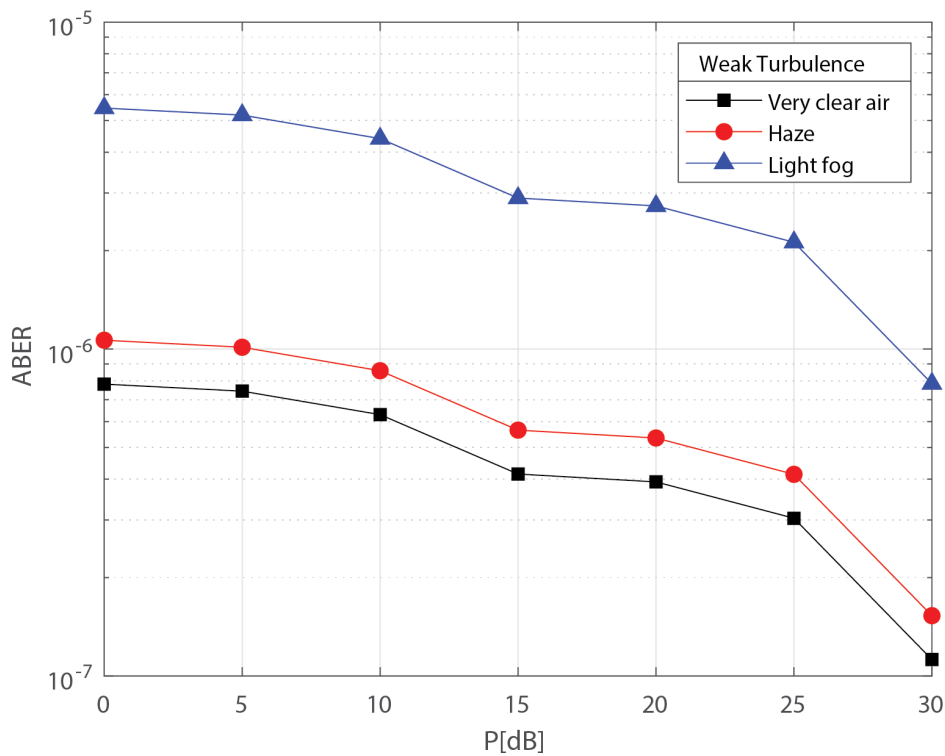


**Figure 6.51:** ABER performance of 4-PPM for different weather condition under weak turbulence.

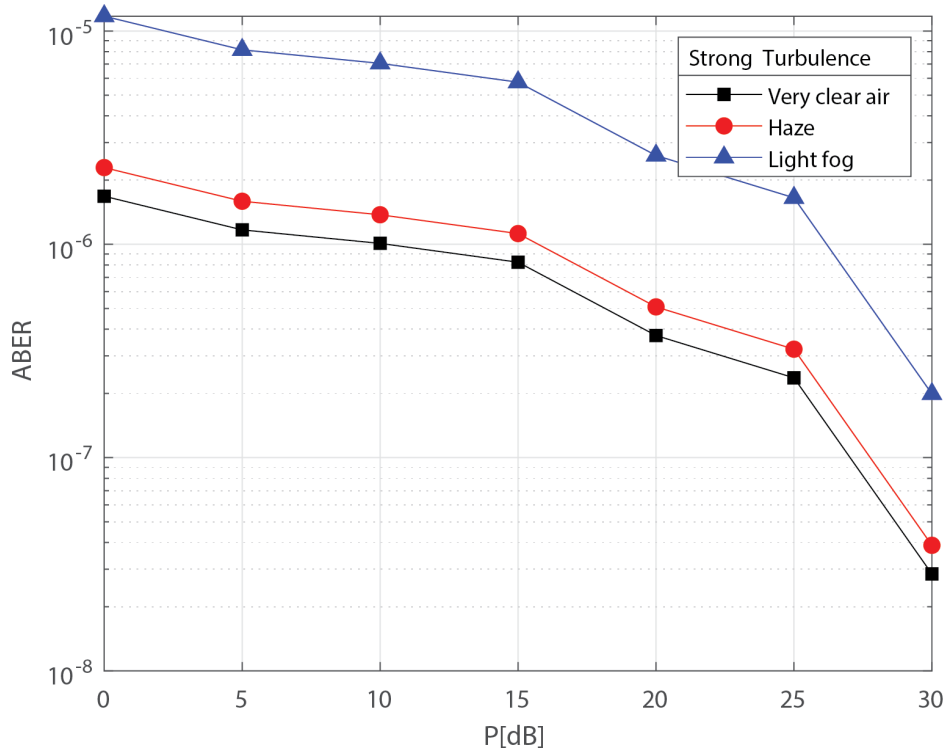


**Figure 6.52:** ABER performance of 8-PPM for different weather condition under strong turbulence.

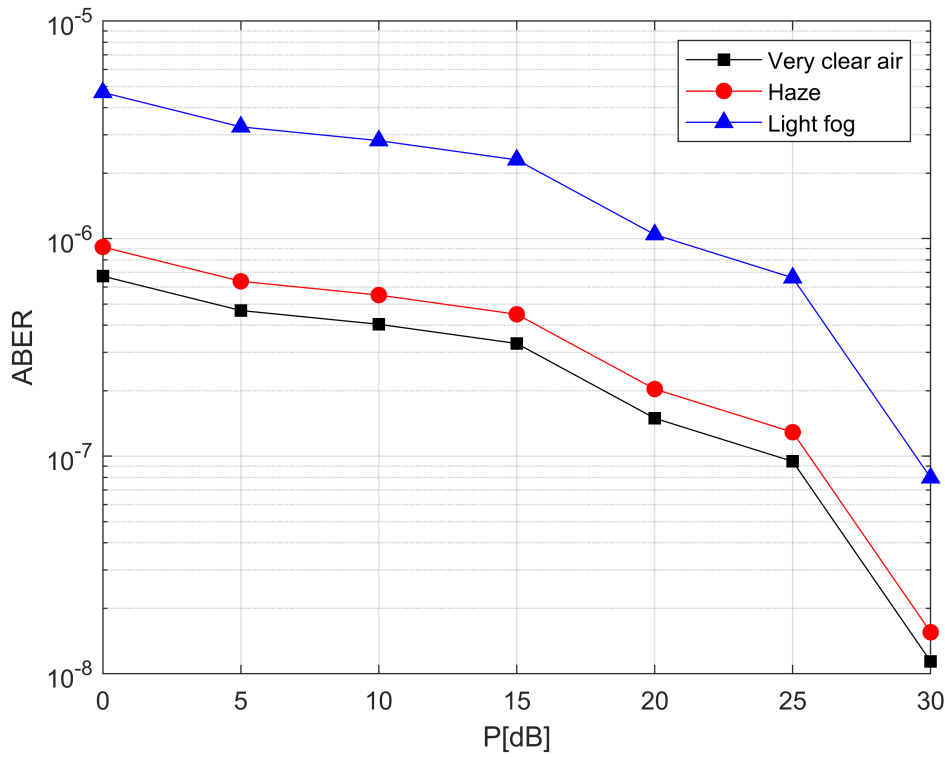


**Figure 6.53:** ABER performance of 8-PPM for different weather condition under weak turbulence.

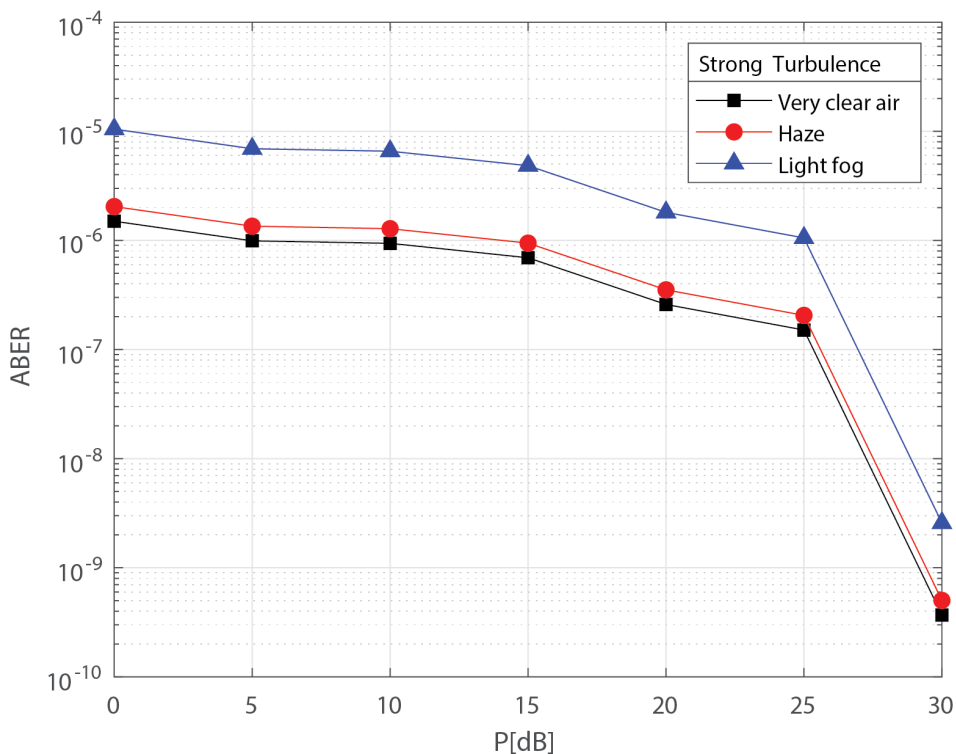


**Figure 6.54:** ABER performance of 16-PPM for different weather condition under strong turbulence.

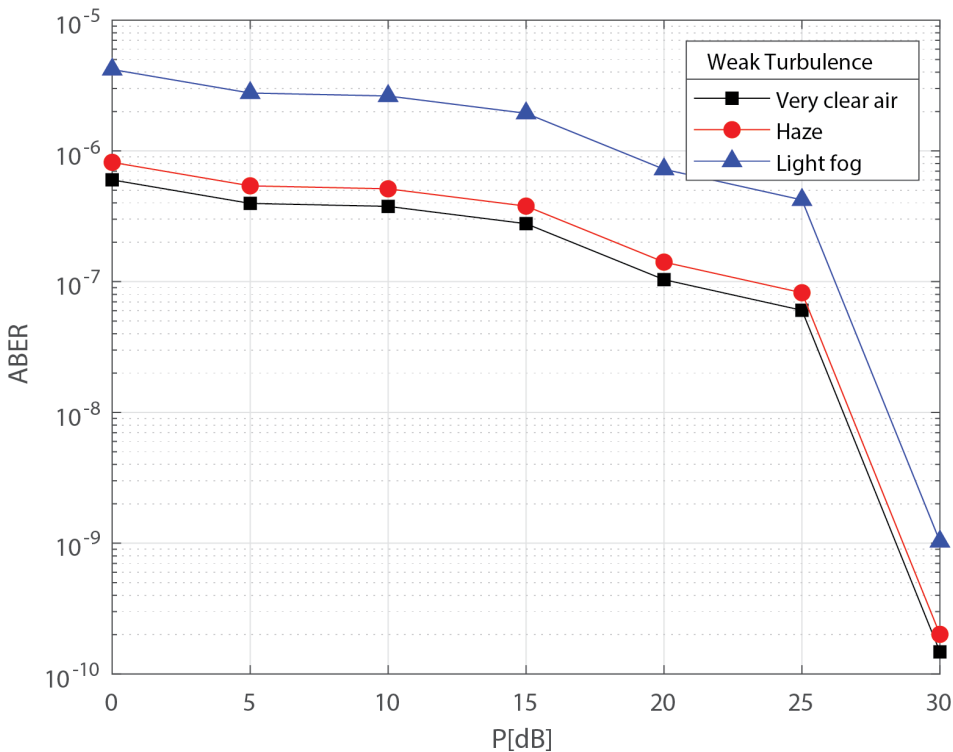


**Figure 6.55:** ABER performance of 16-PPM for different weather condition under weak turbulence.

Under weak turbulence at 30 dB power in figure 6.51, for 4-PPM ABER is more than  $10^{-8}$ ,  $10^{-8}$  and  $10^{-7}$  for clear air haze and light fog and in figure 6.53 for 8-PPM ABER is  $10^{-8}$ ,  $10^{-8}$  and  $10^{-7}$  for light fog. In figure 6.55, 16-PPM we can see that the ABER is very near to  $10^{-10}$  for clear air and haze where for light fog = ABER is  $10^{-9}$ . Now after observing the M-PPM modulation scheme it can be seen that when value of M is increased for both strong and weak turbulence the ABER is decreases, so 16-PPM proves to be the best as compared with 4-PPM and 8-PPM.

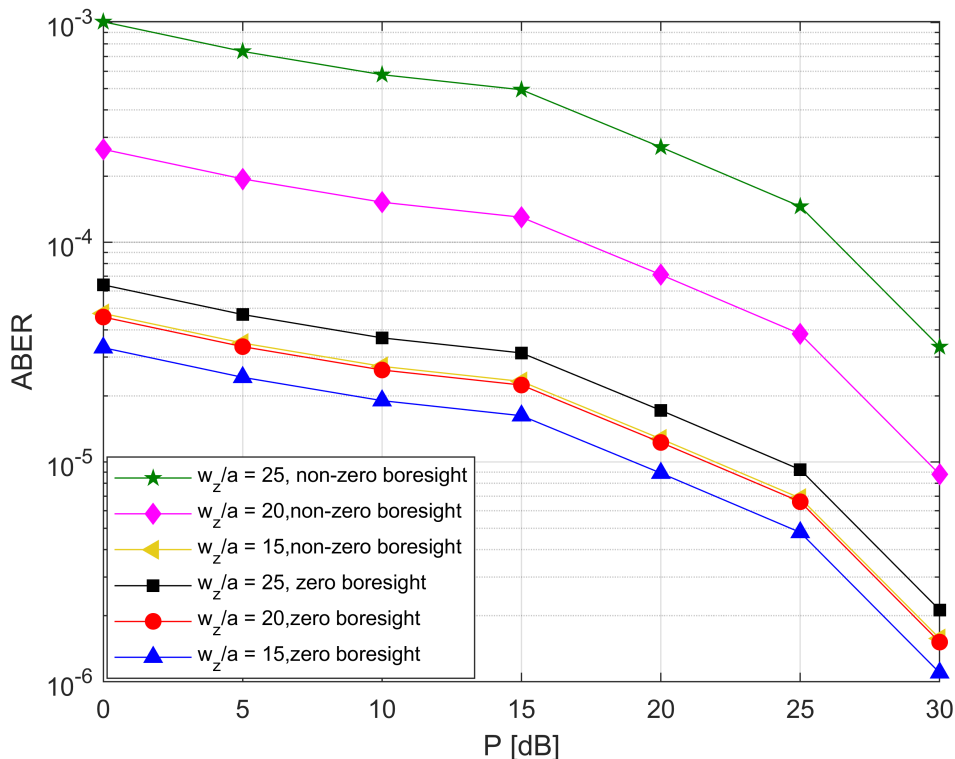
Now for strong turbulence 16-PPM, 8-PPM, BPSK, QPSK, DPSK, 4-QAM, this 6 modulation schemes are giving the best results , Moreover for Weak turbulence 16-PPM, 8-PPM, BPSK, DPSK, NRZ-OOK this 5 modulation schemes are giving the best results to achieving lowest ABER value at 30 dB power. In weak to strong turbulence condition among BPSK, 16-PPM, 8-PPM modulations, 16-PPM shows the best results among all of the above-mentioned modulation schemes.

### 6.3.4 ABER Performance for Different Beam-Width

The simulation results on ABER performance of different modulation schemes for different normalized beam width impact over Málaga ( $\mathcal{M}$ ) Turbulence channel is given below:

The figures (6.56 to 6.69) attached below represents the ABER performance of different modulation scheme for different normalized beam width ( $\omega_z/a = 15, 20$  and  $25$ ) over Málaga ( $\mathcal{M}$ ) atmospheric turbulence channel by considering the both effect of zero boresight pointing error and non-zero boresight pointing error. Here we have used eight different modulation schemes and they are BPSK, QPSK, DPSK, RZ-OOK, NRZ-OOK, M-PPM, M-PAM and M-QAM (Where,  $M = 4, 8, 16$ ).

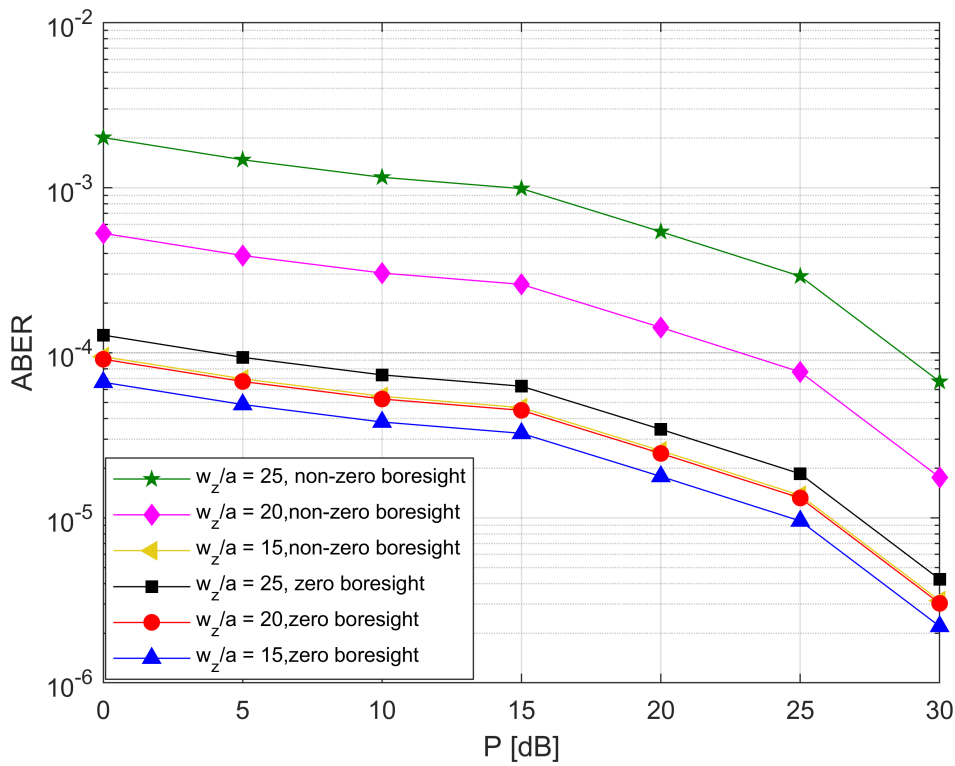
First of all, in figure 6.56, we can see the ABER performance of BPSK modulation for fixed values  $\alpha = 3.99$ ,  $\beta = 2$ ,  $z = 4$  km,  $a = 0.1$  m,  $s = 0.3$  m and different value of beam width. We know that pointing error has effects of the beam width, jitter variance and aperture radius.



**Figure 6.56:** ABER performance of BPSK for different beam width.

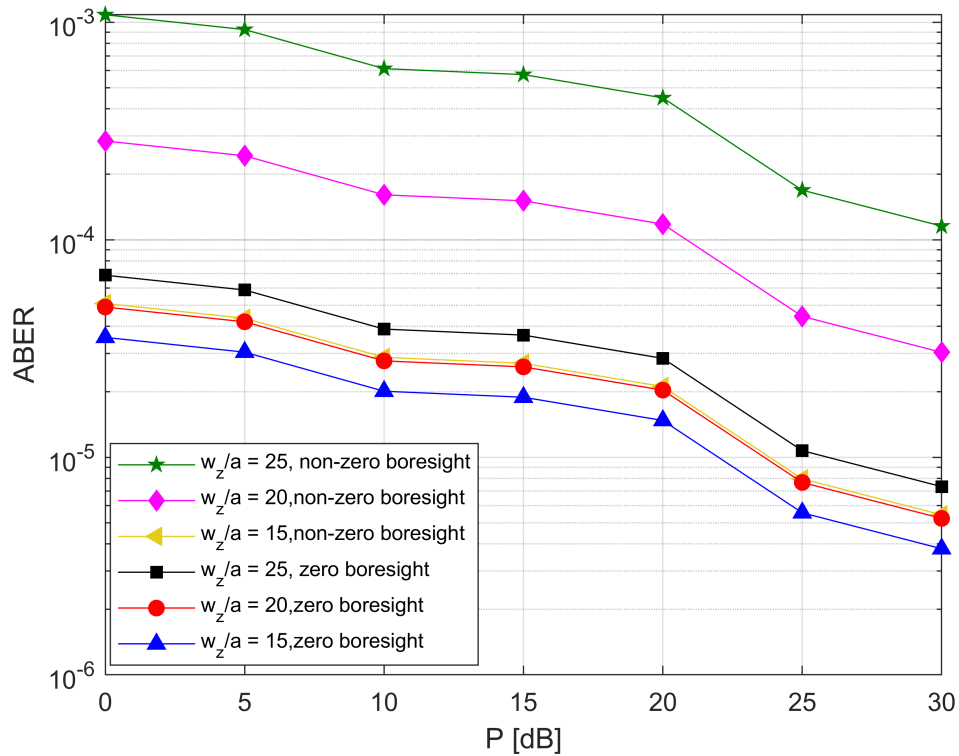
It can be inferred through the figures for the founded result that the performance of the ABER increases with the increasing value of  $\omega_z/a$ . As predicted, we can see from the figures that the value of ABER for non-zero boresight and zero boresight differ for a specific beam width. As for example, when  $\omega_z/a = 25$  the value of ABER at 0 dB power for non-zero boresight is  $10^{-3}$

and for zero boresight is  $6.4 \times 10^{-5}$ . So, we can see the growth of a non-zero boresight for a change in the beam width is giving a more noticeable effect on the performance of ABER. Like the previous parameters also for beam width the ABER performance is becoming well with the increasing value of transmit power that means here also at high power we will get better performance which actually is a constant behavior. Also, we can see from the figure that the performance for  $\omega_z/a = 15$  non-zero boresight and  $\omega_z/a = 20$  zero boresight has very small difference in between.

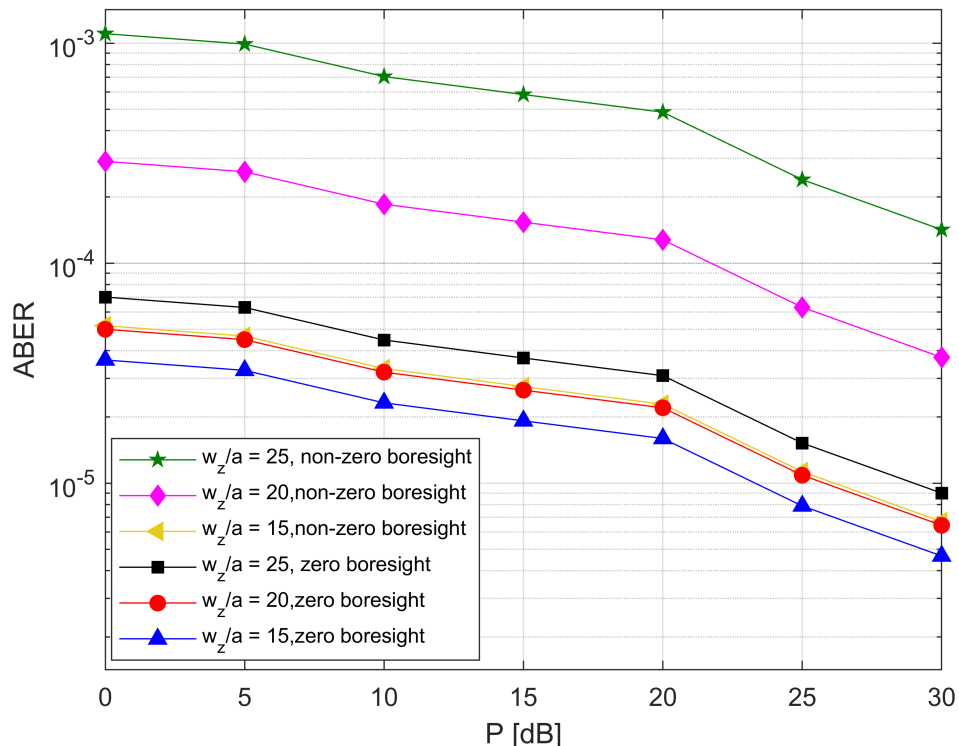


**Figure 6.57:** ABER performance of QPSK for different beam width.

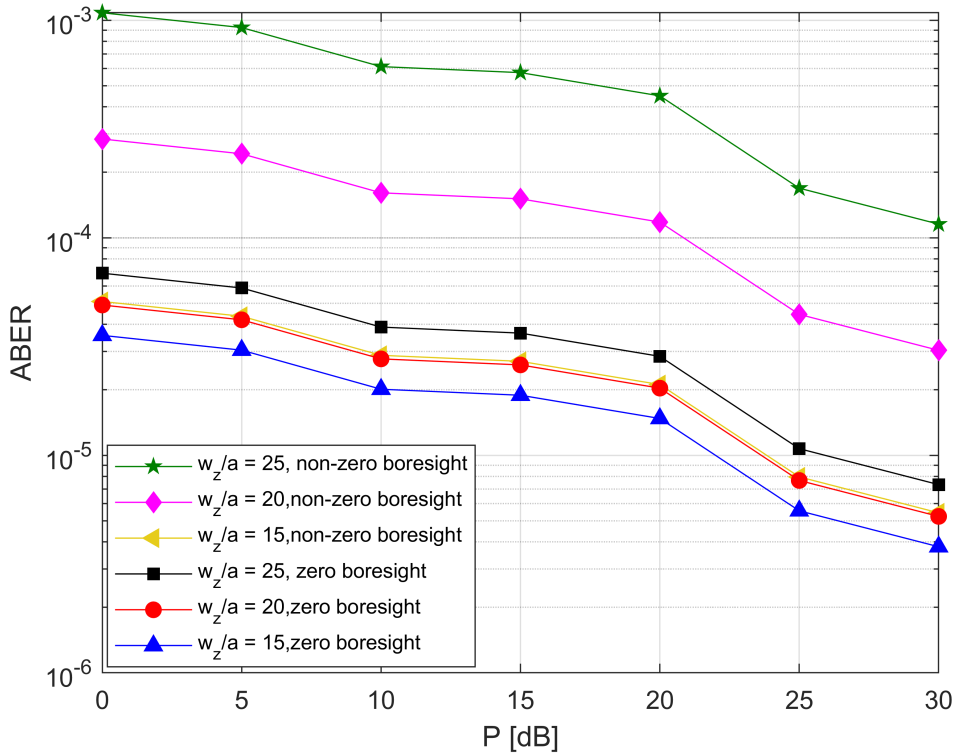
The ABER performance under strong turbulence of QPSK and DPSK modulation respectively for different normalized beam width is shown in figure 6.57 and 6.58. If we compare them with the ABER performance of BPSK modulation shown in figure 6.56, we can see that the performance of ABER for DPSK modulation at low power is almost same as BPSK but at high power we are getting far better result compare to both QPSK and DPSK.



**Figure 6.58:** ABER performance of DPSK for different beam width.



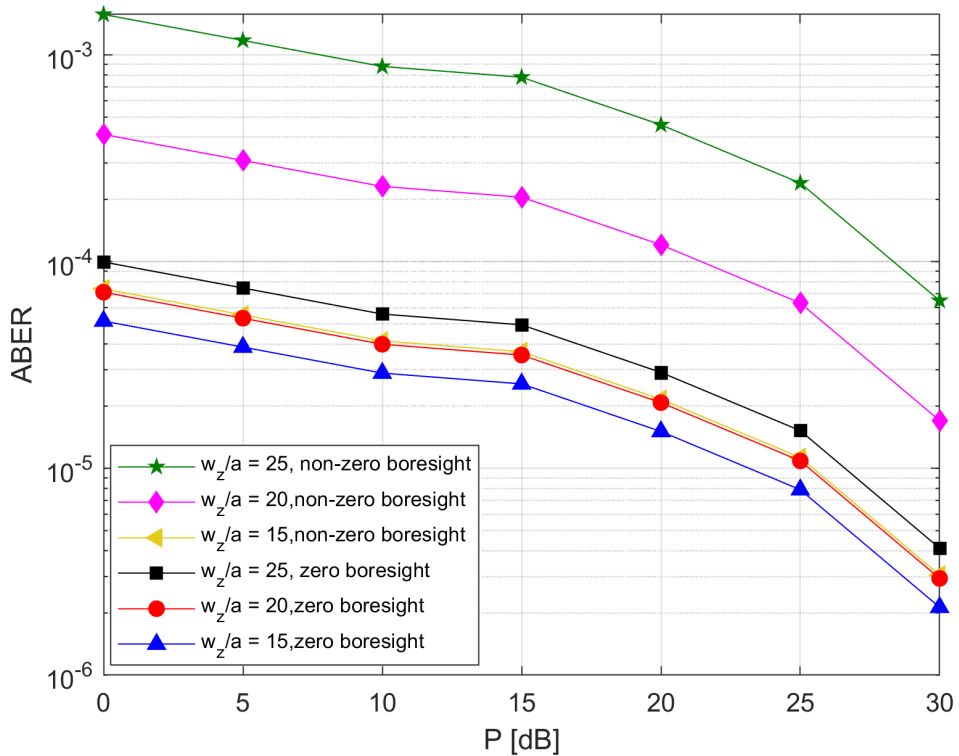
**Figure 6.59:** ABER performance of RZ-OOK for different beam width.



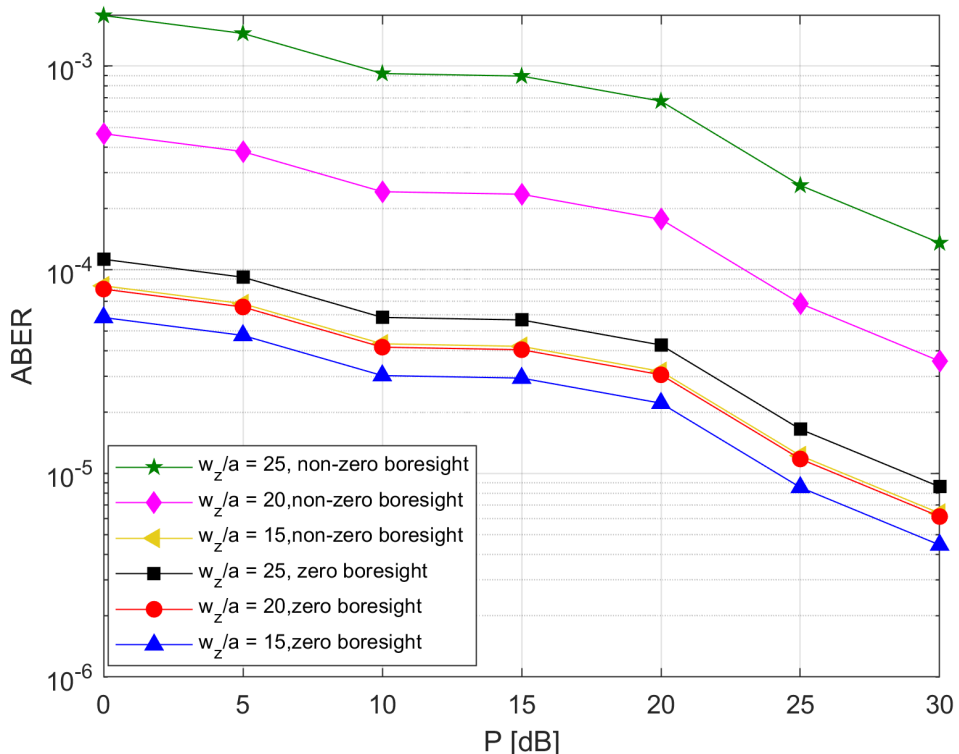
**Figure 6.60:** ABER performance of NRZ-OOK for different beam width.

In figure 6.59 and 6.60 we can observe the relation between the ABER and transmit power of RZ-OOK and NRZ-OOK modulation for different normalized beam width. At low power like 0 dB there is too small difference at the performance of ABER for RZ-OOK and NRZ-OOK. But with the increasing value of power it can clearly observe that the ABER performance of RZ-OOK is better than NRZ-OOK.

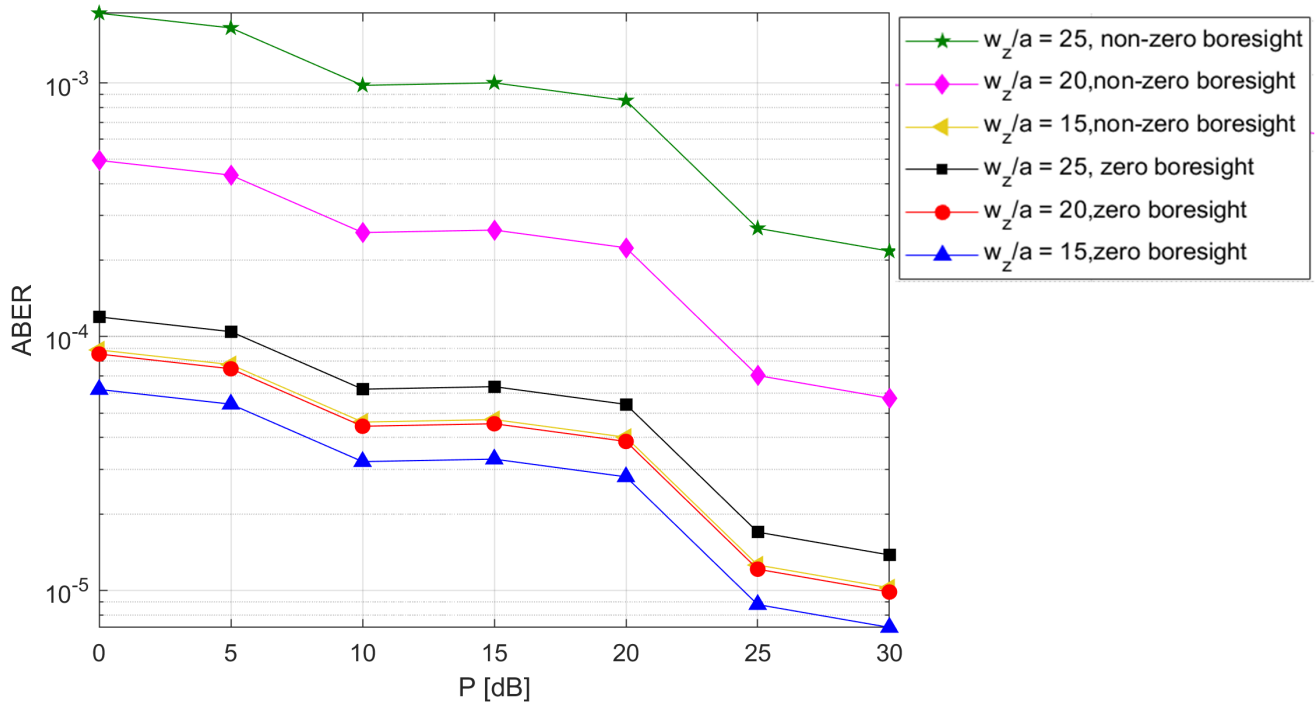
From figure 6.61, 6.62 and 6.63, we can depicts the ABER versus transmit power of 4-QAM, 8-QAM and 16-QAM modulation for different normalized beam width. It can be observed from these figures that with the increasing value of M, the value of ABER is increasing that means the performance of ABER is degrading. Also, there is noticeable similarity between BPSK and 4-QAM. From there graph it can be confirmed that they are giving same ABER performance.



**Figure 6.61:** ABER performance of 4-QAM for different beam width.



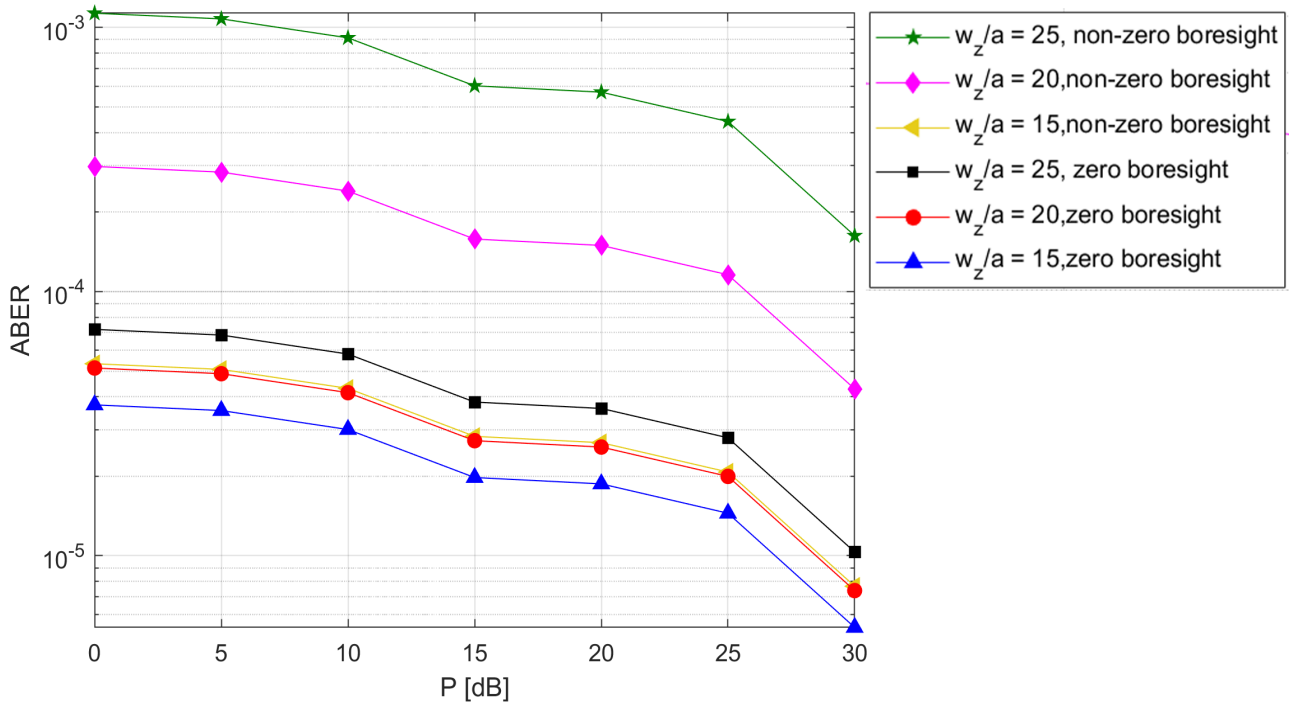
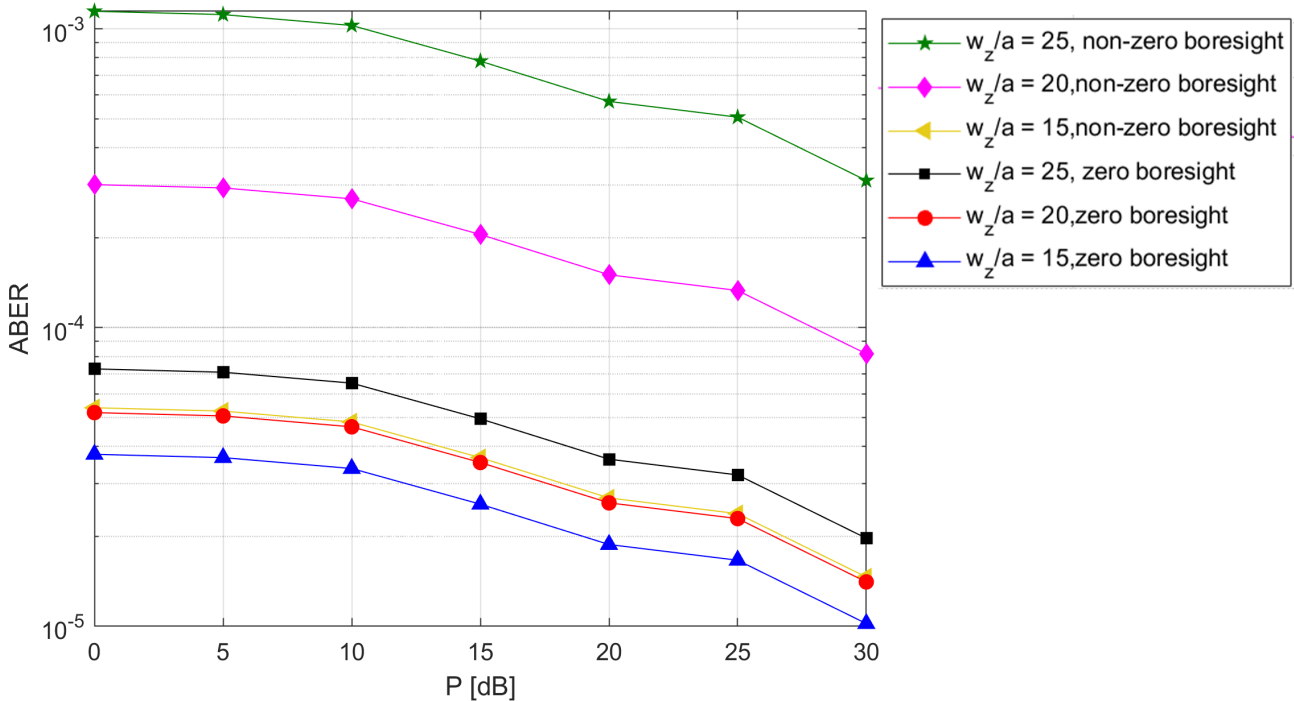
**Figure 6.62:** ABER performance of 8-QAM for different beam width.

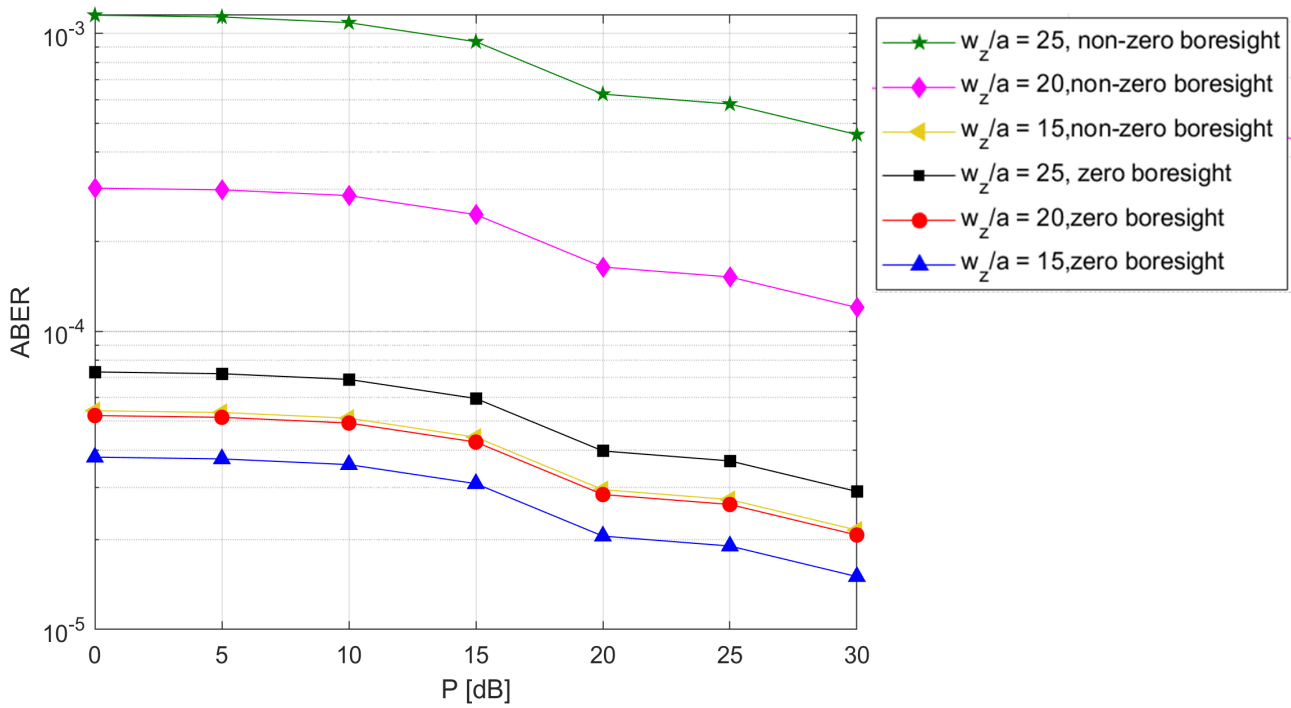


**Figure 6.63:** ABER performance of 16-QAM for different beam width.

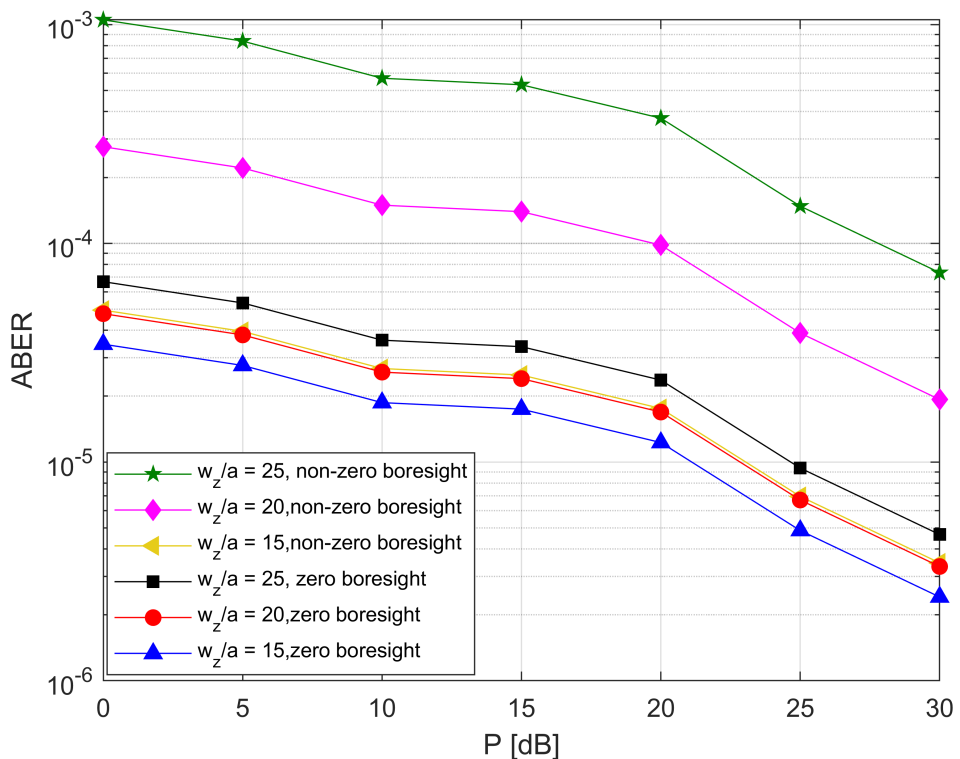
In figures 6.64, 6.65 and 6.66, we can notice the performance of ABER of 4-PAM, 8-PAM and 16-PAM modulation respectively for different normalized beam width. From these attached figures we can get the idea that with the increasing value of M, the value of ABER is decreasing that means the performance of ABER is getting better. Again for 16-PAM we can see that after 25 dB transmit power value of ABER suddenly fall which is clearly noticeable.

We can see the change of ABER against the transmit power of 4-PPM, 8-PPM and 16-PPM modulation respectively for different normalized beam width in figure 6.67, 6.68 and 6.69. From these figures, we can see that with the increasing value of M, the performance of ABER is getting better. By comparing with 4-PPM and 8-PPM, it can be observed that 16-PPM is giving better result than them.

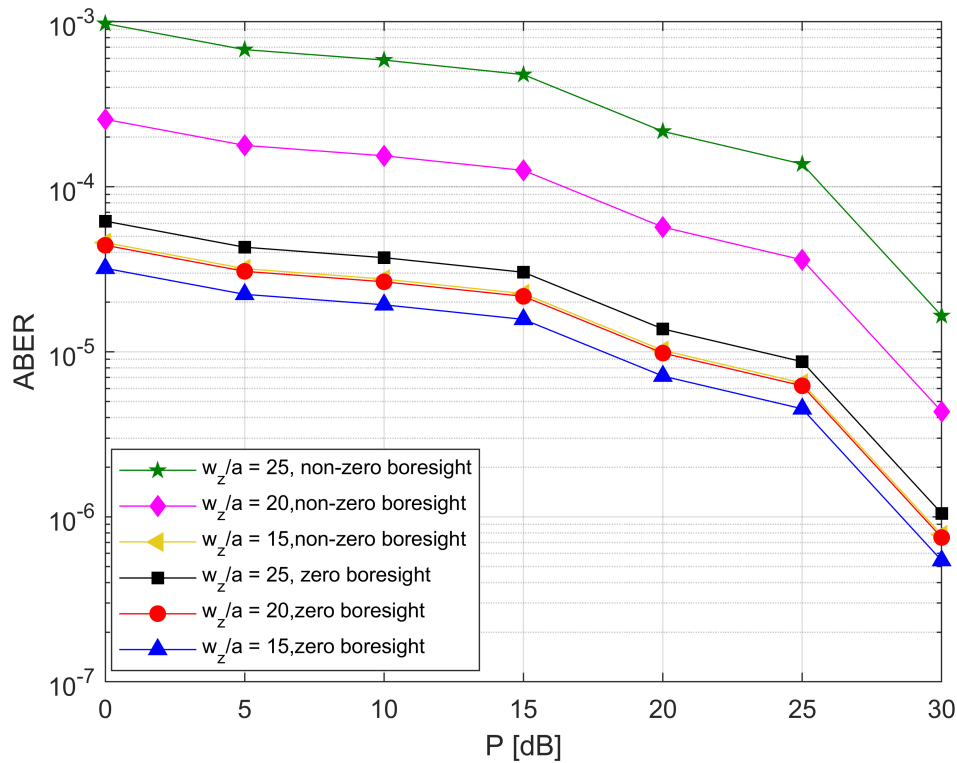
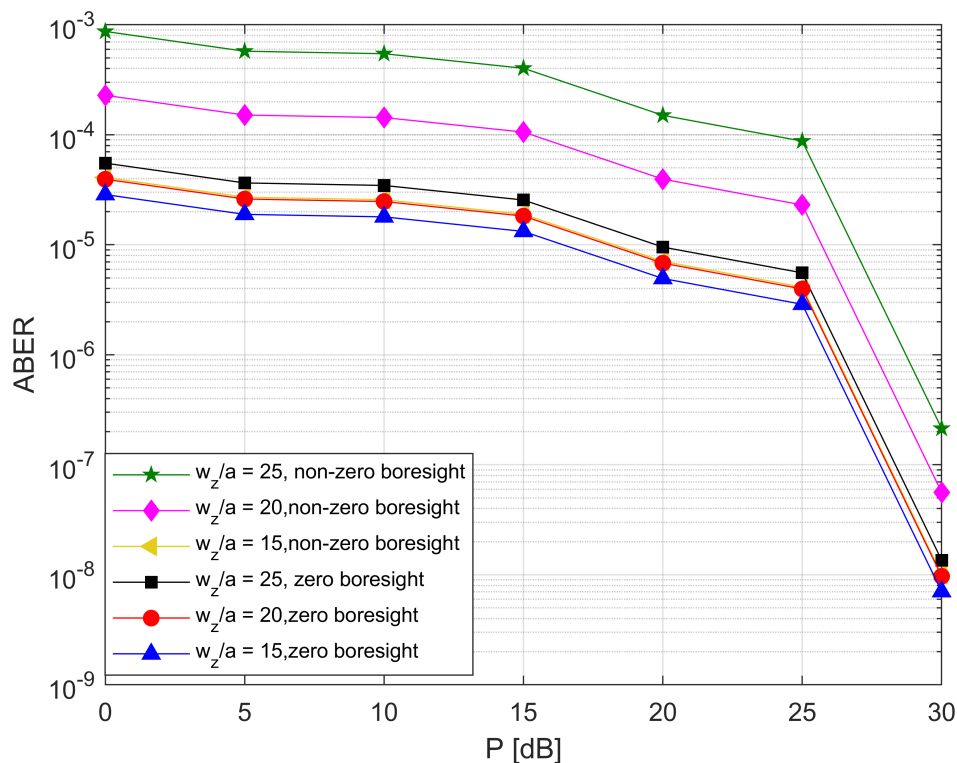
**Figure 6.64:** ABER performance of 4-PAM for different beam width.**Figure 6.65:** ABER performance of 8-PAM for different beam width.



**Figure 6.66:** ABER performance of 16-PAM for different beam width.



**Figure 6.67:** ABER performance of 4-PPM for different beam width.

**Figure 6.68:** ABER performance of 8-PPM for different beam width.**Figure 6.69:** ABER performance of 16-PPM for different beam width.

Finally, we can conclude that among all these modulation scheme, 16-PAM, 8-PAM, 16-PPM, 8-PPM, BPSK are giving better ABER performance for different beam width in FSO system where, 16-PAM modulation is giving the best performance.

# **Chapter 7**

## **Conclusion**

### **7.1 Overall Conclusion and Future work**

In this thesis, we are analyzing the BER performance analysis of the FSO communication system over the Málaga ( $\mathcal{M}$ ) turbulence channel with zero and non-zero boresight pointing errors under different modulation techniques. We have identified the possible Impact of the Málaga ( $\mathcal{M}$ ) turbulence channel in presence of various effects like pointing errors, different link distances, different weather conditions, and different normalized beam widths to analyze the performance of the average BER of the FSO system for the different modulation schemes. For our system, we are doing a channel model by considering the effects of atmospheric attenuation, Málaga ( $\mathcal{M}$ ) atmospheric turbulence, zero and non-zero boresight pointing errors under the IM/DD detection technique. We have used two analytical closed-form representations of the probability density function for a zero and non-zero boresight pointing error respectively for the FSO system over Málaga ( $\mathcal{M}$ ) turbulence in the presence of pointing errors.

From our first Investigation, we got that 16-PPM, 8-PPM, BPSK, 4-PPM, DPSK, QPSK, 4-QAM these are best suitable modulation technique showing the best results to achieving the lowest ABER value when we consider the impact of zero boresights pointing error and Non-zero boresight pointing error for different values of  $\alpha$  and  $\beta$ . Moreover, wheres 16-PPM is giving the best ABER performance compared to the rest of the modulation schemes used here and whereas M-PAM gives the worst performance.

In our second Investigation, we observe that for different propagation link distances ( $z = 1, 2, 3, 4$  Km) these four modulation scheme such as BPSK, RZ-OOK, 8-QAM, and 16-PPM giving the best ABER performance. Then from our 3rd Investigation, we infer that if use this BPSK, 16-PPM, 8-PPM modulations techniques to analyze the performance of channel for different weather (Very clear, Haze, light fog) conditions under weak to turbulence condition, the system

gives lowest ABER. So, from our last finding, we get that when we analyzing the influence of a different normalized beamwidth change over Málaga ( $\mathcal{M}$ ) Turbulence channel presence of both observed zero and non zero boresight cases 16-PAM,16-PPM,8-PPM,4-QAM modulation gives the best performance. Where 16-PAM shows the best results among them.

So, finally after analyzing all our findings we can say that our FSO system under the Málaga ( $\mathcal{M}$ ) turbulence channel with zero and nonzero boresight pointing error giving overall the best average bit error performance when we are used 16-PPM and BPSK modulation techniques.

The performance of the optical signal in free space suffers through phase fluctuations and irradiance due to the atmospheric turbulence and pointing error which degrades the quality of the signal and deteriorates the long-distance efficiency of the communication. In the near future, to improve our recent works for the FSO system, we can explore the following which are as follows:

- The use of the Maximum Transmission Ratio (MRT) technique can enhance the performance of FSO systems.
- We can reduce the atmospheric turbulence effect over Málaga ( $\mathcal{M}$ ) distribution by sending the same signal at different wavelengths, such as the technique of wavelength diversity and time diversity technique.
- As the MIMO technique offers a significant improvement in data throughput and link range despite extra bandwidth or transmitting capacity, it is frequently used in wireless communication technology. So, we can introduce MIMO in the future.
- Besides, we can use a hybrid modulation technique to see the performance of FSO for this channel set up.
- Other performance parameters such as ergodic capacity, outage capacity, etc. under the current channel can be examined for the purpose of our future work.
- In addition, various FSO atmospheric turbulences can be further explored in terms of optical CDMA or optical code division multiple access, optical Direct Sequence (DS) CDMA, and optical CPDM or optical circular polarization division multiplexing, etc.

## 7.2 Challenges of FSO

Now-a-days, Free Space Optics (FSO) is becoming a feasible, high bandwidth wireless replacement of optical fiber. Key advantages of FSO over optical fiber is its quick implementation time, low-cost and for being more efficient. On the other hand, the drawback of FSO compared to optical fiber is that atmospheric laser power attenuation is unpredictable and challenging to determine, also for being weather airports, the availability of links can be calculated for any FSO device as a function of distance. These availability curves provide a clear indication of the appropriate link distances in a given geographical region for FSO systems. Other potential major users of FSO systems are carriers and ISPs particularly for last-mile metro access applications [8]. To use in telecommunications applications, FSO systems should need to satisfy much higher availability criteria. The availability of the carrier-class is normally Regarded to be 99.999 percent. Backing up the FSO link with a lower data rate radio frequency (RF) link would be a more feasible approach for expanding the high availability range. Here the use of a hybrid FSO/RF system will expand the connection range of 99.999 percent to longer distances and open the carriers to a much broader metro/access market [24]. It is necessary to note that there would be a small decrease in total bandwidth as the connection range increases.

# References

- [1] *Fso history and technology.*  
<http://www.laseroptronics.com/index.cfm/id/57-66.htm>.  
(Accessed on 11/28/2020).
- [2] <https://functions.wolfram.com/>.
- [3] <http://www.laseroptronics.com/index.cfm/id/57-66.htm>.
- [4] A. ABDI, W. C. LAU, M.-S. ALOUINI, AND M. KAVEH, *A new simple model for land mobile satellite channels: first-and second-order statistics*, IEEE Transactions on Wireless Communications, 2 (2003), pp. 519–528.
- [5] A. AL-HABASH, L. C. ANDREWS, AND R. L. PHILLIPS, *Mathematical model for the irradiance probability density function of a laser beam propagating through turbulent media*, Optical engineering, 40 (2001), pp. 1554–1563.
- [6] M. C. AL NABOULSI, H. SIZUN, AND F. DE FORNEL, *Fog attenuation prediction for optical and infrared waves*, Optical Engineering, 43 (2004), pp. 319–330.
- [7] H. AL-QUWAIEE, H.-C. YANG, AND M.-S. ALOUINI, *On the asymptotic ergodic capacity of fso links with generalized pointing error model*, in 2015 IEEE International Conference on Communications (ICC), IEEE, 2015, pp. 5072–5077.
- [8] W. ALHEADARY, *Free space optics for 5G backhaul networks and beyond*, PhD thesis, 2018.
- [9] W. G. ALHEADARY, K.-H. PARK, AND M.-S. ALOUINI, *Performance analysis of subcarrier intensity modulation using rectangular qam over malaga turbulence channels with integer and non-integer  $\beta$* , Wireless Communications and Mobile Computing, 16 (2016), pp. 2730–2742.
- [10] S. H. ALI, *Advantages and limits of free space optics*.
- [11] J. B. ANDERSEN, *Stastistical distributions in mobile communications using multiple scattering*, 2002.
- [12] L. C. ANDREWS, R. L. PHILLIPS, AND C. Y. HOPEN, *Laser beam scintillation with applications*, vol. 99, SPIE press, 2001.

- [13] I. S. ANSARI, M.-S. ALOUINI, AND J. CHENG, *Ergodic capacity analysis of free-space optical links with nonzero boresight pointing errors*, IEEE Transactions on Wireless Communications, 14 (2015), pp. 4248–4264.
- [14] I. S. ANSARI, H. ALQUWAIEE, E. ZEDINI, AND M.-S. ALOUINI, *Information theoretical limits of free-space optical links*, in Optical Wireless Communications, Springer, 2016, pp. 171–208.
- [15] I. S. ANSARI, F. YILMAZ, AND M. ALOUINI, *Performance analysis of free-space optical links over málaga( $\mathcal{M}$ ) turbulence channels with pointing errors*, IEEE Transactions on Wireless Communications, 15 (2016), pp. 91–102.
- [16] N. ARAKI AND H. YASHIMA, *A channel model of optical wireless communications during rainfall*, in 2005 2nd International Symposium on Wireless Communication Systems, IEEE, 2005, pp. 205–209.
- [17] S. ARNON, *Effects of atmospheric turbulence and building sway on optical wireless-communication systems*, Optics letters, 28 (2003), pp. 129–131.
- [18] B. BAG, A. DAS, A. CHANDRA, AND R. RÓKA, *Performance analysis of fso links in turbulent atmosphere*, in Design, Implementation, and Analysis of Next Generation Optical Networks: Emerging Research and Opportunities, IGI Global, 2020, pp. 100–156.
- [19] S. BEA AND M. TEICH, “fundamentals of photonics”, Wiley, (1991), p. 313.
- [20] R. BOLUDA-RUIZ, A. GARCÍA-ZAMBRANA, B. CASTILLO-VÁZQUEZ, AND C. CASTILLO-VÁZQUEZ, *Impact of nonzero boresight pointing error on ergodic capacity of mimo fso communication systems*, Optics express, 24 (2016), pp. 3513–3534.
- [21] D. K. BORAH AND D. G. VOELZ, *Estimation of laser beam pointing parameters in the presence of atmospheric turbulence*, Applied optics, 46 (2007), pp. 6010–6018.
- [22] ———, *Pointing error effects on free-space optical communication links in the presence of atmospheric turbulence*, Journal of Lightwave Technology, 27 (2009), pp. 3965–3973.
- [23] N. D. CHATZIDIAMANTIS, H. G. SANDALIDIS, G. K. KARAGIANNIDIS, S. A. KOTSOPoulos, AND M. MATTHAIOU, *New results on turbulence modeling for free-space optical systems*, in 2010 17th International Conference on Telecommunications, IEEE, 2010, pp. 487–492.
- [24] M. Z. CHOWDHURY, M. K. HASAN, M. SHAHJALAL, M. T. HOSSAN, AND Y. M. JANG, *Optical wireless hybrid networks: Trends, opportunities, challenges, and research directions*, IEEE Communications Surveys & Tutorials, 22 (2020), pp. 930–966.
- [25] M. Z. CHOWDHURY, M. T. HOSSAN, A. ISLAM, AND Y. M. JANG, *A comparative survey of optical wireless technologies: Architectures and applications*, IEEE Access, 6 (2018), pp. 9819–9840.

- [26] A. S. J. CHOYON AND R. CHOWDHURY, *Performance comparison of free-space optical (fso) communication link under ook, bpsk, dpsk, qpsk and 8-psk modulation formats in the presence of strong atmospheric turbulence*, Journal of Optical Communications, 1 (2020).
- [27] J. H. CHURNSIDE AND S. F. CLIFFORD, *Log-normal rician probability-density function of optical scintillations in the turbulent atmosphere*, JOSA A, 4 (1987), pp. 1923–1930.
- [28] S. J. DOLINAR, J. HAMKINS, B. E. MOISION, V. A. VILNROTTER, AND H. HEMMATI, *Optical modulation and coding*, Wiley-Interscience, 2006.
- [29] T. Y. ELGANIMI, *Studying the ber performance, power-and bandwidth-efficiency for fso communication systems under various modulation schemes*, in 2013 IEEE Jordan Conference on Applied Electrical Engineering and Computing Technologies (AEECT), IEEE, 2013, pp. 1–6.
- [30] B. EPPEL, *Simplified channel model for simulation of free-space optical communications*, Journal of Optical Communications and networking, 2 (2010), pp. 293–304.
- [31] N. ERMOLOVA AND S.-G. HAGGMAN, *Simplified bounds for the complementary error function; application to the performance evaluation of signal-processing systems*, in 2004 12th European Signal Processing Conference, IEEE, 2004, pp. 1087–1090.
- [32] H. A. FADHIL, A. AMPHAWAN, H. A. SHAMSUDDIN, T. H. ABD, H. M. AL-KHAFAJI, S. ALJUNID, AND N. AHMED, *Optimization of free space optics parameters: An optimum solution for bad weather conditions*, Optik, 124 (2013), pp. 3969–3973.
- [33] A. A. FARID AND S. HRANILOVIC, *Outage capacity optimization for free-space optical links with pointing errors*, Journal of Lightwave technology, 25 (2007), pp. 1702–1710.
- [34] Z. GHASSEMLOOY, S. ARNON, M. UYSAL, Z. XU, AND J. CHENG, *Emerging optical wireless communications-advances and challenges*, IEEE journal on selected areas in communications, 33 (2015), pp. 1738–1749.
- [35] Z. GHASSEMLOOY, J. PEREZ, AND E. LEITGEB, *On the performance of fso communications links under sandstorm conditions*, in Proceedings of the 12th International Conference on Telecommunications, IEEE, 2013, pp. 53–58.
- [36] Z. GHASSEMLOOY, W. POOPOLA, AND S. RAJBHANDARI, *Optical wireless communications: system and channel modelling with Matlab®*, CRC press, 2019.
- [37] Z. GHASSEMLOOY, W. O. POOPOLA, AND E. LEITGEB, *Free-space optical communication using subcarrier modulation in gamma-gamma atmospheric turbulence*, in 2007 9th International Conference on Transparent Optical Networks, vol. 3, IEEE, 2007, pp. 156–160.
- [38] Z. GHASSEMLOOY, S. ZVANOVEC, M.-A. KHALIGHI, W. O. POOPOLA, AND J. PEREZ, *Optical wireless communication systems*, 2017.

- [39] A. GOLDSMITH, *Wireless communications*, Cambridge university press, 2005.
- [40] A. S. HAMZA, J. S. DEOGUN, AND D. R. ALEXANDER, *Classification framework for free space optical communication links and systems*, IEEE Communications Surveys & Tutorials, 21 (2018), pp. 1346–1382.
- [41] T. S. HANZRA AND G. SINGH, *Performance of free space optical communication system with bpsk and qpsk modulation*, IOSR Journal of Electronics and Communication Engineering (IOSRJECE), 1 (2012), pp. 38–43.
- [42] D. HOSSEN AND G. S. ALIM, *Performane evaluation of the Free Space Optical (FSO) communication with the effects of the atmospheric turbulances*, PhD thesis, BRAC University, 2008.
- [43] S. HRANILOVIC, *Wireless optical communication systems*, Springer Science & Business Media, 2006.
- [44] A. A. IBRAHIM, S. Ö. ATA, E. ERDOĞAN, AND L. DURAK-ATA, *Performance analysis of free space optical communication systems over imprecise malaga fading channels*, Optics Communications, 457 (2020), p. 124694.
- [45] M. IJAZ, Z. GHASSEMLOOY, S. ANSARI, O. ADEBANJO, H. LE MINH, S. RAJBHANDARI, AND A. GHOLAMI, *Experimental investigation of the performance of different modulation techniques under controlled fso turbulence channel*, in 2010 5th International symposium on telecommunications, IEEE, 2010, pp. 59–64.
- [46] M. IJAZ, Z. GHASSEMLOOY, J. PESEK, O. FISER, H. LE MINH, AND E. BENTLEY, *Modeling of fog and smoke attenuation in free space optical communications link under controlled laboratory conditions*, Journal of Lightwave Technology, 31 (2013), pp. 1720–1726.
- [47] M. IJAZ, Z. GHASSEMLOOY, S. RAJBHANDARI, H. LE MINH, J. PEREZ, AND A. GHOLAMI, *Comparison of 830 nm and 1550 nm based free space optical communications link under controlled fog conditions*, in 2012 8th International Symposium on Communication Systems, Networks & Digital Signal Processing (CSNDSP), IEEE, 2012, pp. 1–5.
- [48] Y. JAHIR, M. ATIQUZZAMAN, H. REFAI, AND P. G. LOPRESTI, *Performance evaluation of aodvh: An ad hoc networking scheme for hybrid nodes*, in 2010 13th International Conference on Computer and Information Technology (ICCIT), IEEE, 2010, pp. 165–169.
- [49] A. JURADO-NAVAS, J. GARRIDO-BALSELLS, J. F. PARIS, M. CASTILLO-VAZQUEZ, AND A. PUERTA-NOTARIO, *Further insights on málaga distribution for atmospheric optical communications*, in 2012 International Workshop on Optical Wireless Communications (IWOW), IEEE, 2012, pp. 1–3.

- [50] A. JURADO-NAVAS, J. M. GARRIDO-BALSELLS, J. F. PARIS, M. CASTILLO-VÁZQUEZ, AND A. PUERTA-NOTARIO, *Impact of pointing errors on the performance of generalized atmospheric optical channels*, Optics express, 20 (2012), pp. 12550–12562.
- [51] A. JURADO-NAVAS, J. M. GARRIDO-BALSELLS, J. F. PARIS, A. PUERTA-NOTARIO, AND J. AWREJCEWICZ, *A unifying statistical model for atmospheric optical scintillation*, Numerical simulations of physical and engineering processes, 181 (2011).
- [52] J. KAUFMANN, *Free space optical communications: An overview of applications and technologies*, in Proceedings of the Boston IEEE Communications Society Meeting, 2011.
- [53] G. KAUR, H. SINGH, AND A. S. SAPPAL, *Free space optical using different modulation techniques—a review*, International Journal of Engineering Trends and Technology (IJETT), 43 (2017), pp. 109–115.
- [54] K. KAUR, R. MIGLANI, AND J. S. MALHOTRA, *The gamma-gamma channel model-a survey*, Indian J. Sci. Technol, 9 (2016), pp. 10–13.
- [55] D. KEDAR AND S. ARNON, *Urban optical wireless communication networks: the main challenges and possible solutions*, IEEE Communications Magazine, 42 (2004), pp. S2–S7.
- [56] R. KENNEDY, *Communication through optical scattering channels: An introduction*, Proceedings of the IEEE, 58 (1970), pp. 1651–1665.
- [57] I. I. KIM, B. MCARTHUR, AND E. J. KOREVAAR, *Comparison of laser beam propagation at 785 nm and 1550 nm in fog and haze for optical wireless communications*, in Optical Wireless Communications III, vol. 4214, International Society for Optics and Photonics, 2001, pp. 26–37.
- [58] Y. KONO, A. PANDEY, AND A. SAHU, *Ber analysis of lognormal and gamma-gamma turbulence channel under different modulation techniques for fso system*, in 2019 3rd International Conference on Trends in Electronics and Informatics (ICOEI), IEEE, 2019, pp. 1385–1388.
- [59] S. MA, Y.-T. LI, J.-B. WU, T.-W. GENG, AND Z. WU, *Performance analyses of subcarrier bpsk modulation over m turbulence channels with pointing errors*, Optoelectronics Letters, 12 (2016), pp. 221–225.
- [60] A. K. MAJUMDAR AND J. C. RICKLIN, *Free-space laser communications: principles and advances*, vol. 2, Springer Science & Business Media, 2010.
- [61] A. MALIK AND P. SINGH, *Free space optics: current applications and future challenges*, International Journal of Optics, 2015 (2015).

- [62] S. MALIK AND P. K. SAHU, *Performance analysis of free space optical communication system using different modulation schemes over weak to strong atmospheric turbulence channels*, in Optical and Wireless Technologies, Springer, 2020, pp. 387–399.
- [63] D. S. MINI SENGAR, *Effect of atmospheric turbulence on ber performance of fso system based on various modulation techniques*, International Journal of Modern Communication Technologies & Research (IJMCTR), Volume-7 (, Issue-4, April 2019).
- [64] S. S. MUHAMMAD, P. KOHLDORFER, AND E. LEITGEB, *Channel modeling for terrestrial free space optical links*, in Proceedings of 2005 7th International Conference Transparent Optical Networks, 2005., vol. 1, IEEE, 2005, pp. 407–410.
- [65] N. M. NAWAWI, *Wireless Local Area Network System Employing Free Space Optic Communication Link*, PhD thesis, Universiti Teknologi Malaysia, 2009.
- [66] V. V. NIKULIN AND R. KHANDEKAR, *Performance of laser communication uplinks and down-links in the presence of pointing errors and atmospheric distortions*, in Free-Space Laser Communication Technologies XVII, vol. 5712, International Society for Optics and Photonics, 2005, pp. 37–45.
- [67] H. E. NISTAZAKIS, T. A. TSIFTSIS, AND G. S. TOMBRAS, *Performance analysis of free-space optical communication systems over atmospheric turbulence channels*, IET communications, 3 (2009), pp. 1402–1409.
- [68] N. A. M. NOR, I. M. RAFIQUL, W. AL-KHATEEB, AND S. A. ZABIDI, *Environmental effects on free space earth-to-satellite optical link based on measurement data in malaysia*, in 2012 International Conference on Computer and Communication Engineering (ICCCE), IEEE, 2012, pp. 694–699.
- [69] B. OLIVIERET ET AL., *Free-space optics, propagation and communication*, Book, ISTE, 6 (2006).
- [70] G. G. PETER, S. R. WILLIAM, R. MAHON, L. M. JAMES, S. F. MIKE, R. S. MICHELE, R. S. WALTER, B. X. BEN, R. B. HARRIS, I. M. CHRISTOPHER, ET AL., *Modulating retro-reflector lasercom systems at the naval research laboratory*, in 2010-MILCOM 2010 MILITARY COMMUNICATIONS CONFERENCE, IEEE, 2010, pp. 1601–1606.
- [71] M. PETKOVIĆ AND G. DJORDJEVIĆ, *Average ber of dual-branch fso system employing sim-bpsk influenced by malaga atmospheric turbulence with pointing errors*, environment, 1 (2017), p. 3.
- [72] W. O. POPOOLA AND Z. GHASSEMLOOY, *Bpsk subcarrier intensity modulated free-space optical communications in atmospheric turbulence*, Journal of Lightwave technology, 27 (2009), pp. 967–973.

- [73] W. O. POPOOLA, Z. GHASSEMLOOY, AND V. AHMADI, *Performance of sub-carrier modulated free-space optical communication link in negative exponential atmospheric turbulence environment*, International Journal of Autonomous and Adaptive Communications Systems, 1 (2008), pp. 342–355.
- [74] K. PRABU, D. S. KUMAR, AND T. SRINIVAS, *Performance analysis of fso links under strong atmospheric turbulence conditions using various modulation schemes*, Optik, 125 (2014), pp. 5573–5581.
- [75] W. K. PRATT, *Laser communication systems*, New York, Wiley, 1969.
- [76] M. O. PRUDNIKOV A.P., BRYCHKOV Y.A., *Integral and series*, Fizmatlit, Moskva, 2003., 2nd Ed., (2003).
- [77] A. RAHMAN, M. S. ANUAR, S. A. ALJUNID, AND M. N. JUNITA, *Study of rain attenuation consequence in free space optic transmission*, in 2008 6th National Conference on Telecommunication Technologies and 2008 2nd Malaysia Conference on Photonics, IEEE, 2008, pp. 64–70.
- [78] S. K. A. M. M. RAJAN MIGLANI1, SACHAL CHARAK2, *A review on fso by using different modulation techniques*, International Journal of Engineering & Technology, (2018).
- [79] R. RAMIREZ-INIGUEZ, S. M. IDRUS, AND Z. SUN, *Optical wireless communications: IR for wireless connectivity*, CRC press, 2008.
- [80] K. RAMMPRASATH AND S. PRINCE, *Analyzing the cloud attenuation on the performance of free space optical communication*, in 2013 International Conference on Communication and Signal Processing, IEEE, 2013, pp. 791–794.
- [81] M. ROUSSAT, R. A. BORSALI, M. CHICK-BLED, ET AL., *Dual amplitude-width ppm for free space optical systems*, International Journal of Information Technology and Computer Science (IJITCS), 4 (2012).
- [82] R. K. Z. SAHBUDIN, M. KAMARULZAMAN, S. HITAM, M. MOKHTAR, AND S. B. A. ANAS, *Performance of sac ocdma-fso communication systems*, Optik-International Journal for Light and Electron Optics, 124 (2013), pp. 2868–2870.
- [83] H. SAMIMI, *Distribution of the sum of k-distributed random variables and applications in free-space optical communications*, IET optoelectronics, 6 (2012), pp. 1–6.
- [84] H. G. SANDALIDIS, T. A. TSIFTSIS, G. K. KARAGIANNIDIS, AND M. UYSAL, *Ber performance of fso links over strong atmospheric turbulence channels with pointing errors*, IEEE Communications Letters, 12 (2008), pp. 44–46.

- [85] V. SASO, B. MILOSEVIC, AND S. JOVKOVIC, *Ber performance analysis of various fso modulation formats*.
- [86] V. SHARMA AND G. KAUR, *High speed, long reach ofdm-fso transmission link incorporating ossb and otsb schemes*, Optik, 124 (2013), pp. 6111–6114.
- [87] G. SHAULOV, J. PATEL, B. WHITLOCK, P. MENA, AND R. SCARMOZZINO, *Simulation-assisted design of free space optical transmission systems*, in MILCOM 2005-2005 IEEE Military Communications Conference, IEEE, 2005, pp. 918–922.
- [88] M. K. SIMON AND M.-S. ALOUINI, *Digital communication over fading channels*, vol. 95, John Wiley & Sons, 2005.
- [89] J. SINGH AND N. KUMAR, *Performance analysis of different modulation format on free space optical communication system*, Optik, 124 (2013), pp. 4651–4654.
- [90] N. S. SINGH AND G. SINGH, *Performance evaluation of log-normal and negative exponential channel modeling using various modulation techniques in ofdm-fso communication*, International Journal of Computers & Technology, 4 (2013), pp. 639–647.
- [91] S. VIGNESHWARAN, I. MUTHUMANI, AND A. S. RAJA, *Investigations on free space optics communication system*, in 2013 International Conference on Information Communication and Embedded Systems (ICICES), IEEE, 2013, pp. 819–824.
- [92] S. J. VLADIMIR SASO, BORIVOJE MILOSEVIC, *Ber performance analysis of various fso modulation formats*, International Journal of Innovations in Engineering and Technology (IJIET), 14 (2019).
- [93] F. WANG, G. HU, T. DU, Y. SUN, X. HAO, J. CHEN, AND P. WU, *Performance research of mppm-qpsk modulation signal for free space optical communication*, Optics Communications, 457 (2020), p. 124646.
- [94] P. WANG, R. WANG, L. GUO, T. CAO, AND Y. YANG, *On the performances of relay-aided fso system over m distribution with pointing errors in presence of various weather conditions*, Optics Communications, 367 (2016), pp. 59–67.
- [95] H. WEICHEL, *Laser beam propagation in the atmosphere*, vol. 10319, SPIE press, 1990.
- [96] H. WILLEBRAND AND B. S. GHUMAN, *Free space optics: enabling optical connectivity in today's networks*, SAMS publishing, 2002.
- [97] H. A. WILLEBRAND AND B. S. GHUMAN, *Fiber optics without fiber*, IEEE spectrum, 38 (2001), pp. 40–45.

- [98] F. YANG AND J. CHENG, *Coherent free-space optical communications in lognormal-rician turbulence*, IEEE communications letters, 16 (2012), pp. 1872–1875.
- [99] F. YANG, J. CHENG, AND T. A. TSIFTSIS, *Free-space optical communication with nonzero boresight pointing errors*, IEEE Transactions on Communications, 62 (2014), pp. 713–725.
- [100] L. YANG, X. GAO, AND M.-S. ALOUINI, *Performance analysis of free-space optical communication systems with multiuser diversity over atmospheric turbulence channels*, IEEE Photonics Journal, 6 (2014), pp. 1–17.
- [101] W. O. P. Z. GHASSEMLOOY, *Terrestrial free space optical communication*, Optical Communications Research Group, NCR Lab., Northumbria University, Newcastle upon Tyne, (2010).
- [102] S. A. ZABIDI, W. AL KHATEEB, M. R. ISLAM, AND A. NAJI, *The effect of weather on free space optics communication (fso) under tropical weather conditions and a proposed setup for measurement*, in International Conference on Computer and Communication Engineering (ICCCE'10), IEEE, 2010, pp. 1–5.
- [103] S. A. ZABIDI, M. R. ISLAM, W. AL KHATEEB, AND A. W. NAJI, *Investigating of rain attenuation impact on free space optics propagation in tropical region*, in 2011 4th International Conference on Mechatronics (ICOM), IEEE, 2011, pp. 1–6.
- [104] H. ZHANG, H. LI, X. DONGYA, AND C. CHAO, *Performance analysis of different modulation techniques for free-space optical communication system*, Telkomnika, 13 (2015), p. 880.
- [105] X. ZHU AND J. M. KAHN, *Free-space optical communication through atmospheric turbulence channels*, IEEE Transactions on communications, 50 (2002), pp. 1293–1300.